DESIGNING A RIG FOR INVESTIGATING THERMAL FATIGUE OF BIMETALLIC WELDS

A thesis submitted

in fulfillment of the requirement for the award of the degree

of

Doctor of Philosophy

in

Mechanical Engineering

by

Hamender Kumar Aggarwal

Regd. No. 950808002

DEPARTMENT OF MECHANICAL ENGINEERING

THAPAR UNIVERSITY PATIALA-147004,

PUNJAB, INDIA

April, 2017

CERTIFICATE

This is to certify that the thesis entitled "**DESIGNING A RIG FOR INVESTIGATING THERMAL FATIGUE OF BIMETALLIC WELDS**", which is being submitted by Mr. Hamender Kumar Aggarwal to the Department of Mechanical Engineering, Thapar University, Patiala in the fulfillment of the requirements for the award of the degree of **DOCTOR OF PHILOSOPHY,** is a record of bonafied research work carried out by him under our guidance and supervision. The matter presented in this thesis has not been submitted either in part or full to any other university or institute for the award of any degree.

Rahul Chhibber

Dr. Rahul Chhibber
Assistant Professor
Department of Mechanical Engineering
Indian Institute of Technology, Jodhpur

Dr. Navneet Arora
Professor
Department of Mechanical and Industrial Engineering
Indian Institute of Technology, Roorkee

Rajeev Mehta
20/04/2017

Dr. Rajeev Mehta
Professor
Department of Chemical Engineering
Thapar University, Patiala

ACKNOWLEDGEMENT

My deepest gratitude and appreciation is extended to the ones who helped me in making this study possible. They made the past few years a learning and memorable period of my life.

I am very grateful to the authorities of the Thapar University, Patiala for providing me an opportunity to carry out my research work. By the end of my Ph.D. journey, I realize that it is the team work that has got me here. It is a matter of honour and privilege for me to offer grateful acknowledgement to my supervisors: Dr. Rahul Chhibber, Assistant Professor, Department of Mechanical Engineering, Indian Institute of Technology, Jodhpur, Rajasthan, India, Dr. Navneet Arora, Professor, Department of Mechanical and Industrial Engineering, Indian Institute of Technology, Roorkee, Uttrakhand, India and Dr. Rajeev Mehta, Professor, Department of Chemical Engineering, Thapar University, Patiala, Punjab, India. They were always there with all kinds of support and inspiration, wise counsel, imbuing academic discipline, clear thinking, excellent guidance, constant encouragement, constructive criticism and valuable suggestions. Without their kind and patient instructions, it is impossible to finish this thesis.

I would like to express my indebtedness to Dr. Parkash Gopalan (Director, Thapar University, Patiala), for their continuous encouragement, inspiration and support. I am also very much thankful to Prof. Dr. O. P. Pandey (Dean, Research and Sports Projects, Thapar University, Patiala), who helped me a lot tying the loose ends. Sincere thanks are also due to my fellow Ph.D. colleagues, Naveen Kumar, Yogesh Kumar Singla, Department of Mechanical and Industrial Engineering, Indian Institute of Technology, Roorkee, Uttrakhand, India and Deen Bandhu Chhotu Ram University of Science and Technology, Murthal, Haryana, India in funding for project of thermal fatigue test rig. This work is just a small drop in the ocean of knowledge created by the celebrated authors whose published work has been consulted and referred in my research work.

I also like to acknowledge SAI Labs and Thapar University for sample analysis.

My thanks to all my lab mates of Deen Bandhu Chhottu Ram University of Science and Technology, Murthal, Haryana, India, especially Sh. Desh Raj Singh (In-charge, Forging shop), M. R. Saini, Mahender, Surender Khatri (electrician) and who has contributed a lot in completing the experimental work and all those who wished my

success. Special thanks are due to my family from the bottom of my heart, my mother Padma Gupta and my father Sh. Yog Raj Gupta and elder brother Dr. Rajeev Aggarwal, Bhabhi Sangeeta, sister, Dr. Savita Kansal and sister-in-law Surender Kansal for giving me their selfless roc-solid support and encouragement. Special thanks are also due to my wife, Reema and my kids, Sugandha and Keshav for their love and support. My family has continuously supported me in my research. My research work would not have been possible without the support of my wife and my kids.

Finally, I thank Sh. Prabhu Ji (Kangra Ashram) for his mercy and grace for supporting me at each step. Without Him, I couldn't stay patience and my health during this journey. I pray for the continuous protection by the Prabhu Ji and wish to move to the next phase of my life.

I offer my regards and thanks to all those who helped and supported me in any respect during the completion of the thesis.

(Hamender Kumar Aggarwal)

ABSTRACT

The bimetallic welds between ferritic plain carbon steels or low alloy steels and austenitic stainless steels being used in nuclear power plants impose a challenge towards the structural integrity assessment for researchers not only due to the different metallurgical zones, having a gradient in chemistry and mechanical properties but also due to the high temperature operating conditions and the temperature variations over the length of operation.

Thermal fatigue is a phenomenon where a structural damage occurs when a material is subjected to cyclic thermal changes that may lead to initiation and growth of cracks and eventually lead to fracture after an exposure to sufficient amount of cycling. The thermal strains and associated thermal stresses are generated in the material when exposed to a temperature gradient, over a number of repeating cycles. This process is referred to as thermal fatigue. The magnitude of the thermal stresses generated in the case of thermal shock, is greater due to steeper temperature gradients in comparison to that observed for gradual change in temperature.

To investigate the effect of the resulting stresses on mechanical behaviour of the reactor components, it is necessary to perform fatigue test under thermal test loading. The present work addressed the problem of evaluation of mechanical behaviour of bimetallic welds under thermal fatigue conditions by developing a test rig for simulating thermal fatigue conditions at laboratory scale and using the experimental test rig to study the mechanical behaviour of bimetallic welds exposed to thermal fatigue conditions. The effect of testing parameters such as the number of cycles, notch radius in specimen (defining degree of constraint) and heating time (corresponds to temperature gradient during heating) was observed in bimetallic weld zone, heat affected zone on the ferritic side of the plain carbon steel and the base materials namely stainless steel 304 L and plain carbon steel SA516 grade 70.

CONTENTS

LIST OF FIGURES

LIST OF TABLES

ABBREVIATIONS AND NOTATIONS

°C	Degree Centigrade
°F	Degree Fahrenheit
AC	Alternate Current
ASM	American Society for Metals
ASME	American Society of Mechanical Engineers
AWS	American Welding Society
BMWs	Bimetallic Welds
BS	British Standards
BWR	Boiling Water Reactors
CDZ	Carbon Depleted Zone
CGHAZ	Coarse Grain Heat Affected Zone
CNC	Computerized Numerical machine
Cr	Chromium
C_{ss}	Specific Heat of Stainless Steel
CTE	Coefficient of Thermal Expansion
Cu	Copper
DM	Demineralized
EDX	Energy Dispersive X-ray
ER	Electrode
f	Frequency
FAZ	Fully Austenitic Zone
f_c	Critical Frequency
g/cc	Gram per cubic centimeter
GMAW	Gas Metal arc welding
GPa	Giga Pascal
GTAW	Gas Tungsten arc welding
HAZ	Heat Affected Zone
HE	Heat Exchanger
HT	Heating Time
in	Inches
IR	Infra-Red
$J/g-^0_C$	Joule per gram degree centigrade
kg/hr	kilogram per hour
kHz	kilo Hertz
kW	kilo Watt
kW/cm^2	kilo Watt per square centimeter
L	Length
LAS	Low Alloy Steel
LEFM	Linear Elastic Fracture Mechanics
Mn	Manganese
Mo	Molybdenum
MPa	Mega Pascal

Ni	Nickel
NOC	Number of Cycles
NR	Notch Radius
P	Power
PWRs	Pressurized Water Reactors
q	Water Flow Rate
RF	Rated Frequency
S	Sulphur
Sec	Seconds
SEM	Scanning Electron Microscope
Si	Silicon
SS	Stainless Steel
TCS	Thermal Cyclic Shock
TF	Thermal Fatigue
TR	Transmit Receiver
UTS	Ultimate Tensile Strength
V	Volume
Vs	Verses
W	Weight
W/m-K	Watt per meter Kelvin
YS	Yield Strength
K	Stress Intensity Factor
Δt	Temperature Difference
ρ	Density

CHAPTER 1
INTRODUCTION

1.0 Overview

This chapter is aimed at understanding the importance of thermal fatigue in industrial components. The need for present research work has been highlighted. The chapter ends with in the overview of the thesis.

1.1 Introduction

The phenomenon of thermal fatigue as a cause of damage is observed in different locations in various industries such as in turbine blades in power plants, rolling mill cylinders in rolling mills, moulds in die casting industry, bimetallic weld joints in nuclear reactors. With the increase in the life of the nuclear power plants the thermal fatigue becomes a more potent threat towards undermining the structural integrity of the nuclear reactor components by emerging as a major cause for the damage to its components.

The initiation and growth of cracks due to thermal shock cycles or repeated thermal shocks is due to the restraint of thermal expansion and contraction of material as it is exposed to thermal shock environment (rapid change in temperature). Restraint may be internal or external depending upon the condition, internal constraint results from the thermal gradient across the thickness of material, as the heat is not able to flow quickly across the thickness of the specimen. On other hand external constraints mean some external forces act upon the specimen that is alternately heating and cooling. If changes in temperature are severe and resulting strain is large enough then localized plastic deformation can occur.

The thermal shock stresses are transient in nature. Cracking due to thermal shock is a major issue in the thermal power station equipment such as in boiler equipment thermal shock cracking is an inevitable effect in normal operation with startup and shut down process. Effect of thermal shock stresses result in opening of crack means exposing to environment that behaves as aqueous in nature that may lead to corrosion. Thus corrosion plays an important role during fatigue (thermal shock cycle).

Thermal shock cycles is sometimes referred as thermal fatigue and the study is focused on the thermal fatigue in thermal and nuclear power industries, where time dependent effect can be presumed to be negligible and only thermal stresses is used

to analyze the event due to thermal shock cycles in the temperature ranges from 20-300°C (operating temperature of nuclear power plant).

The bimetallic weld joints being an integral part of nuclear power plant components used for connecting the low and high temperature sections are exposed to thermal fatigue conditions. The structural integrity assessment of these bimetallic joints is an important task for the researchers.

1.2 Organization of the thesis

This thesis is organized into seven chapters and the essence of each chapter is detailed below:

The **Chapter 1** outlines the introduction to the research topic and the organization of the thesis.

The **Chapter 2** provides a detailed literature survey on the investigations carried out by various researchers on the topic of thermal fatigue.

The **Chapter 3** deals with the problem formulation. The need of the research is highlighted; the research objectives are identified and the research plan is discussed.

The **Chapter 4** discusses the experimental designing of the thermal fatigue test rig. It discusses the design of various individual components of the test rig and also discusses the basis for selection of various design parameters.

The **Chapter 5** presents the experimentation carried out using the test rig with the evolved design matrix for experimentation and the experimental investigations on obtaining the mechanical behavior of the various test specimens subjected to thermal fatigue conditions at laboratory scale.

The **Chapter 6** provides the results and discussion obtained in the thesis.

The **Chapter 7** presents the conclusions of the research work and suggests the scope for further research in the area.

In the end, the list of references is given.

CHAPTER 2
LITERATURE REVIEW

2.0 Overview

This chapter is aimed at reviewing the literature related to the present investigation. The various sections in the chapter discuss about thermal fatigue of Bimetallic welds, thermal cycling in nuclear reactors, thermal shock failure mechanism, factor influencing joint integrity and safety and latest research work carried in this area. Based on the outcome of above stated review, gapes and opportunities have been discussed in the end of the chapter.

2.1 Pressure Vessel

i. The various shapes of pressure vessels are generally used to contain any media at elevated temperature and pressure. This is made possible by using various fastening devices to hold the pressure vessel shell together by connecting and securing mating parts (Decamp, 1998) [38]. The pressure vessels experience dynamic and static loading conditions. With the ever expanding needs of the modern world the need for the use of more efficient materials in terms of resistance at elevated temperatures, resistance to corrosion and neutron irradiation and requirement of higher impact and fatigue strength are increasing day by day (Harvey, 1969) [64].

ii. To the pressure vessel base are also attached by welding the necessary appurtenances, such as nozzles, support attachments, access openings, etc. Stress construction factors in welded joints arise through these means.

iii. The metallurgical structure of the weld metal with respect to the adjacent parent metal (Esterling, 1983) [51] (Findley, 1947) [52].

iv. The occurrence of welding defects, such as porosity, slag inclusions, and shrinkage cracks.

v. The weldment geometry- profile and contour of reinforcement, fillets, transition, etc., including surface finish (Harvey, 1969) [64]

2.1.1 Pressure Vessel Material

During the use of pressure vessel design approach, using the ASME Code, Section VIII, Division 1, it is assured that a higher factor of safety is adopted to allow for the existence of highly localized stresses (Denis, 2004) [39].

The different components (shells, nozzles, flanges, studs, etc.) of the pressure vessels are made of different materials. Different types of materials generally used in pressure vessel design as per temperatures conditions are given in table 2.1 (Denis, 2004) [39].

Table 2.1 Type of material generally used in pressure vessel design

	Design Temperature, °F	Material	Plate	Pipe	Forgings	Fittings	Bolting
Cryogenic	−425 to −321	Stainless steel	SA-240-304, 304L, 347, 316, 316L	SA-312-304, 304L, 347, 316, 316L	SA-182-304, 304L, 347, 316, 316L	SA-403-304, 304L, 347, 316, 316L	SA-320-B8 with SA-194-8
	−320 to −151	9 nickel	SA-353	SA-333-8	SA-522-1	SA-420-WPL8	
Low temperature	−150 to −76	3½ nickel	SA-203-D	SA-333-3	SA-350-LF63	SA-420-WPL3	SA-320-L7 with SA-194-4
	−75 to −51	2½ nickel	SA-203-A				
	−50 to −21	Carbon steel	SA-516-55, 60 to SA-20	SA-333-6	SA-350-LF2	SA-420-WPL6	
	−20 to 4		SA-516-All	SA-333-1 or 6			SA-193-B7 with SA-194-2H
	5 to 32		SA-285-C	SA-53-B SA-106-B	SA-105 SA-181-60,70	SA-234-WPB	
Intermediate	33 to 60 61 to 775		SA-516-All SA-515-All SA-455-II				
Elevated Temperature	776 to 875	C-½Mo	SA-204-B	SA-335-P1	SA-182-F1	SA-234-WP1	
	876 to 1000	1Cr-½Mo	SA-387-12-1	SA-335-P12	SA-182-F12	SA-234-WP12	
		1Cr-½Mo	SA-387-11-2	SA-335-P11	SA-182-F11	SA-234-WP11	
	1001 to 1100	2¼ Cr-1Mo	SA-387-22-1	SA-335-P22	SA-182-F22	SA-234-WP22	with SA-193-B5 SA-194-3
	1101 to 1500	Stainless steel	SA-240-347H	SA-312-347H	SA-182-347H	SA-403-347H	SA-193-B8 with SA-194-B
		Incoloy	SB-424	SB-423	SB-425	SB-366	
	Above 1500	Inconel	SB-443	SB-444	SB-446	SB-366	

From Bednar, H.H., *Pressure Vessel Design Handbook*, Van Nostrand Reinhold Co., 1981.

To provide superior mechanical properties the use of low alloy steels (LASs) and stainless steels (SSs) is adopted in the primary system of the pressurized water reactors (PWRs) (Castro, 1974) [24] (Pavlyuk, 1986) [108]. The low alloy steel clad with stainless steel is used for the main primary coolant piping , whereas the use of stainless steel is adopted for the branch lines to provide corrosion resistance and suitable strength (Khan, 2011) [82]. The use of stainless steel filler or Inconel based filler is used to join the Low alloy steel components to the pipes made of stainless steels to form the bimetallic welds (Devis, 1993) [36]. The stainless steel filler or Inconel based filler is known to reduce the differences in the coefficient of thermal expansion and metal chemistry between the two metals being joined (Swindeman)

[128] [129]. The locations of the bimetallic weld in PWRs I shown in Fig. 2.1. As can be seen from the figure 2.1; a number of locations in primary piping systems contain bimetallic welds (Changheui, 2008) [25] (Kuwabara, 1992) [91].

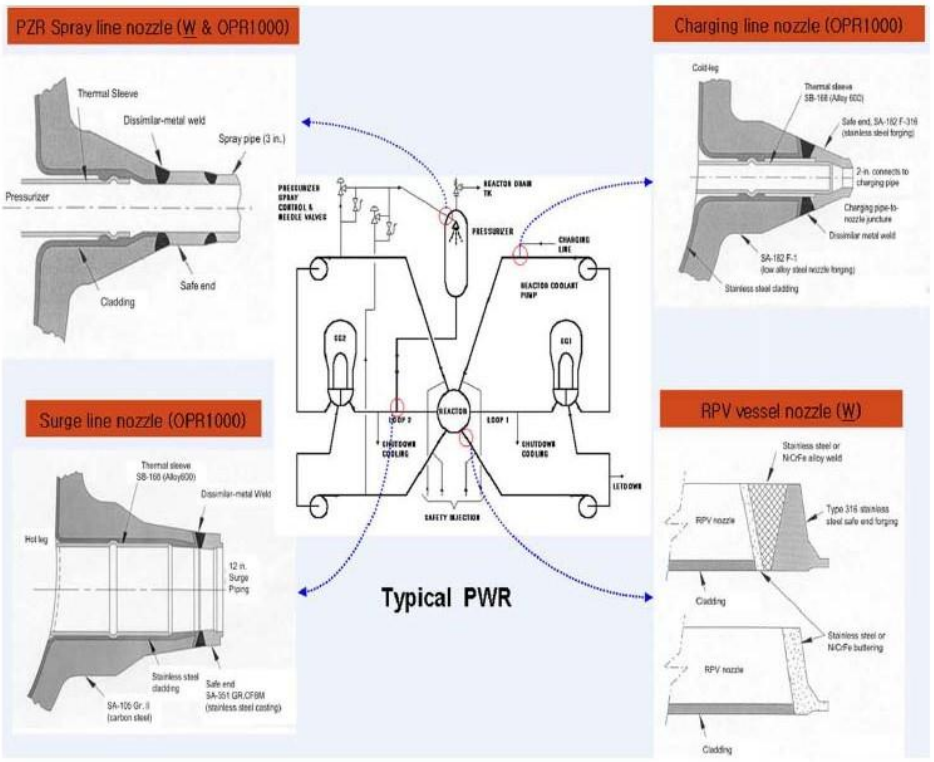

Fig. 2.1 Locations of bimetallic weld in typical PWR

2.2 Introduction to Thermal Fatigue

The volume of a solid body increases or expands when the temperature of that body is raised. This change of volume is called “thermal expansion” and the term “thermal strain” refers to the unit change of a linear dimension that is associated with the rise in temperature. No internal stress is produced in a solid material if the temperature increase is the same in all parts of the body and if the volume change is unrestrained (Schwam D. 2004) [118].

In a solid that is restrained so that it cannot expand (or contract) freely, a temperature change gives rise to a stress called a "thermal stress." A mechanical deformation is uniquely related to and concurrent with a thermal stress. A thermal-stress deformation that is recovered or relieved when the restraint is removed is said to be an elastic deformation. A thermal-stress deformation that is not recovered when the restraint is removed is said to be a plastic deformation. Plastic deformations can result from large thermal stresses, high temperatures, or long duration of stress application.

The elastic and plastic deformation together constitute the internal, or mechanical-load, strain which hereafter will be referred to simply as mechanical strain. The mechanical strain at a point is always related to the stress at that point and this stress can be produced independently of the temperature. A mechanical strain is not uniquely dependent on temperature, but a thermal strain is dependent on temperature. A thermal strain can occur without producing a thermal stress (i.e., in an unrestrained body), but a thermally induced stress (in a restrained body) always produces or is accompanied by a mechanical strain (Anderson, 1959) [5], (Baldwin, 1957) [10]. In thermal-fatigue tests there are, therefore, three kinds of strain: thermal strain, mechanical strain, and geometric strain. A thermal strain is that strain produced by temperature change. A mechanical strain is that strain which is produced by a stress, and there is no intrinsic difference between a thermal stress and a mechanical stress. A geometric strain is that which can be physically measured by a displacement. The geometric, or observed, strain is the algebraic sum of the mechanical strain and the thermal strain. A repeated fluctuation of temperature in a restrained solid produces cyclic thermal stresses (and strain), leading ultimately to failure. The name "thermal fatigue" is applied to failures produced by cyclic thermal stresses. The cyclic mechanical strains associated with the thermal stresses may be only elastic, or they may contain both elastic and plastic components (Zuchowski R., 2000) [144].

The conventional thermal-fatigue experiment can be simply described as the alternate heating and cooling of a thin-walled tubular specimen in a device that restricts the longitudinal movement of the specimen.

A significant critical review of the subject of thermal fatigue by T. C Yen, 1961 [141] has included a brief discussion of the test method and summarizes the two major difficulties of the conventional thermal-fatigue test namely, the lack of a uniform temperature throughout the length of a tubular specimen and the measurement of the mechanical strain especially the plastic component, produced by restrained thermal cycling. For several years thermal-fatigue testing was pursued with vigor and gained widespread attention. Interest abated, however, when apparent lack of success met efforts to obtain good agreement between the experimental results and the lives of service applications, or between thermal-fatigue and isothermal strain-fatigue data. No satisfactory explanation of the dilemma was universally accepted, and a shadow of

doubt began to cloud the experimental method. The value of the thermal-fatigue test has been contested by critics because many believe that the published methods of determining the plastic-strain values are questionable, that any calculated value of plastic strain may be gravely in error, that the construction of a stress-strain diagram is not possible, and that the plastic strain per cycle indeed becomes an elusive quantity to calculate (Zhang, 2002) [145]. The reasons for doubting the validity of the results of the conventional test have not rested simply on prejudice. The thermal coefficient, modulus of elasticity and strength properties all vary with temperature, which in this test varies with time, the temperature at any instant of time varies throughout the length of the specimen. Thus the problem has appeared to be too complex to deduce the stress-strain cycle of the material. Thermal-fatigue reports often do not relate how the plastic strain values were calculated and are vague about how other data were obtained. A clear, critical analysis of the published methods of determining the plastic strain has not yet appeared. The possible reasons why thermal-fatigue data do not always show good agreement with isothermal strain-fatigue results are generally not discussed. **A need exists to analyze the experimental testing problem and to suggest possible alternatives.**

2.3 Thermal Shock

The thermal stresses arise due to the expansion or contraction due to the temperature variation. Heating or cooling of a component or structure is hindered or prevented. Thermal shock events generally occur in plant involving water and steam when cold water strikes on the heated surface. Heating of component creates stresses due to non-uniform heating. Surrounding component is at different temperature and when it tries to contract, it produces compressive stresses. Each part of the body try to expand and contract with different amount, but each part will be constrained to some degree by a neighbouring region. This leads to a system of transient strains and associated stresses that is commonly called "**thermal shock**".

Three forms of failure generally occurred due to thermal shocks:-

1. Fatigue, due to repeated thermal for long period of time, result in crack initiation and then growth of crack (Keinanen, 1995) [76].
2. Creep failure when temperature is more than the critical temperature following the shock, in which residual stresses relaxation of weld produces void on the material grain boundaries.

3. Fracture, which is a rapid extension of a preexisting defect or crack in the component occurring during a single shock (Denys, 1987) [40].

2.4 Thermal Cyclic Shock (TCS) Vs Thermal Fatigue (TF)

Thermal fatigue and Thermal cyclic shock are not same in the context of development of stress due to change in temperature. Thermal fatigue is the development cyclic stress resulting from temperature variation from minimum to maximum whereas thermal shock cycle is the subset of thermal fatigue. In TCS, temperature distribution is transient in nature and thus follows the non-linear temperature distribution by rapid change in operating condition. Thermal fatigue is the strain controlled fatigue divided into two ways first one is thermal mechanical fatigue and other one is thermal stress fatigue. In thermal mechanical fatigue the external constraints is due to structural supports or other member connected to the component. In thermal stress fatigue case internal constraints occur when adjacent elements of the component are at different temperature or made of different material. This is the case of thermal shock condition when a component is heated non-uniformly then steep temperature gradient is developed (Ciepiere, 2002) [30]. Cooled region prevent the expansion of heated zone thus developing a self-equilibrium stress condition within the component. Same phenomena occur when cooling the heated component that prevents cooler area from contracting.

2.5 Thermal Fatigue of Bimetallic Welds

The use of bimetallic welds between low alloy steel and stainless steel is being frequently used in the pressurized water reactors (PWR) and boiling water reactor (BWR) designs, where the low alloy steel is used in relatively low temperature condition and stainless steel is used for components exposed to elevated temperature conditions. (Dahlberg, 2011) [35] (Haddar, 2012) [63] (Ikka, 2001) [68], (Chhibber, 2006) [27].

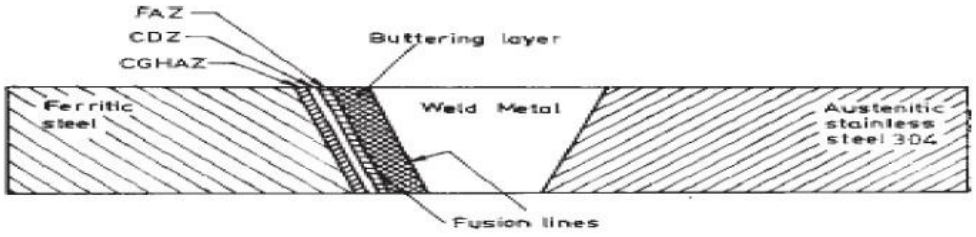

Fig. 2.2 Metallurgical discontinuities in Bimetallic welds (Chhibber, 2006) [27]

Welding of bimetallic welds is facilitated in the nuclear power plant to join stainless steel with ferritic steel (Buckthorpe, 1997) [19]. To join the bimetallic welds buttering is employed for the safety purpose. Coolant pipe that is of stainless steel is attached to ferritic steel of reactor vessel (Dennis, 2004) [39] (Harvey, 1969) [64]. Surge, spray lines are also connected with bimetallic weld joint with the nozzles. The most common material is of type 316 stainless steel is welded with type 308 stainless steel. For buttering of above dissimilar alloy SS 309 L buttering filler is used (Khan M.K., 2014) [83] . Metallurgical discontinuity depends upon the type of filler material and material used for buttering (ASM Handbook, 1993) [7]. Stress concentration occurs in welded joint due to the weld metal geometry (Bushboom, 1986) [23]. Mismatch effect in strength of weld plays an important role for the fatigue failure (Changheui, 2008) [25]. During thermal shock cycles of dissimilar weld metal there is a development of strain due to difference in coefficient of thermal expansion. Ferritic steel is generally softer and during post weld heat treatment the migration of carbon from the buttering layer to the matrix of ferritic steel and thus during heating and cooling strain produced is restrained by the harder and stronger, rich carbon zone in ferritic stainless steel material (Richard E book, 2001) [116] (ASME Boiler and Pressure Vessel Code, 2010) [115].

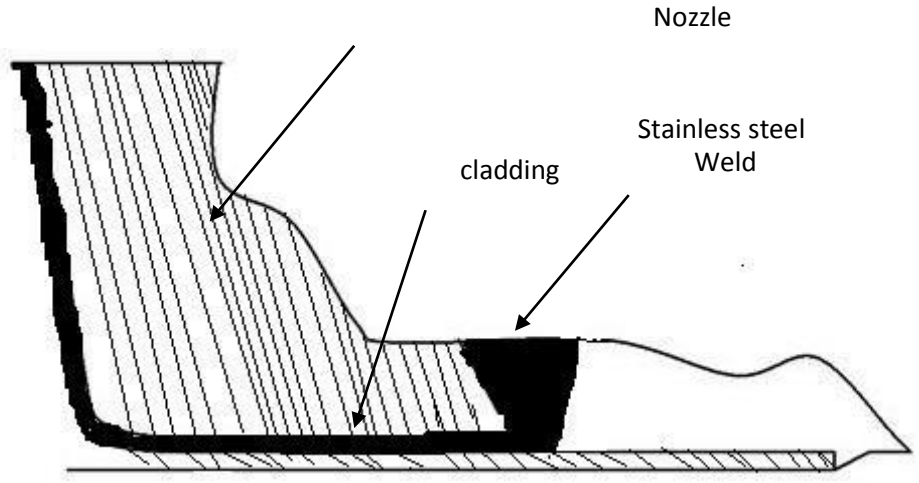

Fig. 2.3: Dissimilar metal weld

It is observed that due to difference in mechanical properties of base metal, weld metal and heat affect zone in similar weld metal results in crack initiation and propagation under thermal cyclic shock (Kadlec, 2012) [73] (Ginsztler, 1986) [60] (Kerezsi, 2001) [78].

During many elevated temperature applications for energy conversion systems, the use of bimetallic weld joints containing austenitic stainless steels and chromium–molybdenum ferritic steels is common (Sireesha, 2002) [124]. The early service failures owing to the number of start –up and shut down cycles during operation has been reported in the literature (Klueh, 1982) [86] (Elmer, 1982) [47] (Sudha, 2006) [127]. The role of the thermal stresses occurring due to temperature fluctuations and their effect on the degradation of the properties at the interfaces of these joints is highlighted in some of these studies.

2.6 Thermal Cycling in Nuclear Reactors

Thermal shock conditions are introduced in the nuclear reactors during rapid shut down of the reactor system. Due to large thickness materials involved and the temperature gradient the differential expansion and contraction conditions during thermal shocks lead to tensile thermal stresses resulting in incremental crack and leading to eventual cracking with increased number of shocks (Clayton, 1983) [32].

2.7 Effect of Thermal Cycling

The bimetallic weld joints are prone to frequent failures (Blumer, 1984) [16] and these failures are generally attributed to one or more of the following causes (Bhaduri, 1989) [14]:-

i. Thermal stresses induced in BMWs due to large difference in coefficients of thermal expansion (CTE).
ii. Residual stresses present in the BMWs.
iii. Martensite formation in BMWs.
iv. Carbon migration.
v. Preferential oxidation at the interface.

2.7.1 Thermal stresses

In the nuclear reactor system containing different component made with different materials and exposed to heavy variable mechanical and thermal shock loads during service lead to development of stresses which accumulate and may cause high level of stress concentration at certain regions leading to the formation of cracks (Abdulaliyev, 2007) [1].

2.7.2 Residual stresses

It is evident from the literature available that in the bimetallic welds the heat affected zone in the ferritic steel side or the region near the interface between ferritic steel and austenitic stainless steel is prone failure as high residual stresses are generated in this region due to the mismatch in thermal expansion coefficients of the two base metals.

Various researchers have investigated the fracture toughness degradation , generation of residual stresses and damage in base metals, HAZ region and weld region (Joseph, 2005) [71] (korolev, 1975) [87] (Kumar, 2015) [89].

2.7.3 Martensite formation

The formation of martensitic region in the partially mixed zone of the weld having a composition gradient from the ferritic interface to stainless steel side leads to development of sharp micro-structural and mechanical property gradients across the weld interface and is responsible for early service failure of bimetallic welds at higher operating temperatures (Dupont, 2007) [43] (Johansson, 1956) [70].
The use of Nickel-based filler metals prolong the life of austenitic-to ferritic dissimilar welds as it use produces a thinner martensite layer compared to stainless steel filler metals (Self, 1984) [119].

2.7.4 Carbon migration from the ferritic steel

The phenomenon of carbon migration occurs across the weld metal interface from ferritic steel to austenitic stainless steel in bimetallic welds during elevated temperature exposure. The elemental carbon diffusion across the bimetallic weld joint depends on the base metals and weld metal chemistry. The elemental carbon diffusion is caused by the decomposition of the carbide in the ferritic steels. Research efforts have been carried out by researchers to understand the carbon migration kinetics in bimetallic welds (Mitchell, 1978) [102].

2.7.5 Preferential stress-oxidation

The failure of the bimetallic weld joint is also caused by the preferential stress-oxidation at the weld metal/ferritic steel interface of bimetallic welds. The failure analysis revealed that an oxide-filled notch is generated on the outside diameter of the ferritic steel adjacent to the weld crown. The eventual failure is caused due to the propagation of the oxide notch through the tube-wall thickness (Bhaduri 1989 [14]).

2.8 Thermal Shock Failure Mechanisms

Thermal shock cycle consists of tensile and compressive stresses and corresponding strains are produced. During compressive part of the cycle the increase in temperature lowers the yield strength of material thus compressive strain becomes plastic under restricted distortion of specimen (Kerezsi, 2000) [79] (Buessem, 1955) [20].

On the other hand in tensile part of the cycle concentrated thermal stress is larger than the yield strength of the material and reversed plastic deformation occurs (Kerezsi) [80-81]. If the number of thermal shock cycle exceeded the limit then localized deformation cause a fatigue crack. Suppose a surface at lower temperature suddenly come in contact with hot fluid than surface tends to expand against the remaining material and developed compressive stresses (curve OQ in figure 2.1).

Further when subjected to rapid cooling surface shows tensile stresses (point 'S') and the core of material experience compressive stress shown in Fig. 2.1.

Thermal fatigue of steel in the temperature ranges from 25-300°C, results into precipitation of transition carbide. In steel with carbon content above 0.2% the phenomena is accompanied by increase in hardness, whereas steel with carbon percentage less than 0.2% , prefer to diffuse at the boundaries or at the dislocations sites during cooling, further no much carbon is left in solution to precipitate upon reheating.

Mechanism that is responsible to degradation of thermal fatigue life of welded joint is stress/ strain concentration within a joint due to the inelastic behaviour of heat affected zone (HAZ), base metal, and weld metal. Second is the strength variation within joint. As it is very well known that content of δ-ferrite is larger in weld metal than base metal. And last one is effect of notch due to strain concentration at the welded joint. Creep effect is not considered during thermal fatigue as the maximum temperature is 300°C and at this temperature no creep phenomena occurs.

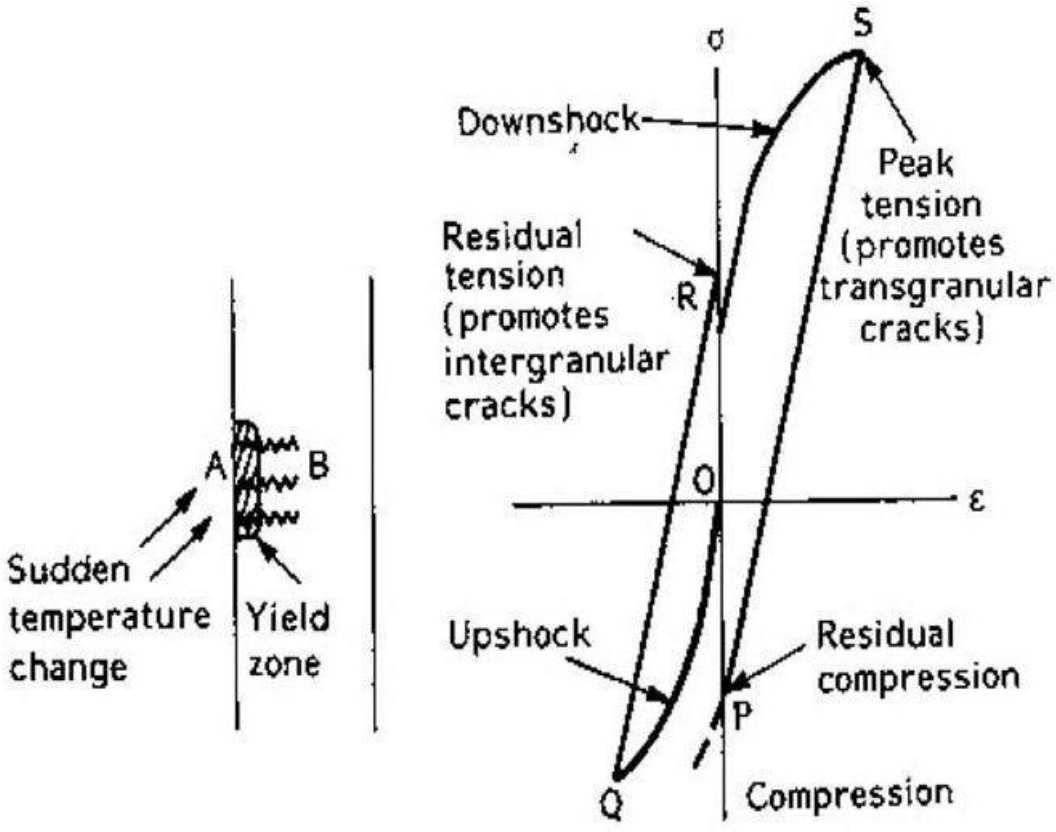

Fig. 2.4 Hysteresis Loop at the Surface of a Material Subjected to Cyclic Heating and Cooling

A brief background on the thermal fatigue research is presented here. Particularly the attempt is made on the general history of thermal fatigue research carried out by the various researchers.

2.9 Issues with Bimetallic Welds

The bimetallic welds made using ferritic or low alloy steel and austenitic stainless steel are considered to be a grave area of concern from issues arising due to the fabrication and structural integrity assessment challenges imposed by these joints.

Several researchers tried to explore the different facets to address the fabrication and structural integrity assessment issues engulfing the use of bimetallic welds. (Dupont, 2007) [43] (EO Correa) [48-50] (Klueh) [85-86] (Elmer, 1982) [47] (Abdulaliyev, 2007) [1] Agbadual, 2011) [2] (IAEA Report, 2003) [6] (Beres, 2003) [13] (Sireesha, 2002) [124].

The major challenge arrives from the different physical and chemical properties of the base metals, their different microstructures, different dilution characteristics, different element transfer mechanisms, and variation in process characteristics employed to join these metals and alloys.

The effect of thermal cycling further aggravates the problem by imposing additional thermal stresses during cycling to constrained geometries. The degradation of thermal power plant components is greatly dependent on the use of bimetallic welds. Various researchers have studied the degradation and failure of the welds and the base material components (Keim Elisabeth, 2012) [75] (Sudha, 2006) [127]. Researchers have also explored the use of different filler materials to investigate the failure of these welds under conditions of addition of different alloying elements (Self, 1984) [119] (Becker, 1967) [11] (Buni, 2004) [21]. The most of the failure investigations have been carried out for the ferritic heat affected zone and the use of a transition layer enriched in nickel and chromium content has also been explored (Bhaduri, 1999) [14] (Tucker, 1956) [133].

2.10 Factors Influencing Joint Integrity of Weld Metal.

The factors such as metallurgical zones, geometric defects, weld metal composition, weld metal dilution during fusion welding, phase transformations during heating affect the integrity of the weld joint. Researchers have worked on these issues for different combinations of bimetallic welds (Devaux, 2000) [41] (Kenneth, 1975) [77] (Eckel, 1964) [46] Christoffel, 1956) [29] (Yusufzai M.Z.K. 2012) [143] (Pham, 2013) [109]. The selection of filler material, the metallurgical behavior of weld alloy, its mechanical and physical properties, mutual solubility between metals in case of dissimilar metal welds, formation of intermetallic compounds at the interface and inside the weld microstructure are some of the major concerns while designing a weld joint (AWS Handbook, 1982) [3]. The role of different operating conditions such as elevated temperature, high humidity, corrosive environment are also the major concerns for the evaluation of the weld joint integrity. Repeated temperature cycling under harsh environments may require the weld to be designed in such a way to have high stress corrosion cracking resistance. The repeated expansion and contraction may result in developing the residual stresses in the weld and weld should be designed so that the residual stresses do not affect its performance and component integrity.

The concept of alloying addition and providing an interface layer so as to minimize the sharp transition in microstructures and properties along with elemental compositions by using the buttering layer facilitates the prolonged life of the weld joint as the buttering layer provides a barrier layer for carbon migration at elevated temperatures (Mitchell, 1978) [102] (Meyer, 2001) [101].

2.10.1 Welding Process Considerations

Literature is available where the process parameter optimization and modelling for different welding processes has been discussed (Fussel) [56,57], (Singh G.) [121,122]. Similarly for arc welding processes, flux modeling and optimization has also been a major area of investigation (Kumar, 2016) [90] (Pandey N.D., 1994) [107] (Yusufzai, 2012) [142].The three most popular arc welding processes utilized for Joining nuclear welds are SMAW, GMAW and GTAW.

The selection of the suitable welding process is one of the most important considerations for the fabrication of the bimetallic weld. The selection of the suitable welding process would be governed by the thickness of the base metals, the type of base metals, availability of suitable filler material and majorly the amount of dilution allowed from case to case basis.

The suitable process parameter selection only follows after the selection of suitable welding process. The welding process can be varied to obtain desired quality welds.

2.11 Residual Stresses

It is known from literature that tensile residual stresses are detrimental to structural integrity of materials. They increase the chances of crack formation and crack propagation in the material that results in damage of the material and hence a thorough mapping of residual stresses becomes a primary task (Murugan, 2001) [103] (Joseph, 2005) [71] (Brickstad, 1998) [18] (Gordon, 1966) [61] (Dean, 2006) [37].

The generation of residual stresses in the materials and their mapping techniques and classification have been too studied by various researchers (Murugan, 1996) [104] (Masubuchi, 1980) [100] (Hass, 1982) [62] (Kasatkin, 1981) [74].

Residual stresses adversely affect the service behavior of the structure. Their effect is subtle, far-reaching, and occasionally disastrous. Stress corrosion cracking

and hydrogen induced cracking of a weldment can occur without any external loading in the presence of residual stresses.

A significant detrimental effect of residual stresses is the intergranular stress corrosion cracking in austenitic stainless steel. In addition such stresses appear to accelerate all forms of corrosion. The tensile nature of residual stresses may cause brittle fracture.

The buckling strength of a material may decrease due to the initial distortion in the material and compressive residual stresses. Since in regions where both the residual and applied stresses are compressive they are additive, so that the critical applied load will be lower in the presence of such a residual stress system than that there were no residual stresses.

The fatigue behaviour of the welded assemblies is influenced by the residual stresses because the local stresses result from the superposition of welding residual stresses and of the variable stresses in service. When compressive residual stresses exist in regions near the surface of a plate, the fatigue strength may be increased.

Residual stresses are of yield-point magnitude at room temperature that would cause preferential creep, highly localized at the weld region, and in due course give rise to premature failure (Masubuchi, 1980) [100].

The fracture toughness of the brittle material reduces with increase in magnitude of residual stresses. The generation of residual stresses is also dependent on the nature of material. For ductile material the residual stresses do not affect much on its fracture strength as compared to brittle material. (birger, 1985) [15] (Lobanov, 1998) [96]. The residual stresses can also be useful and intentionally induced as into auto frettage. This process involves over straining the tube or pressure vessel, by application of high internal pressure. The material at the inner surface yields with the plastic deformation penetrating deeper and deeper into the cylinder wall as the pressure is increased. The compressive stresses thus induced increase the pressure that can be sustained by cylinder in service.

Major factors responsible for setting up of Residual Stresses:-

1. Qualities of the parent metal and filler rod or electrode,
2. Shape and size of weld,
3. Comparative weights of weld metal and parent metal,

4. Type of joint and method used in making weld (e.g. tacking, back-step sequence, etc.)
5. Heat input into the weldment i.e. on flame size in oxyacetylene welding; and current, electrode size and welding speed in arc welding.
6. Type of structure and neighbouring joints.
7. Expansion and contraction (free or constrained component).
8. Rate of cooling.
9. Stresses already present in the weld metal (Lobanov, 2005) [97].

2.11.1 Methods of Relieving or Controlling Welding Residual Stresses

Residual stresses are virtually elastic deformations which posses some potential energy accumulated in a body. The main feature of residual stress relieving is that they can be avoided only through metal plastic deformation. Where, how and when to develop deformation are important points of the problem.

The choice of residual stress relieving method greatly depends on the kind of residual stresses and its negative effect on the weld structure. Reducing welding Residual stresses consists, of the following possibilities:

(i) Decreasing the level of residual stresses, in particular the maximum tensile stress level,

(ii) Decreasing the zones with high residual stresses,

(iii) Decreasing the degree of multi-axiality of residual tensile stresses.

To achieve these aims the following methods are employed: (i) Design consideration (ii) Material consideration (iii) Heat treatment (iv) Mechanical stress relieving process (a) Shot peening (b) Hammer peening 11 (v) Vibration stress relief (vi) Explosive treatment.

2.11.2 Role of residual stresses in structural integrity assessment

The residual stress determination and mapping of welds is an important part of the structural integrity assessment procedures as it is known that tensile residual stresses are responsible for the degradation and failures in welds.

The knowledge of residual stresses and their treatment has become increasingly important in strength calculations particularly with respect to dealing with assurance of containment and damage assessment of structural parts where fatigue and fracture modes have to be considered Leggatt et al., 2008 [94].

Residual stresses in welds may in some cases reach yield stress and can result in a reduction in fatigue strength and premature failure of a structural part. (Chibber et. al) [27] [28].

2.12 Research Work by other Researchers in structural integrity assessment of bimetallic welds and in research domain of Thermal fatigue

From the literature of National Advisory Committee for Aeronautics Washington DC (1954), some researcher had worked on the topic. In the year 1949, Bradshaw, F. J. [17] worked on thermal stresses in Non-ductile materials. In 1955, Buessem [20] presented their work on the ring test and its applications to thermal shock problems. In 1952, Bentele, M and Lowthian, C. S [12] presented on the topic of thermal shock tests on gas turbine materials. Mechanism of failure of high Nickel-Alloy turbojet combustion liners was reported by Weeton and John W in 1949 [136].

The thermal shock resistance of metallized hollow ceramic cylinders quoted by Westbrook, J. H. in 1949 [137]. Cooper, A. L. at al. in 1951 [34] studied the elevated temperature properties of titanium carbide base ceramic containing nickel or iron. As seen the theory and industrial implications of thermal stresses in metals is an old and well established subject in engineering and it was not recognized as a field until the 1950s.

Dong, 1990 [42] investigated fracture prediction models and studied the effect of under/over matching joints on the accuracy of these models.

Hayashi, 1998 [65] performed thermal fatigue strength studies of 304 stainless steel in stimulated boiling water reactor environment.

Many researchers have stimulated the fatigue behaviour of various materials and structures (Janssens, 2009) [69], (Niffenegger, 1998) [105]. Also some of the researchers have done the mathematical modeling and numerical investigation of various process parameters involved in welding (Singh R., 2016) [123], (Ancelet, 2008) [4].

Research work by scientists like Manson and Coffin in the year 1954 [33] was carried out aimed at undertaking a complete investigation of the thermal fatigue phenomenon using both experimental and theoretical approaches and provide an initial framework further experimental and theoretical investigations in the 1970s.

The work during its initial phase was largely focused upon determination of the effect of temperature cycling on low cycle fatigue strength of materials (Reddy G.V.P., 2008) [114]. Shuji Taira, 1973 [120] performed studies on thermal fatigue and low cycle fatigue at elevated temperatures and developed a relationship between them.

J. P. Gauther and P. Peterson in the year 1989 [58] used the servo-hydraulic machines for experimental setup for determining the effects of high cycle random loading in austenitic stainless steels. In addition, fatigue at elevated temperature was performed by Howes MAH in 1973 [67] using the fluidized bed technique.

In addition to various test methods, the concentration was also carried out on identifying crack initiation for use in life prediction rather than monitoring the crack growth (Lloyd G.J., 1980) [95]. A British Scientist named White DJ in 1969 [138] contributed in the field by providing a more comprehensive review of investigations on thermal stresses and thermal fatigue.

With the development of Linear Elastic Fracture Mechanics (LEFM) approach in 1970s, it became more and more evident that the stress intensity factor (ΔK) was an acceptable parameter for modelling of the crack growth for small plastic strain values.

In light of this the objective of the thermal fatigue experimentation and theoretical investigations changed from determining lifetime predictions to identification of crack growth relationships with thermal fatigue correlating the effect of minimum and maximum temperature, strain range, mean strain and cycle shape on the stress intensity factor (ΔK). Rau et al. in 1973 [113] carried out crack growth investigations in turbine blade steels.

Pistorius PGH et al. in 1995 [110] worked on thermal fatigue of steel tires on urban railway systems. Several symposia also sponsored by ASTM have been held on the topic.

Wlliams, 2013 [139] developed a model for predicting the remaining fatigue life of welded joints.

Some other researchers (Takagaki, 2006) [130] have also worked to assess the fatigue damage while others have utilized experimental techniques such as induction heating Stanley Z. (1988) [126] to create experimental test rigs for research.

A very brief description for the work done in the area of thermal fatigue and structural integrity assessment of bimetallic welds by different researchers is presented as below:

[1] J. P. Gauther, P. Petrequin, (1989) [58], the effect of high cycle random loading at 330ºC and at 550ºC on the fatigue resistance of stainless steels type 316LN has been investigated.

[2] B. T. Timofeev et al.(1997) [132], the research article provides the fracture toughness test results of 15X2MFA steel (10 heats), 15X2MFAA steel (six heats) materials and their welds which are used in manufacture VVER-440 reactor pressure vessels

[3] Genki et al.(1997) [59], this research article describes some recent research activities on probabilistic fracture mechanics (PFM) to establish standard procedures for evaluating failure probabilities of nuclear Pressure vessel and piping performed by the Japan Atomic Energy Research Institute (JAERI).

[4] B. Kerezsi, A. G. Kotousov and J. W. H. Price (2000) [79], carried out experimental research work for development of an experimental test rig for investigating crack growth in pressure vessels and piping equipment under thermal fatigue conditions at laboratory scale.

[5] E. Visca et al. (2000) [135], carried out research activity aimed at defining a suitable method in order to qualify junctions between armour materials and heat sink of plasma facing components (PFCs) mock-ups in ITER.

[6] F. De. Backer et al.(2000) [8], carried out studies to evaluate micro-structural changes during fatigue loading. The work aimed at development of an assessment scheme for the evaluation of the residual lifetime of components.

[7] T. Hirose et al.(2000) [66], a new fatigue test machine with a laser extensometer for hot cell usage has been developed. Materials used in this work were Japanese reduced activation ferritic/ martensitic steel (RAFs), JLF-1 (Fe-9Cr-2W-V-Ta) and its weldment.

[8] A. Laukkanen et al. (2001) [92], studied the bimetallic welds and aimed at providing an assessment procedure by combining experimental and numerical fracture mechanics approaches.

[9] B. Kerezsi et al. (2002) [81], examined the use of ASME and British standard codes to estimate the growth of cracks driven mainly by thermal shocks. The

research article describes uses the techniques described in the ASME Boiler and Pressure Vessel code Section XI and British Standard BS7910 for the prediction of crack growth.

[10] Jin-Su Kim et al. (2002) [84], carried out , three-dimensional finite element analysis for various surface cracks to investigate the effect of clad thickness and crack geometry on the constraint effect by using the two-parameter characterization based on the J-integral and the Q-stress.

[11] B. K. Dutta, H. S. Kushwaha (2003) [45], addressed the nature of crack tip constraint conditions in axi-symmetric circumferentially flawed pipe (CFP).

[12] Tarafder, S., et al.(2003) [131], discussed the ductile tearing under constraint conditions of steel used in primary heat transporting piping in the nuclear reactors.

[13] J. W. H. Price et al. (2003) [111], presented an analysis of the thermal shock crack growth mechanisms involved, including an assessment of the environmental effects causing damage in pressurized components.

[14] Changheui Jang et al. (2003) [26], showed that the existence of the stainless cladding that had significant impacts on the RPV failure probabilities.

[15] Ramazan Kacar and Orhan Baylan, (2003) [72], has shown that different filler metals can be used to join austenitic stainless steel to the martensitic stainless steel.

[16] Karl-Heinz Schwalbe et al. (2003) [117], has tried to compare the assessment procedures and methodologies being adopted for fracture assessment.

[17] V. Maillot et al.(2004) [98], studied the stability of the crack networks obtained by thermal fatigue under isothermal load controlled four point bending fatigue test, and some conclusions were drawn on the mechanisms of propagating crack selection.

[18] J. M. Song et al. (2004) [125], this study investigated the tensile properties of spray- formed (SF) and ingot-cast (IC) high-Si aluminum alloys which suffered from cyclic heating/cooling.

[19] S. Marie et al.(2005) [99], worked on the development of a Stress Intensity Factors compendium for cracks in a Reactor Pressure Vessel (RPV) taking into account the cladding.

[20] B. K. Dutta, et al. (2005) [44], described that the structural integrity of components is usually performed using the specimen fracture resistance curve significantly differs from the component fracture resistance.

[21] Claud, E. et al. (2007) [31], In recent years, probabilistic analysis have been playing an increasing role in safety assessments for nuclear power plants (NPPs) in the USA. This paper includes a summary of results from several of those key assessment experiments.

[22] C. M. Lawrence Wu et al. (2006) [93], studied the thermal fatigue behaviour of SiCp/Al composite synthesized by infiltration of molten aluminium alloy into a perform of 65vol. % SiCp. for the crack propagation and fracture surface characteristics.

[23] Rahul Chhibber et al. (2006) [27], presented an effort towards identifying and understanding the problems affecting the BMWs and is well an attempt to highlight the current issues in the structural integrity assessment of structure having these welds.

[24] W. J. Evans et al. (2007) [140] utilized an induction heating/forced air cooling thermal cycle. The paper highlights experience in using this system for strain control TMF testing on INCO718.

[25] V. Firouzdor et al.(2007) [53], in this investigation, the effect of microstructural constituents on thermal fatigue resistance of A319 aluminium casting alloy was studied.

[26] A. Fissolo et al. (2008) [54], investigated the differences between uniaxial and thermal fatigue damage, tests have been carried out using the thermal fatigue devices SPLASH and FAT3D.

[27] N. Ranc et al.(2008) [112], this paper studies the thermal effects associated with the propagation of a fatigue crack in a gigacycle fatigue regime.

[28] E. Paffumi, et al. (2008) [106], the author has contributed towards the development of improved methods for assessing possible thermal fatigue damage in nuclear plant piping systems.

[29] M. Balbi, et al., (2008) [9], the kinetics of microcrack growth during cycling has been studied in a S3205 duplex stainless steel in the as-received and aged (100hr at 475^{o}) conditions

[30] Changheui Jang et al (2008) [25], prepared the dissimilar metal welds composed of low alloy steel, Inconel 82/182weld, and stainless steel by gas

tungsten arc welding and shielded metal arc welding techniques. Microstructures were observed using optical and electron microscopes. Typical dendrite structures were observed in Inconel 82/182 welds.

[31] M. Sireesha et al (2002) [124] discussed the evaluation of the bimetallic joint made using modified 9Cr–1Mo steel (Grade 91) and Alloy 800.

[32] A. Joseph et al (2005) [71] carried out failure analysis on a dissimilar weld joint and showed that a significant number of failures have occurred in the heat affected zone (HAZ) region on the ferritic steel side of such dissimilar weld joints.

[33] R. Foret et al (2006) [55] presented the results of a study of structural changes in laboratory welds of 6CrMo-V 8-3-2 (T25) and X12Cr-Mo-V-Nb 10-1 (P91) steels annealed at temperatures from 600° to 900°C(1112° to 1652°F).

[34] L. Béres et al. (2003) [13] in their paper describes the layered formation in the heterogeneous welded joint and reports on the investigation of the consequences of such diffusion. The principal goal of this investigation was to reduce the probability of cracking during service.

[35] A. Meyer et al (2001) [101] discusses the possibility that diffusion from the weld metal can increase the carbon or nitrogen content of the heat-affected zone, and consequently stabilize grain boundary austenite.

[36] D. J. Kotecki et al (1999) [88], discussed that the upper martensite boundary line from the Schaeffler diagram for stainless steel weld metals can be transposed to the WRC-1992 diagram. However, magnetic measurements and longitudinal face bend tests of weld metals do not show good correspondence to this boundary.

[37] R.L. Klueh et al (1983) [85] developed a simplified thermally accelerated test procedure for investigating failure of bimetallic welds between plain carbon steels and austenitic stainless steels.

[38] Burstown (1998) [22], investigated influence of constraint on crack tip stress fields in strength mismatch welded joints.

2.13 Gaps identified from the Literature Survey

After literature review it was found that some mathematical models for crack initiation and growth developed through thermal fatigue using finite element are available. The predictions of structural behaviour can be validated from these models.

Mechanical fatigue test data for resulting residual stress measurement in austenitic steel is available in literature but residual stresses developed in bimetallic welds are not available. Similarly tensile and fracture mechanical characterization of the different microstructural zones of the bimetallic welds are available, but the thermal fatigue behaviour was not covered on these weldments.

ASME and BSI codes for predicting crack growth is also reported though studies relating to thermal fatigue in composite materials, refractory materials, claddings and thermal barrier coatings etc. are also covered by the various researchers.

In view of above the followings are the gaps that can be summarized:

1. It is clearly evident from the literature survey that a comprehensive analysis of the problems surrounding the bimetallic welds is required. The thermal fatigue appears as one of the major problems in bimetallic welds. The current level of knowledge in this particular area of thermal fatigue is insufficient to undertake the task of fully resolving and accompanying the structural integrity assessment issues.
2. It is also observed that the focus of the contemporary research regarding the in-situ bimetallic weld behaviour in nuclear pressure vessel reactor has been mainly in the development of structure integrity assessment issues that can enhanced the life cycle of the bimetallic welds. However not much work has been reported in the area of thermal fatigue of bimetallic weldments.
3. As on date, no standardized and well documented single method or procedure exists to predict the structural integrity of such complex components as bimetallic welds. Hence, there is a need to investigate the complexities of thermal fatigue behaviour in terms of strength and metallurgical changes to the bimetallic weldment thoroughly.
4. The role of buttering layer also needs to be investigated for the residual stress mapping in the bimetallic welds.
5. The generation and role of residual stresses in the degradation of these welds at these high temperature variations has not been reported.
6. In the area of corrosion behavior of bimetallic welds under thermal fatigue conditions, much work has not been reported. Thus corrosion behavior of bimetallic welds needs to be examined under thermal fatigue conditions.

CHAPTER 3
PROBLEM FORMULATION

3.0 Overview

In this chapter, the need for the present research has been given based on the literature review carried out in Chapter 2 and the gaps identified. It covers the research objectives and the research plan.

3.1 Need for Research

- It is clearly evident from the literature survey that a comprehensive analysis of the problems surrounding the bimetallic welds is required. The thermal fatigue appears as one of the major problems in bimetallic welds. The current level of knowledge in this particular area of thermal fatigue is insufficient to undertake the task of fully resolving and accompanying the structural integrity assessment issues. It is also observed that the focus of the contemporary research regarding the in-situ bimetallic weld behaviour that not much work has been reported in the area of thermal fatigue of bimetallic weldments.
- As on date, no standardized and well documented single method or procedure exists to predict the structural integrity of such complex components as bimetallic welds. Hence, there is a need to investigate the complexities of thermal fatigue behaviour in terms of mechanical behavior that changes to the bimetallic weldment zones thoroughly.

3.2 Research Objectives

Based on the need of research as identified from literature review, the research proposal aims to:

- Design and fabrication of test rig for investigating of the thermal fatigue of bimetallic welds under laboratory conditions.
- To investigate thermal fatigue behaviour of bimetallic welds using above setup.

3.3 Research Plan

3.3.1 Fabrication of the bimetallic weld joints

The bimetallic welds between plain carbon steel SA516 grade 65 and austenitic stainless steel SS 304 L need to be fabricated using SS 309 L buttering layer and

SS 308 L weld filler as per standard welding procedure specification using Tungsten Inert Gas welding process.

3.3.2 Design of test rig for investigating the thermal fatigue behaviour

To simulate the thermal fatigue conditions in laboratory the design specifications of the test rig and its individual components need to be arrived at. The working test rig should be able to conduct repeatedly thermal shock tests on the specimens in the designed range. The temperature over time plots during heating and cooling cycles need to be recorded during the thermal shock tests.

3.3.3 Experimentation

The various design parameters (number of cycles, notch radius, temperature gradient during heating) need to be varied on the test rig to carry out different thermal fatigue tests. The thermal shock tests representing the variation of different process parameters would be carried out on specimen made from four different zones namely the weld zone , SS 304 L base material, SA 516 base material, ferritic heat affected zone.

3.3.4 Analysis of the mechanical behavior under thermal fatigue

The analysis of the mechanical behavior of the bimetallic weld specimen exposed to diff. thermal shock tests need to be carried out to see the response of each zone under thermal fatigue conditions.

The flow chart of the research plan being followed is shown in Figure 3.1. The successful completion of the research work would provide an insight into the thermal fatigue behaviour of bimetallic welds. The research would help to contribute towards generating the much needed useful data to analyse the mechanical behavior of the components using bimetallic welds subjected to repeated thermal shocks.

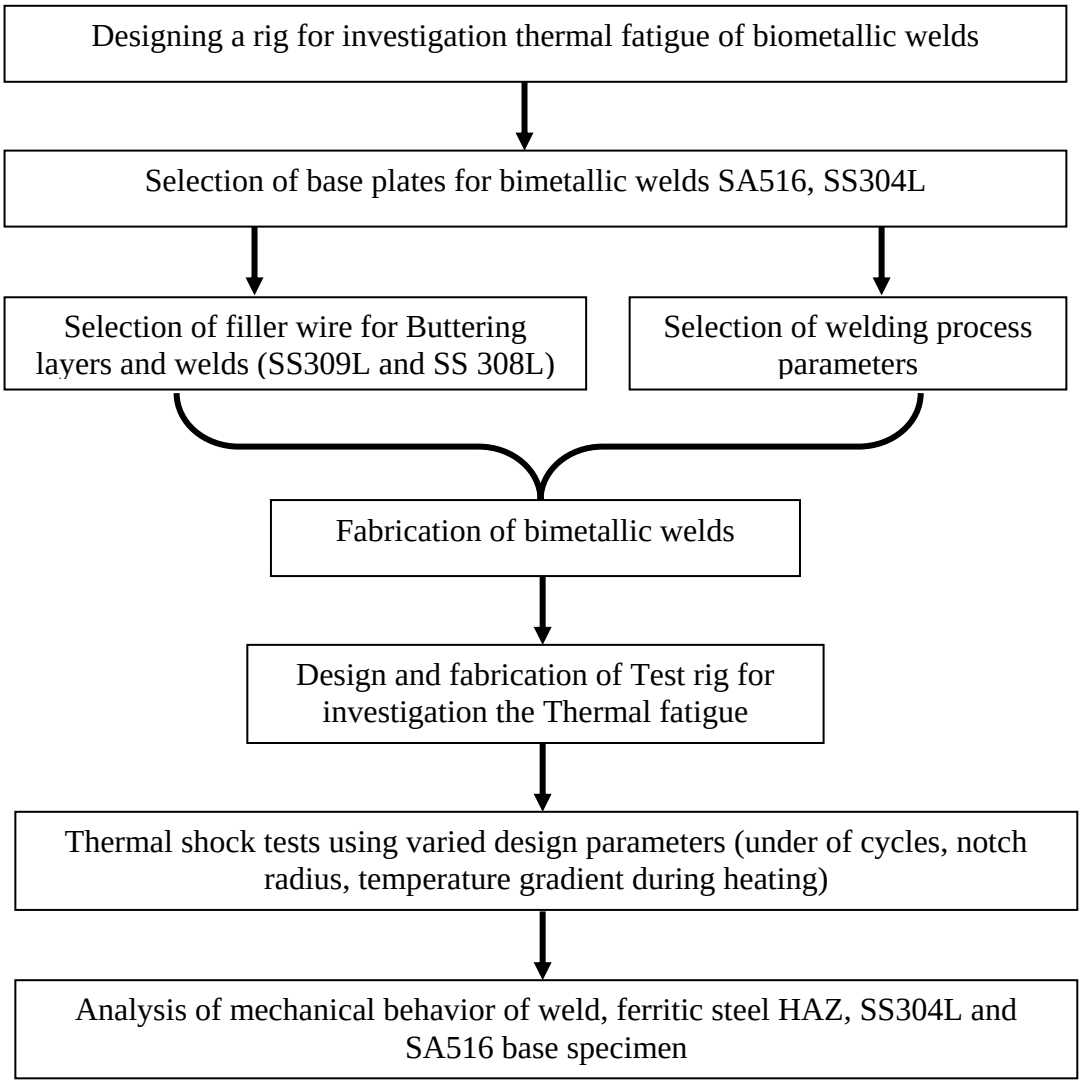

Fig. 3.1 Flow chart of research plan

CHAPTER 4
DESIGNING OF TEST RIG

4.0 Overview

To achieve the research objectives and to execute the research plan mentioned in Chapter 3, a Test Rig was designed to conduct Thermal Fatigue Testing of bimetallic welds by simulating the fatigue conditions at the laboratory scale. This chapter covers the details of design of various components of the test rig i.e. power and frequency selection for induction machine, cooling system, temperature measurement etc.

4.1. Induction Machine

In induction machine heating produced is by non-contact type method. It uses high frequency electricity to heat materials that are by this principle electrically conductive materials that can be heated using high frequency electricity. In this, heat is actually generated inside workpiece and it is a very efficient process. It can be compared with the other heating processes in which the heat is generated in a flame or heating Coil, same is then used to heat the workpiece. Based on the above discussion we can say that the Induction Heating lends itself to some unique applications in different industries. A basic induction heating type of system is shown in Fig. 4.1.

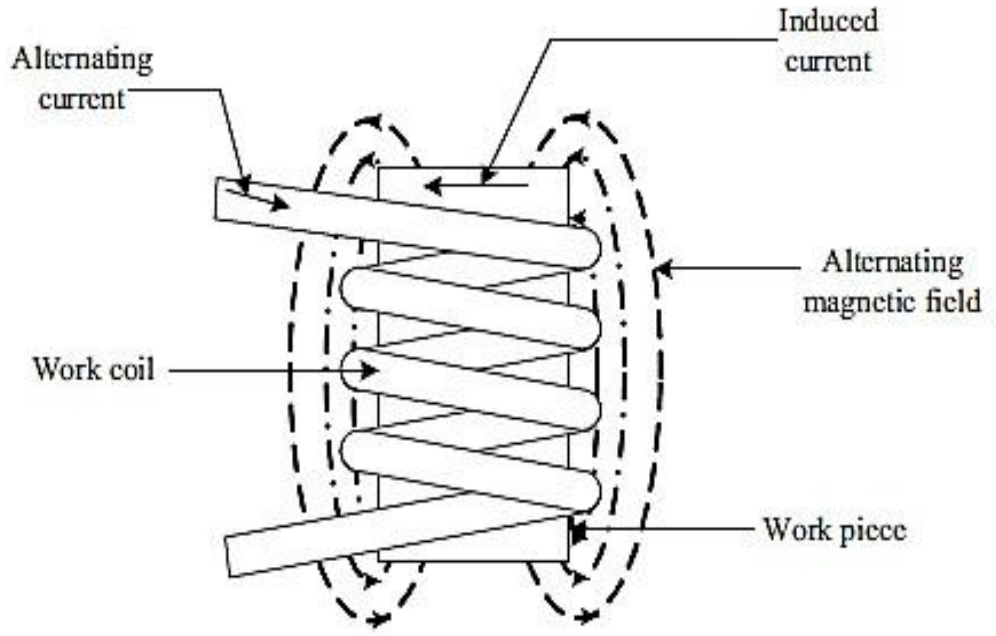

Fig.4.1. Basic Induction Type Heating System [126]

4.2 Principal of Induction Heating

A large AC current is passed through a coil from a high frequency electricity source. An intense and rapidly changing magnetic field in the space is generated within the work coil because of the passing of the current through this coil. The specimen under investigation is placed for heating within this magnetic field. The principal of induction heating is shown in Fig. 4.2. A current flow in the conductive work piece is induced because of this alternating magnetic field. The arrangement of the work coil and the work piece is thus obtained may be considered equivalent to an electrical transformer. Here, coil can be considered like the primary circuit where electrical energy is fed in, and the work piece is considered like a single turn secondary circuit. This circuit is short-circuited. The eddy current thus flows which causes tremendous currents to passes through the work piece.

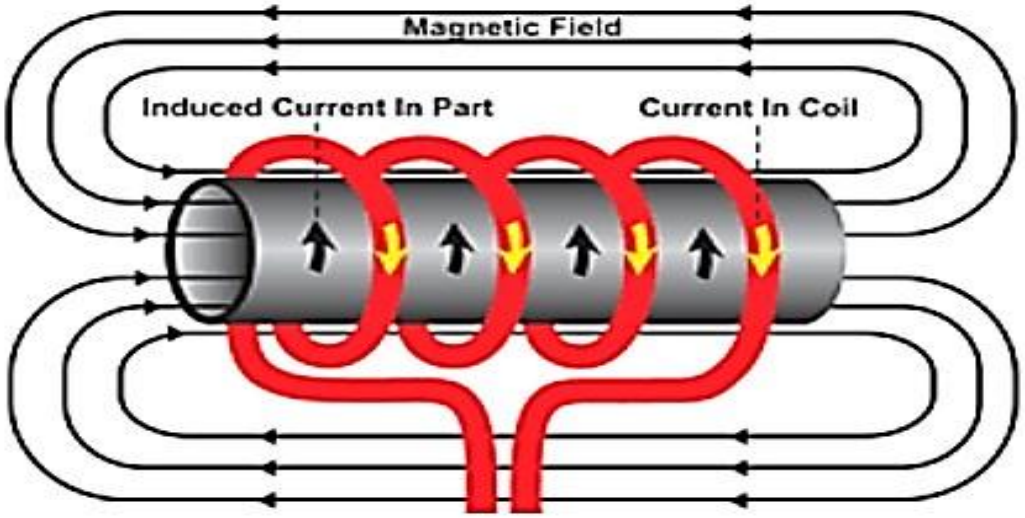

Fig.4.2. Eddy currents induced in work piece [116]

The essential things to implement induction heating are:

1. A source of electrical power with high frequency.
2. A work coil capable of producing the alternating magnetic field.
3. A workpiece which is electrically conductive.

Fig.4.3.Induction heating of 25 mm metal bars using 15 kW at 450 kHz.[116]

Fig. 4.3 is showing the actual induction heating of a cylindrical bar. Between the high frequency source and the work coil an impedance suitable network is usually needed so good power transfer is ensured. The water cooling systems are usually employed in induction heaters to remove waste heat from the work coil. Finally, to control the intensity of the heating action and time some control electronics is usually employed. The system is saved from being damaged by a number of unusual operating situations with the help of control electronics.

4.3 Design Procedures for Through Heating [116]

On the basis of total kilowatt hours of electricity expanded each year, through heating (without melting) is probably the largest single use of induction heating in the metals industry. The principal applications of induction through heating include heating prior to hot working and through heating for purposes of heat treatment.

4.3.1 Selection of Frequency for Through Heating

The selection of frequency for through heating is usually based solely on calculations of reference depth using the critical frequency as a guide line. For these simple geometries, the critical or minimum frequency f is therefore given by [116]

$$\left.\begin{aligned} f_c &= 1.6 \times 10^8\, \rho/\mu a^2 \qquad (a \text{ in in.}) \\ f_c &= 4 \times 10^8\, \rho/\mu a^2 \qquad (a \text{ in cm}) \end{aligned}\right\} \text{Round bar}$$

where a is bar diameter

The critical frequency expressions are function of material resistivity and geometry for which μ = 1. The selection of frequency as per diameter is shown in the Fig. 4.4.

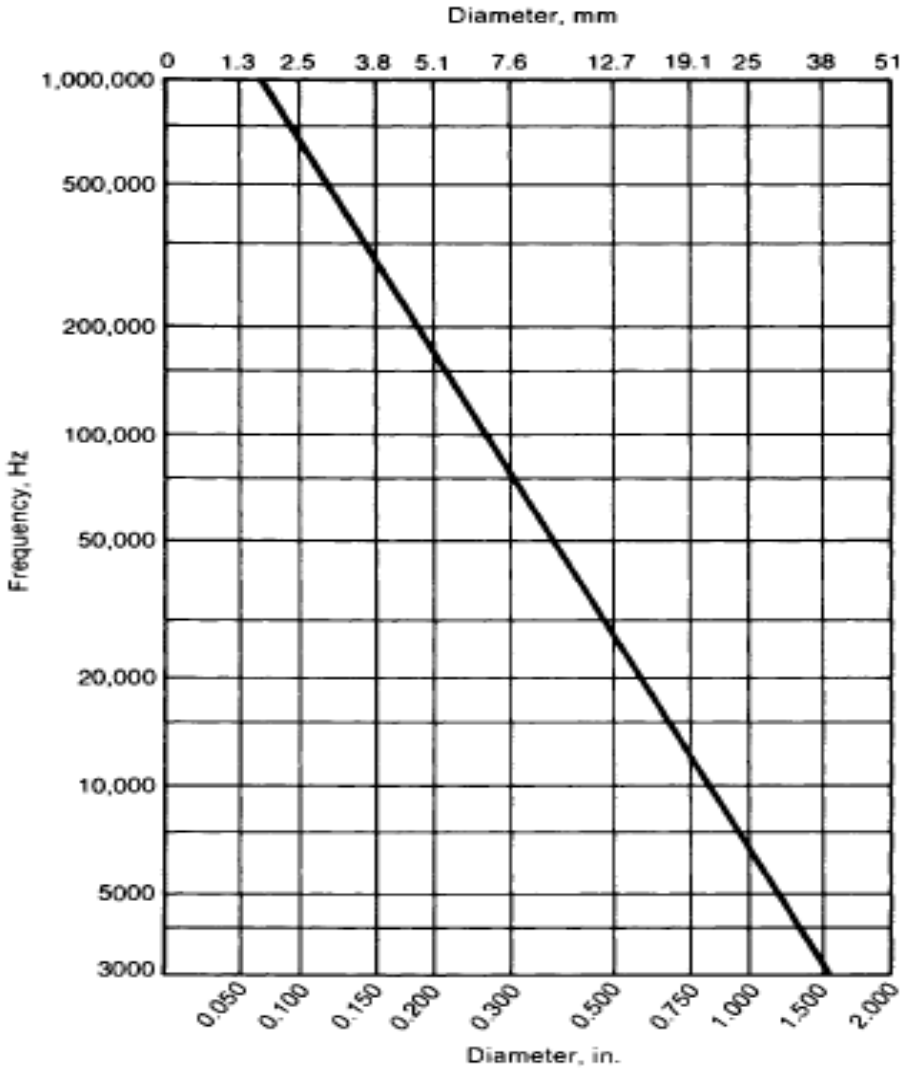

Fig.4.4. Relationship between diameter of round steel bars and minimum generator frequency for efficient austenitizing using induction heating [116]

4.3.2 Selection of Power Rating for Through Heating

During selection of power rating for induction through heating, two factors- material throughput and required temperature uniformity should be evaluated. The first of these, material throughput, determines the over-all power rating because:

Required power = (kilograms/hour throughput) x (kilowatt hours/kilogram)
x (efficiency factor)

The factor kilowatt hours/kilogram is known as the heat content; it is the amount of thermal energy required to heat a given material usually from room temperature to a higher, specified temperature.

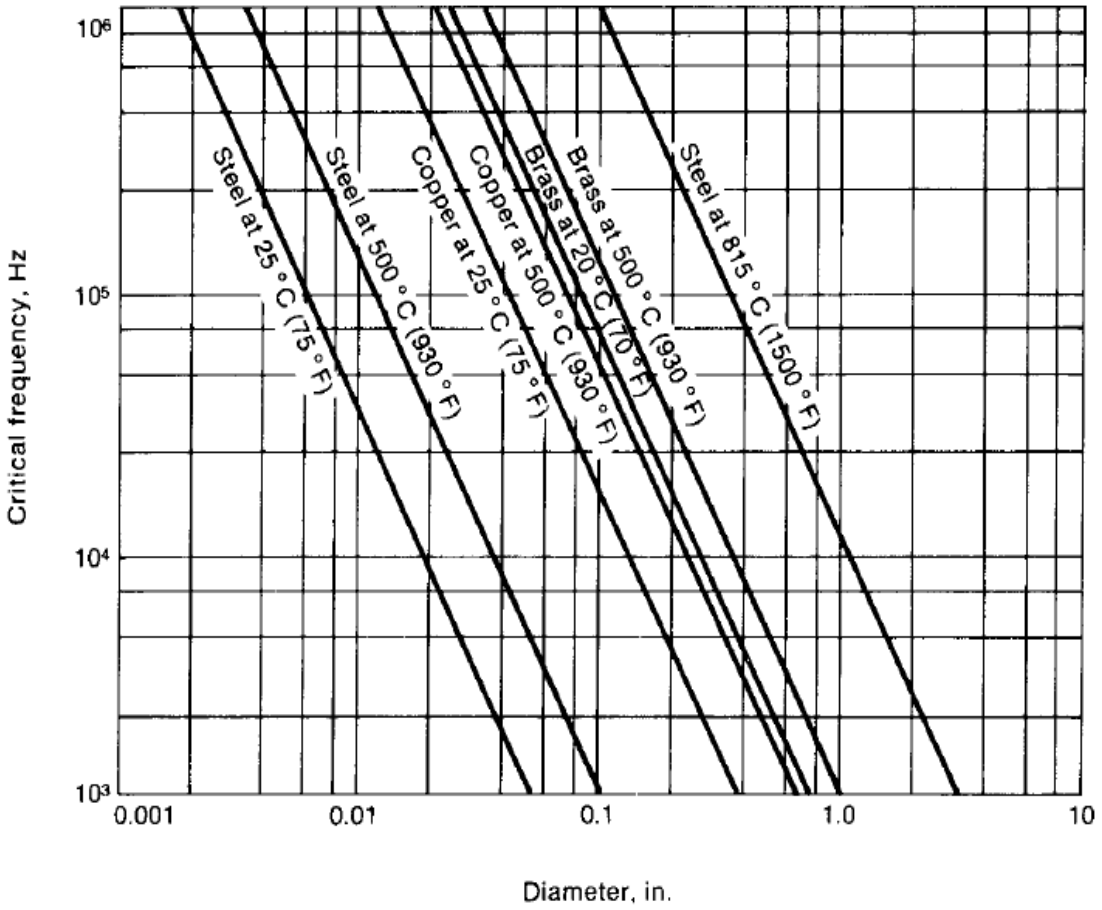

Fig.4.5.Critical frequency for efficient induction heating of several materials.[116]

The power density at the induction coil is the metered output power divided by the amount of work piece surface within the induction coil and is expressed in kW/cm^2. Selection of power and frequency both are equally important. The total power required is equal to the losses in the system and the heat required for work piece.

With the help of the cross-sectional size and the weight of steel to be heated per hour one can define heating systems. Lower power densities and frequencies are used for thorough heating because the work pieces need to have the heat soak and penetrate to the core. Higher productivity is obtained from using more power heating and from heating more work piece area at the same time, thereby not increasing the power density. Higher power densities provide the ability to heat

surfaces more rapidly. However, there may be limitations to the amount of power that an individual induction coil can handle.

Table 4.1 Typical system losses for different induction power supplies

Power supply	Frequency	Terminal Efficiency %	Output Transformer Efficiency %	Coil Efficiency %	System Efficiency %
Solid State	10 kHz	90	75	75	51
Radio	450 kHz	65	60	85	33

The heat content to heat the sample is theoretically selected based on the Fig. 4.6.

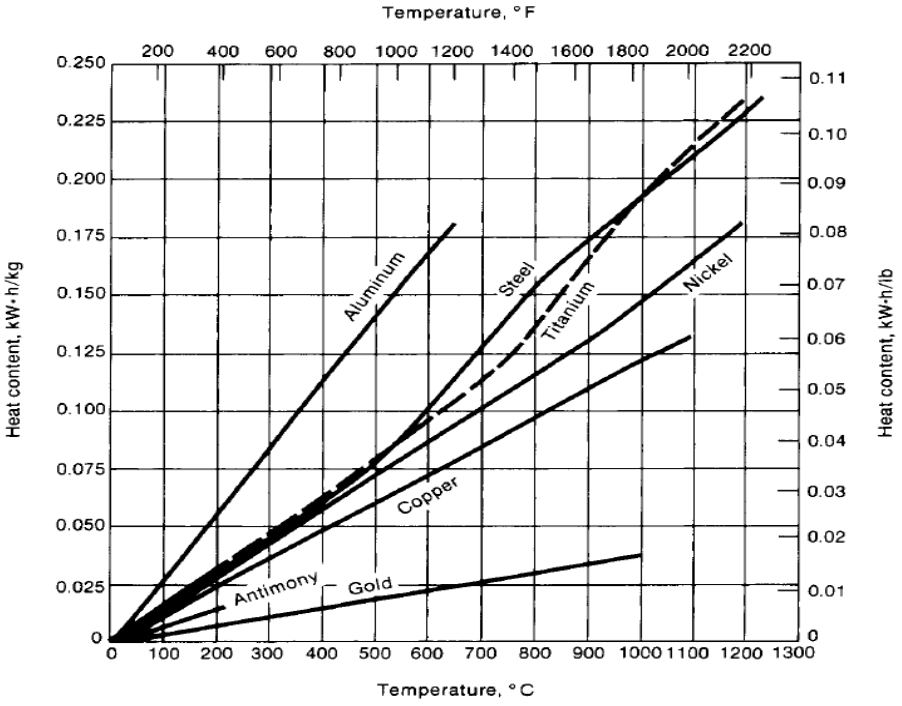

Fig.4.6 Change in specific heat with temperature for materials. [116]

For through-heating applications, the power density should be kept relatively low to allow conduction from the outer layers (which are heated more rapidly by higher current densities) to the inner layers. There will always be a temperature gradient, but this can be minimized by careful selection of induction heating parameters. Neglecting the temperature gradient, the absorbed power depends on the required temperature rise ΔT, the total weight to be heated per unit time W, and the specific heat of the material C. The power P to be supplied to the load is then given by

$$\mathbf{P = W\ C\ \Delta T}$$

To determine the total input power needed from the power source which supplies AC current to the induction coil, the power lost from the work piece due to radiation and convection and the loss in the coil itself due to Joule heating must be added to P. Heat loss by convection is usually small and is neglected in calculations of power requirements for typical rapid-heating applications.

Power losses are of three forms:

- Coupling losses between the coil and the work piece. The percentage of the power supplied to the coil that is transferred to the work piece is a function of the resistivity and permeability of the work piece material, the coil geometry, and the distance between the work piece and the coil.
- Power losses between the output terminals of the power supply and the coil.
- These losses are associated with improper tuning and I^2R losses in the appropriate tank circuit, imperfect impedance matching between the power supply and the work piece/induction coil, and transmission losses between the power supply and the induction coil.
- Power losses within the power supply due to conversion of line frequency to higher-frequency AC.

4.3.3 Hysteresis

Hysteresis losses occur only in magnetic materials such as steel, nickel and a few other metals.

4.3.4 Skin Effect

In induction heating, as the frequency of the heating current tends to concentrate close to the metal surface (work piece).This is referred to as the skin effect. The skin effect is the phenomenon in which electric current flows only in the limited area near surface of conductive material and proximity effect is the phenomenon, which the primary current in the inductor and the secondary current in the conductive material pull each other because the direction of current is opposite direction to each other and flows in the limited area near surface where distance is smallest to each other. The depth depends upon the frequency and as the frequency is higher, the depth becomes smaller [116].

$$\delta = \frac{1}{\sqrt{\pi f \mu \sigma}} (m)$$

μ = specific permeability
f = frequency, Hz

Penetration depth (m)

The reference depth decreases with higher frequency and increase with higher temperature.

4.3.5 Conduction of Heat in Sample

Conduction is the prime phenomenon of heat transfer in the interior of a work piece which is produced by the eddy currents on the surface. Hysteresis produces a secondary effect and is a small producer of heat. Losses due to hysteresis are usually ignored in the heat content calculations for induction processing because of the minor effect. The standard values of SA 516 G70 and SS 304L are shown in table 4.2 and 4.3:-

Table 4.2 Specifications of SA 516 G70

Specification	**Value**	**Unit**
Resistivity	0.0000170	Ohm-cm
Specific heat	0.47	J/g-°C
Melting temperature	1450	°C
Density	7.8	g/cc
Thermal conductivity	52	W/m-K

Table 4.3 Specifications of SS 304L

Specification	**Value**	**Unit**
Resistivity	0.000072-0.00010	Ohm-cm
Specific heat	0.5	J/g-°C
Melting temperature	1400-1450	°C
Density	8	g/cc
Thermal conductivity	18	W/m-K

4.4 Induction Coils

The coil, also known as inductor or induction work coil, is basically a transformer that primarily induces high frequency output of an induction power supply into a work piece, which is effectively the transformer secondary. Coil design is application specific, so the type of coil to be used should be selected before designing fixture.

Coil design considerations for efficiency and use include:

- The coil should be coupled as close to the work piece as possible.
- The leads into the coils must be designed for the best efficiency.
- The coils must be designed so that they are rigid and do not move when power is applied.
- The coils must be designed so that they do not overheat during use and do not develop stress fractures during use. As a rule, lower frequency coils generally operate with higher power inputs, so they require more rigidity and better cooling.
- All coils have significant power losses and need good cooling. Separate high-pressure cooling systems may be necessary for high-power applications.
- The coil must be designed so that the magnetic flux lines produce eddy currents that heat the desired areas. The highest concentration of flux lines is inside the coil, producing the maximum heating rate there.
- Coils can be made with different contours and shapes or can be made with more than one turn.
- Radio frequency (RF) coils need closer coupling and concentricity around workpieces than the lower frequencies.
- Flux concentrators are used to increase coil efficiency or to concentrate the flux to specific areas in the work piece.

4.5 Temperature Measurement

There are various methods of monitoring temperatures during induction heating. The most common techniques make use of thermocouples and radiation detectors. Despite the widespread use of each method, several major problems should be considered before a final selection is made. These include problems of poor work piece surface condition, contact resistance and response time for thermocouples.

Thermocouples

- The temperature of the heated junction is determined by measuring the voltage and referring to calibration tables for the particular thermocouple materials. Thermocouples are of two basic types: contact and noncontact (or proximity).

Contact Thermocouple

- This procedure is impractical for measuring work piece temperatures in most induction heating processes because of the presence of an induction coil (single-shot and scanning applications) or the fact that the part is moving through the coil (scanning methods of induction heating). For this reason, contact thermocouples are normally used during initial trials to set up a particular process.

Non-contact (Proximity) Thermocouples

- To overcome the difficulties associated with scale formation, proximity thermocouples are often utilized. In this type of device, the thermocouple junction is attached to a disk of stainless steel or other high-temperature alloy. The standard values of Coil Material are shown in Table 4.4.

Table 4.4 Specifications of Coil Material

Specification	Value	Unit
Resistivity	$1.7x10^{-8}$ (at 293K)	Ohm-m
Density	7.86	g/cc
Thermal conductivity	350	W/m-K
Permeability	1	Hm
Diameter of coil	4	mm
Length of coil	800	mm

Resistance of conduction coil (R): $R = \rho L/A$

$R = 0.00182$ ohm

4.6 Design Calculations

The calculations for the designing of power supply, frequency, cooling required and thermocouple are given below-

Weight of Specimen

$W = \rho * V$ $V = \pi r^2 I$

$W_w = 0.12$ Kg $= 120$ g $t_R = 25^0C$ $t_{max} = 283^0C$

$C_{SS} = 0.5$ J/g-°C

Energy required for heating the sample to 283^0C

Q = m c dT

Q= 120 x 0.5 x (283-25) Q = 15480 J

Q= 15.48 KJ We need to heat the sample in min. 15 sec.

So max. Heat rate required = 15.48/15 = 1.032 kW

Power Rating

Maximum heating time = 30 sec. Minimum heating time = 15 sec.

From Heat Content Vs Temp. Graph for 300^0C temperature

Required Heat Content = 0.05 kWh/Kg

Number of Cycles per hour (for max. heat rate) = 3600/15

= 240 cycles/hr. Material processed per hour

= 240 x 0.12 kg

= 28.8 kg

Power = (kg/hr) * (kWh/kg)/Efficiency

- The efficiency is assumed to be 0.5 based on the various loses of heat in the coil and other losses.

Power = 28.8 x 0.05/0.5 = 2.88 KW

So we assumed the minimum power required for heating is 3 kW.

Current Requirement

Power (P) = I^2R

3000 = I^2 x 0.00152

I = 1283 A

Cooling Water Requirements:

Cooling water is required because all of the electrical energy consumed is essentially transferred in the form of heat to the cooling water. Except for small radiation losses and residual heat left after quenching, even the heat produced in the workpiece is absorbed by the quenchant, which in turn is cooled through a heat exchanger.

- Inlet temperature of water = 25^0C
- Outlet temperature of water = 55^0C

The following fig. 4.7 [(a) to (c)] are showing the basic schematic of water circulating system.

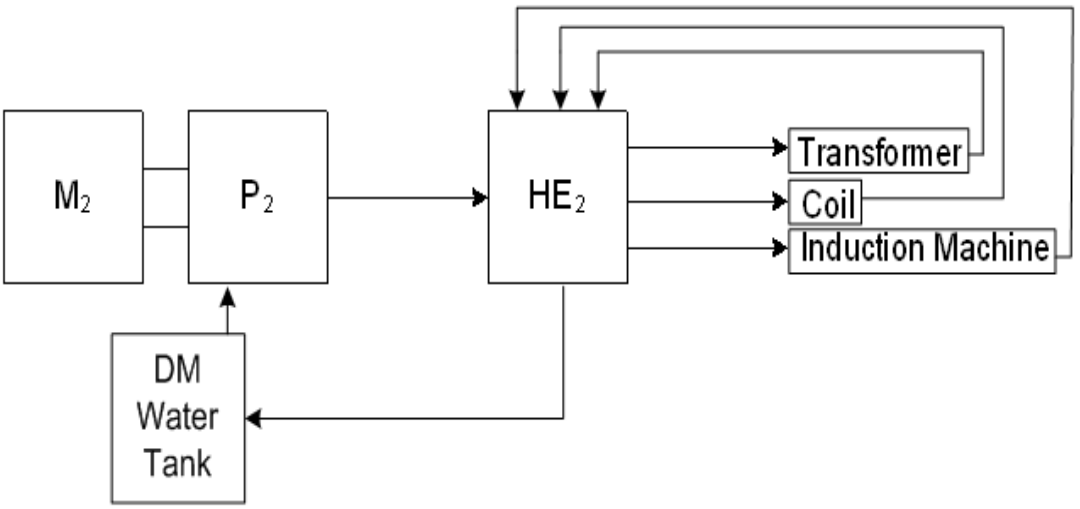

(a)

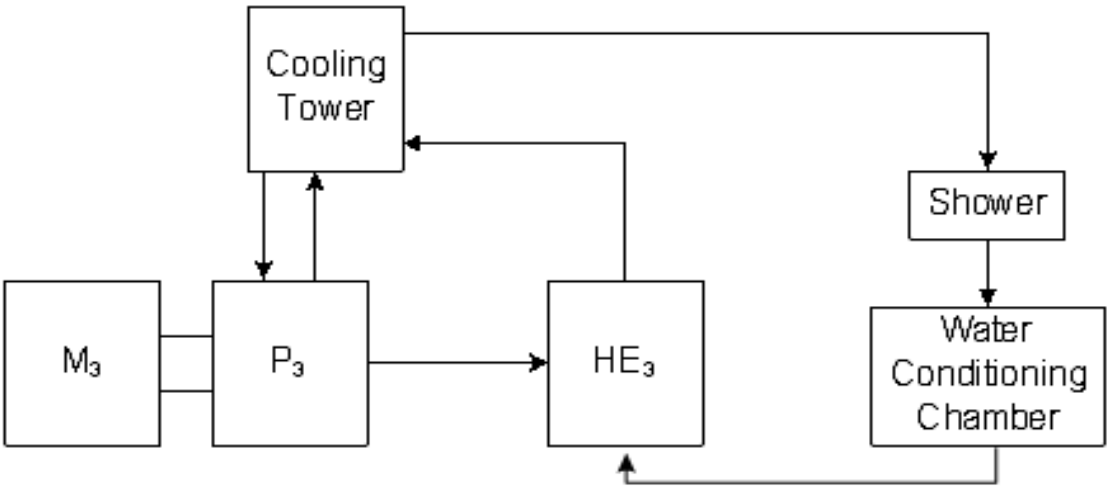

(b)

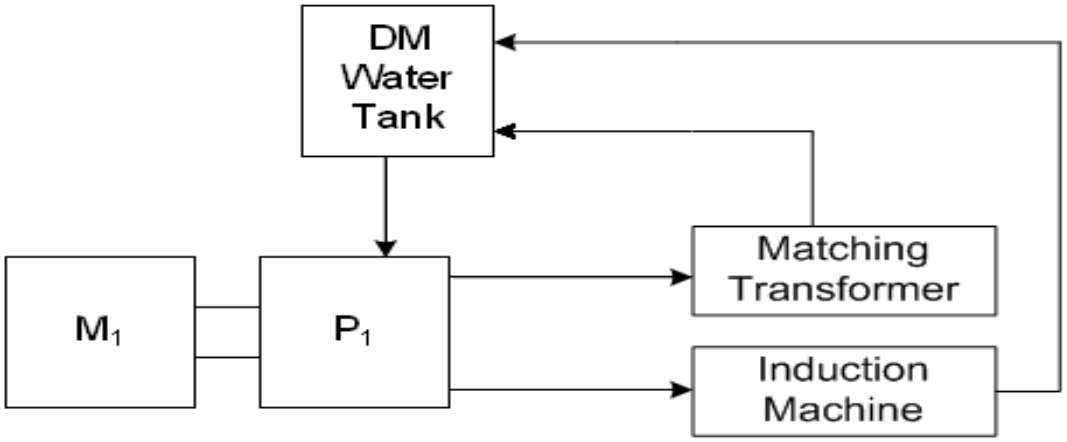

(c)

Fig.4.7 (a) to (c) Schematic of the water circulation in the system

From heat balance equation: Heat loss = Heat gain

Heat loss = Heat released by the sample

Heat gain = Heat absorbed by water

Heat loss = 15.48 KJ in 15 sec.

Required Cooling Rate = 15.48/10 =1.548 or 1.6 KW Flow Rate Required:

Heat gain = m x C_{water}x ΔT

$\Delta T = T_{in} - T_{out}$ Where m is in Kg/sec and C_{water} = 4.18 KJ/Kg-K $T_{in} = 25^0C = 298^0K$

$T_{out} = 55^0C = 328^0K$ Now from heat balance equation

$1.6 KW = m \times 4.18 \times 10^3 \times (328-298)$

m = 0.0128 Kg/sec.

Now Volume flow rate q = m /ρ

q = 0.0128/1000

$= 1.2 \times 10^{-5}$ m^3/sec q = 43.2 ltr/hr

Let q = 50 ltr/hr

4.7 Fabrication of the Test Rig

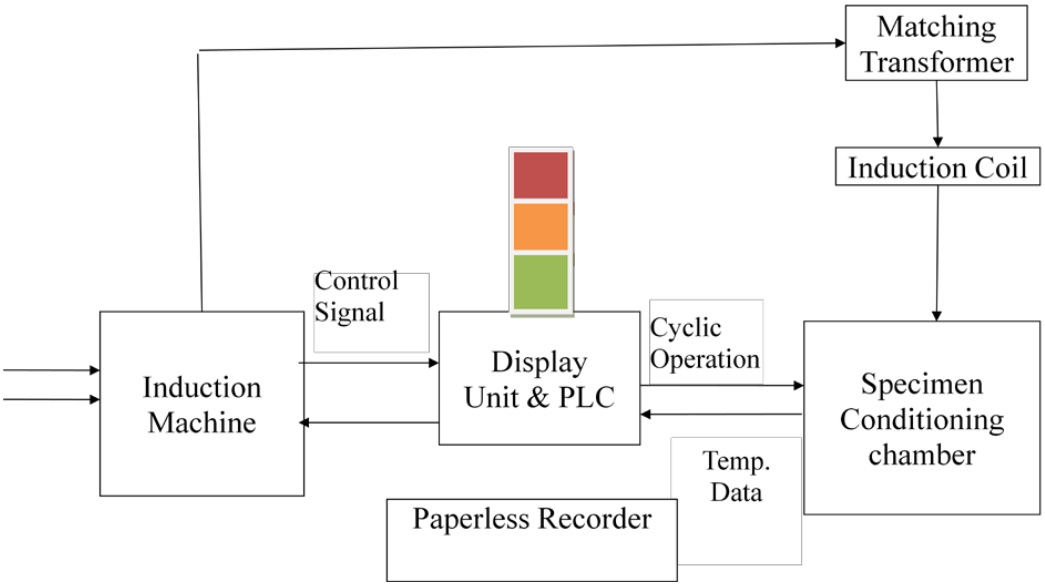

Fig.4.8 Schematic arrangement of developed thermal fatigue test rig

- Induction heating is the most clean, efficient, cost-effective, precise, and repeatable method of material heating available to the industry. Therefore, a test rig has been fabricated to analyze thermal fatigue effects using induction heating and water quenching arrangements. The schematic of the designed test rig is given in fig. 4.8.

The fabricated test rig has the following features:

- The specimen is heated by induction process so that specimen is homogeneously heated without any temperature gradient and the specimen is effectively cooled through a spray arrangement.
- The temperature is sensed by non-contact type IR sensor.
- There is a feedback system for auto heating on/off and cooling on/off when the set values of maximum and minimum temperature are reached.
- There is a counter for measuring number of cycles.
- Digital time and temperature paperless recording system.

4.7.1 Components of Test Rig

The Fig. 4.9 shows the various essential components of the designed test rig.

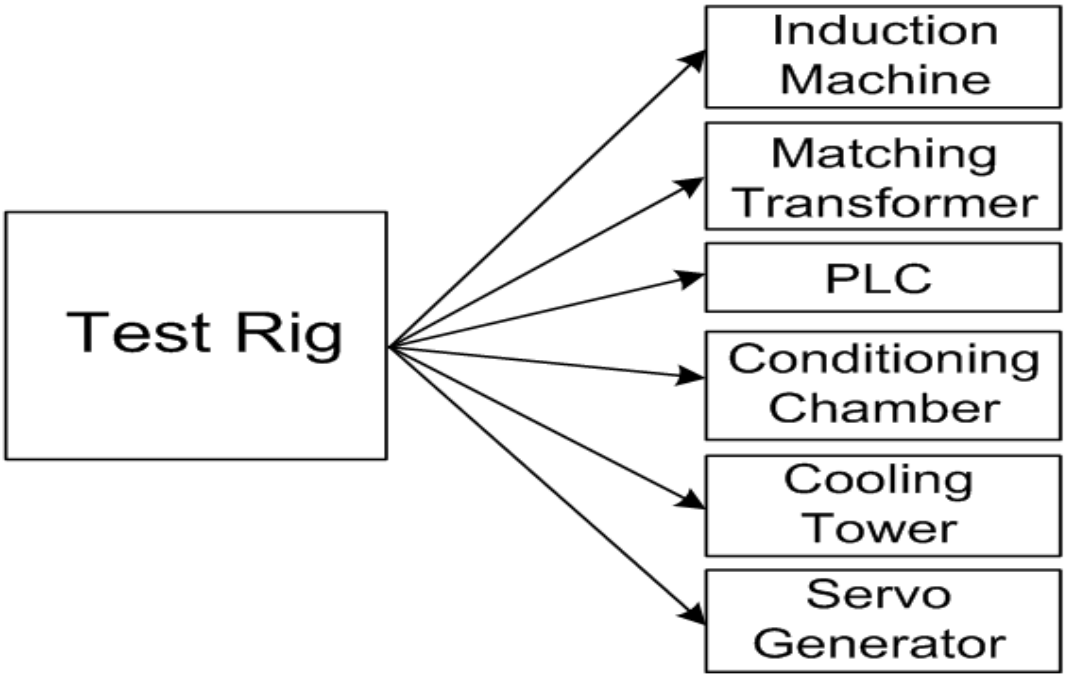

Fig. 4.9 Components of Test Rig

4.7.2 Different Views of Test Rig

The fig. 4.10 showing the different parts of the Test Rig designed.

Fig. 4.10 Overview of the Thermal Fatigue Test Rig

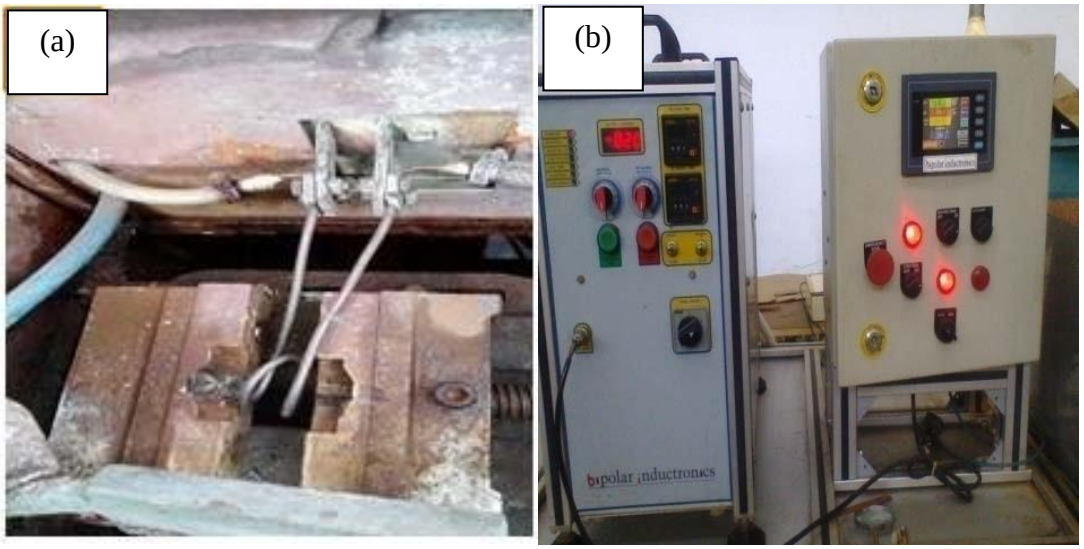

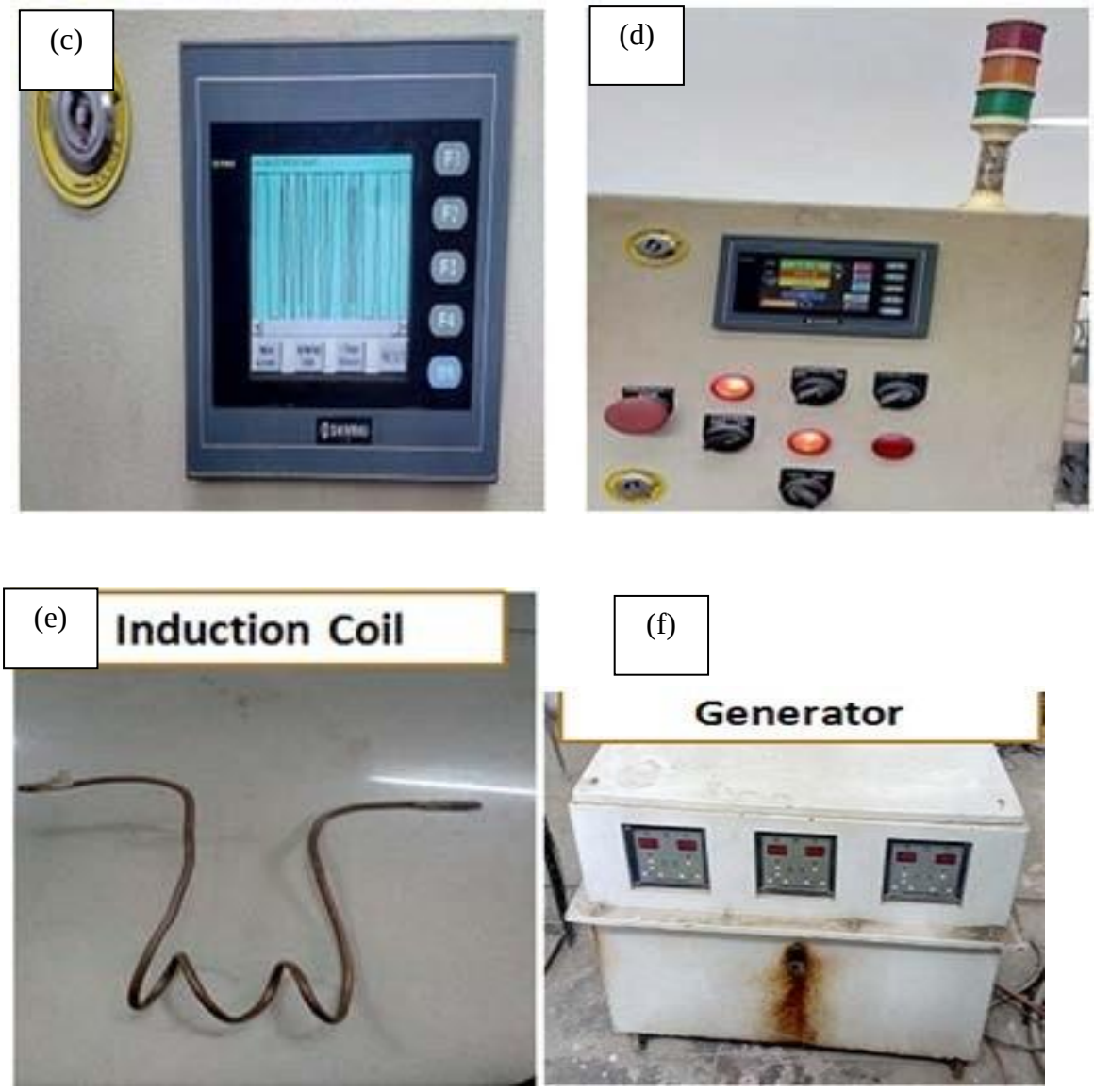

Fig.4.11. (a) Control Panel, (b) Sample heating location with Coil, (c), (d) Control Panel, (e) Copper Coil and (f) Generator.

4.8 Sample Heating

The Time Vs Temperature plots obtained during the heating and cooling cycles are given in Fig. 12 and Fig. 13. The temperature range kept was 283^0C – 25^0C. Cooling time was kept constant for all experiments. The total cycle time is 25 sec or 40 sec as shown in Fig 4.12 and Fig 4.13.

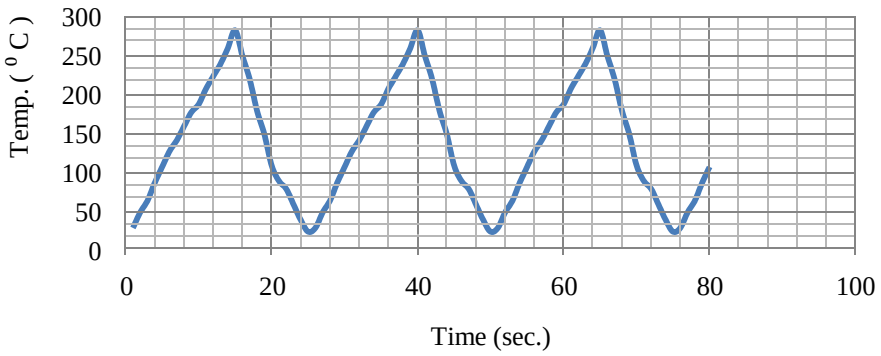

Fig.4.12.Temperature Vs Time profile with 15 sec. heating time followed by 10 sec. cooling time

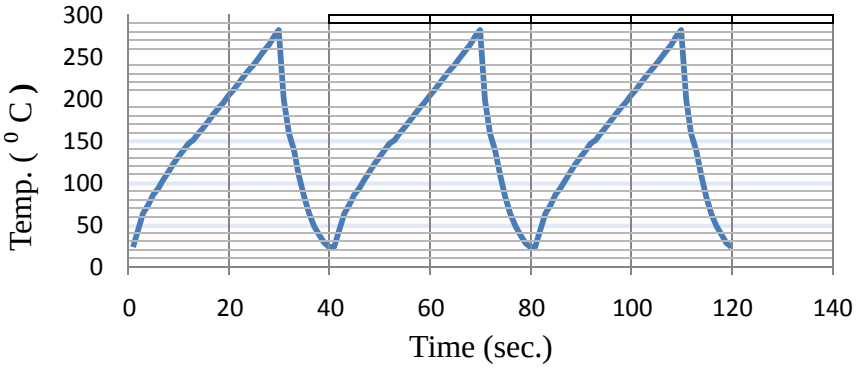

Fig. 4.13.Temperature Vs Time profile with 30 sec. heating time followed by 10 sec. cooling time

As per the details given above, the design of various components and power requirements, a test rig for thermal fatigue testing was got fabricated and installed. Trial runs were made on this test rig and it was found the rig is fit to carry out detailed experimental work to meet the research objectives.

CHAPTER 5
EXPERIMENTAL WORK

5.0 Overview

The present chapter discusses details about the experimental work carried out with the help of this designed test rig (design details mentioned in Chapter 4). This chapter covers experimental scheme, selection of base materials and buttering/filler materials, selection of groove design and preparation, selection of welding process and welding process parameters, selection of buttering layer thickness, specimen preparation, thermal fatigue parameters and measurement of residual stresses.

5.1 Experimental Scheme

Thermal fatigue tests were carried out on the test specimens under controlled thermal fatigue conditions. The thermal fatigue parameters were selected as close to actual industrial situation. The thermal fatigue parameters selected were Heating Time (HT), Notch Radius (NR) and Number of Thermal Shock Cycles (NOC). These factors were considered as three variable factors.

Among these variables, the two variables i.e. Heating Time (HT), Notch Radius (NR) were selected in terms of minimum and maximum values. Thermal fatigue tests were conducted on the four types of specimens having notch in weld metal, ferritic HAZ, SA516 Gr 70 and SS304L. The evolution of thermal fatigue specimens were monitored in terms of weld strength and individual base metals strength. The weld strength was evaluated through ultimate tensile strength, yield strength, percentage elongation and hardness. The studies were carried out for specimens without thermal fatigue and with thermal fatigue. The number of thermal shock cycles given was 500, 1000, 1500 and 3000 cycles. The residual stresses were measured for welded plates to select the thickness of buttering layer.

5.2 Base Materials Selection

The base materials used were austenitic stainless steel plates SS 304 L and plain carbon steel SA516 Gr70 plates. The SS 304L plates were received on complementary basis from Jindal Steels Limited, Hisar and SA 516 Gr70 plates were received from Steel Authority of India Limited. Table 5.1 gives the chemical compositions of the materials used. The chemical composition was determined by Spectro Lab, Delhi.

Table5.1 (a) Chemical composition of Ferritic steel SA 516 grade 70

C	Si	Mn	S	P	Cr	Mo	Fe
0.216	0.238	1.14	0.021	0.022	0.015	0.012	98.28

Table 5.1 (b) Chemical composition of austenitic stainless steel SS 304 L

C	Si	Mn	P	Ni	Cr	Mo	Fe	V
0.014	0.177	1.69	0.023	8.40	18.5	0.147	70.70	0.042

5.3 Filler Metal Selection

Selection of a suitable filler metal is an important factor to produce a sound bimetallic weldment, the selection a suitable filler metal plays a significant role. Here one of objectives is to minimize undesirable metallurgical interactions between the metals. Thus, it is necessary that the filler metal should be compatible with both base metals and be capable of being deposited with a minimum of dilution.

Thus, for welding two dissimilar metals, the following two important criteria for selection of a proper filler metal must be kept in mind:

1. The potential filler metal must satisfy the joint design requirements such as mechanical properties or corrosion resistance.
2. The selected filler metal must fulfill the weldability criteria with respect to dilution, melting temperature and other physical property requirements of the weldment.

Based on the above discussion and cited literature the composition of the filler metals were selected and their compositions are given in Table 5.2 (a) & (b)

Table 5.2 (a) Chemical composition of SS 308 L filler wire

C	Si	Mn	S	Ni	Cr	Mo	Cu
0.01	0.4	1.6	0.01	10.0	20.0	0.1	0.2

Table 5.2 (b) Chemical composition of SS 309 L buttering wire

C	Si	Mn	S	Ni	Cr	Mo	Cu
0.02	0.4	1.6	0.01	13.0	24.0	0.1	

The mechanical properties of the base and filler materials used are shown in Table 5.3

Table 5.3Mechanical and Physical properties of the material used

Type of steel	Tensile strength (MPa)	Yield strength (MPa)	Modulus of Elasticity (GPa)	Thermal Coeff.(10^{-6}m/m^{0}C)
SA 516 Gr70	450-585	240	200	11.7
304 L	480	170	193-200	17.2-18.4
308 L wire	618	460	190-210	17.2-18.4
309 L wire	644	489	190-210	15.0-17.2

5.4 Selection of Groove Design

The weld groove design was selected (shown in fig. 5.1) as per AWS B2.1-1/8-227:2002 for standard welding procedure specification for GTAW of SA516 Gr70 with SS 304 L

using ER309L for buttering layer and ER 308 L for filling the gap.

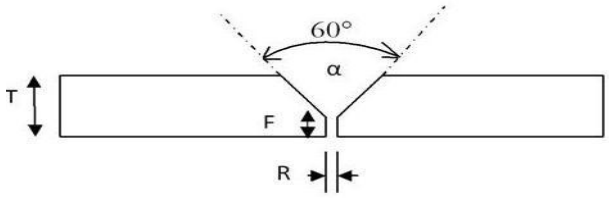

Fig. 5.1 Single-V Groove Joint Design

Where,

R= Root opening

F=Root face

T= thickness of plate

α = groove angle

5.4.1 Preparation of Groove

Austenitic stainless steel plate 304L and plain carbon steel SA 516 grade 70 plates of 32 mm thick as received from the manufacture were cut into size of 150 x 70 x 20 mm on power saw. The groove was prepared as per above said standard. As shown in Fig. 5.2, the weld grooves were prepared in both plates on milling machine. Both the plates were in proper position maintaining the proper gap and rigidly clamped in fixture so that effect of distortion can be nullified. The V-groove prepared for welding as shown in Fig. 5.2.

Fig. 5.2 Plates with V grove

5.5 Selection of Welding Process

5.5.1 Gas Tungsten Arc Welding

GTAW or TIG welding process was selected for preparation of bimetallic welds.

As shown in Fig. 5.3 and Fig. 5.4 there is non-consumable electrode which produces arc between metal to be welded. The weld zone is covered by an inert gas (Argon) to protect from outside atmospheric air and a suitable filler material is used. In the welding torch, tungsten electrode is surrounded by the inert gas and also connected by power source. From the power source current flows in the electrode and also it is cooled by inert gas to prevent the electrode from overheating. The work piece is attached to the other terminal of power source. Fig. 5.5 shows the GTAW welding machine used for preparing bimetallic weldments in present study.

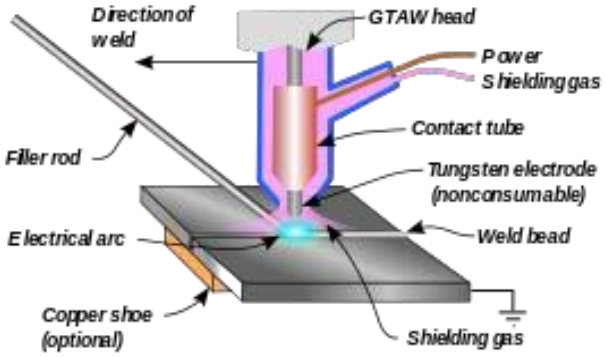

Fig.5.3 Gas-Tungsten Arc Welding (GTAW) Process

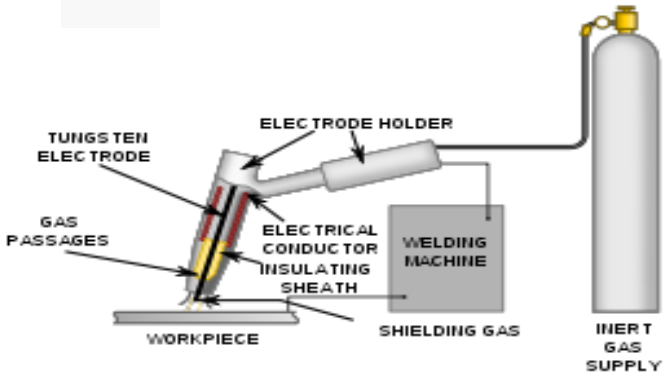

Fig.5.4 GTAW system setup

Fig.5.5 GTAW Welding Machine

5.5.2 Selection of Welding Parameters

The welding parameters were selected AWS B2.1-1/8-227:2002 for standard welding procedure specification for Gas Tungsten Arc Welding of carbon steel to austenitic stainless steel. The welding parameters were modified to improve the final weld quality.

Parameters used during welding of all weld coupons are as follows:

Voltage	
16-24 V Current	140 – 180 A
Polarity	DC, electrode negative
Shielding gas	Argon
Gas flow rate	12 lit./min.
Purity of gas	99.94%

5.6 Buttering Layer

The problem of dilution in austenitic stainless steel filler metal can be controlled by first buttering the joint face of the ferritic steel with 309L or 310L stainless steel filler metal. After machining and inspecting the buttered layer, the joint between the stainless steel component and the buttered steel part can be made using conventional welding method. An appropriate filler metal for welding the stainless steel base metal can be selected.

5.6.1 Selection of Buttering Layer Thickness

Weld coupons without buttering layer and with buttering layer were fabricated. The two buttering layer thicknesses i.e. 4 mm and 6 mm were initially considered for preparing bimetallic welds. All these three cases (without buttering layer and with buttering layer) were compared after welding with regard to residual stresses in longitudinal and transverse directions. The location of various strain gauges fixed at various points of interest is shown in Fig. 5.6. The strain gauges were fixed A, B, C and D with the help of data acquisition system (shown in Fig. 5.7) the results were plotted. From the plotted graphs Fig.5.8 to Fig. 5.13 it can be concluded that maximum residual stresses i.e longitudinal and transverse residual stresses at the weld centre are almost same in all cases. But at the interface of ferritic steel and the buttering layer there is reduction in residual stresses. Thus, welded specimen with 6mm buttering layer has minimum transverse and longitudinal residual stresses as compared to rest of the specimens with 4mm buttering layer and without buttering layer. So all the coupons were prepared with 6 mm buttering layer thickness.

Fig.5.6 Placement of Strain Gauges in different Zones.

Fig.5.7 Strain measurement setup

5.6.2 Residual stresses in welded specimens without and with Buttering Layer

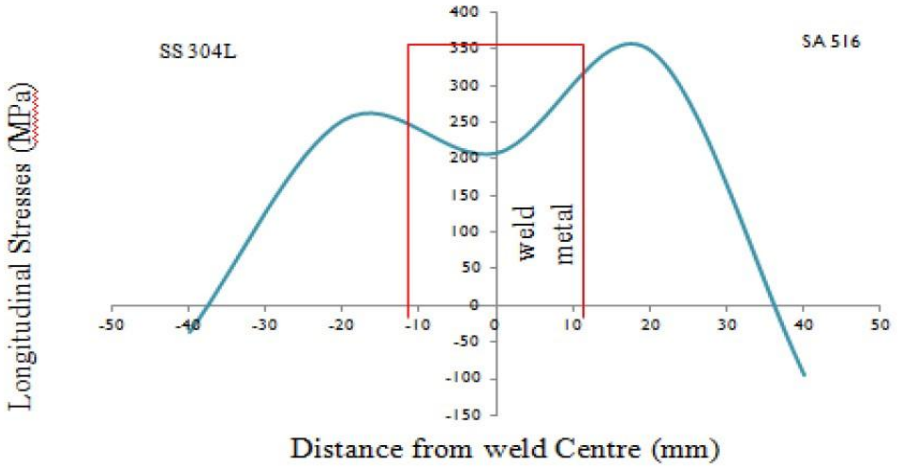

Fig 5.8 Distribution of Longitudinal Residual Stresses in specimen without buttering

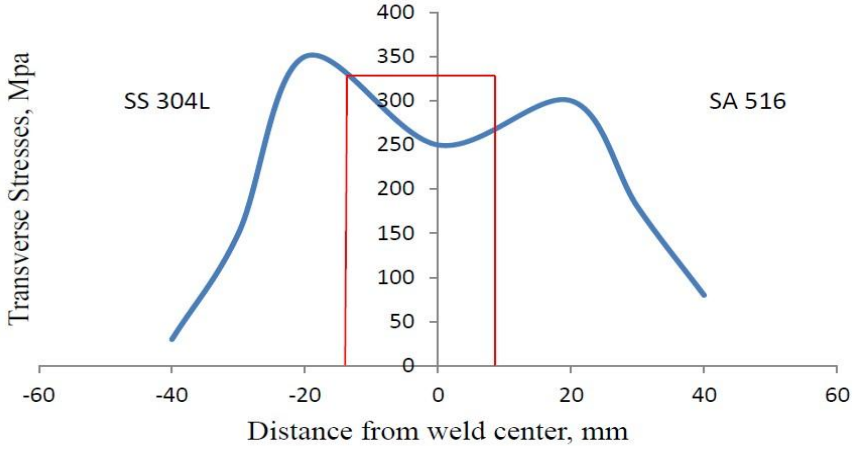

Fig 5.9 Distribution of Transverse Residual Stresses in specimen without Buttering

5.6.3 Bimetallic weld with 4mm buttering layer thickness

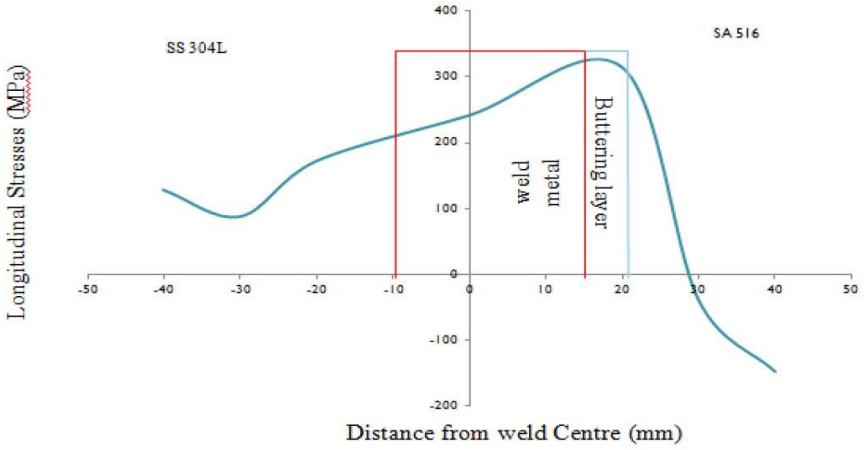

Fig 5.10 Distribution of Longitudinal Residual Stresses in Specimen with 4mm Buttering layer

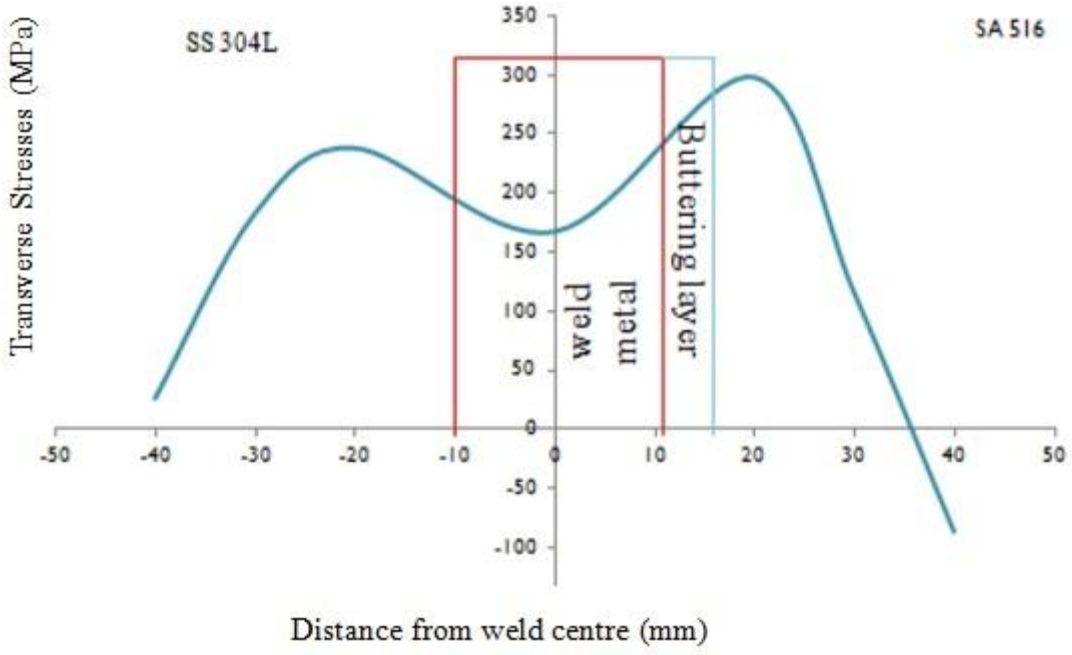

Fig 5.11 Distribution of Transverse Residual Stresses in Specimen with 4mm Buttering Layer

5.6.4 Bimetallic weld with 6mm buttering layer thickness

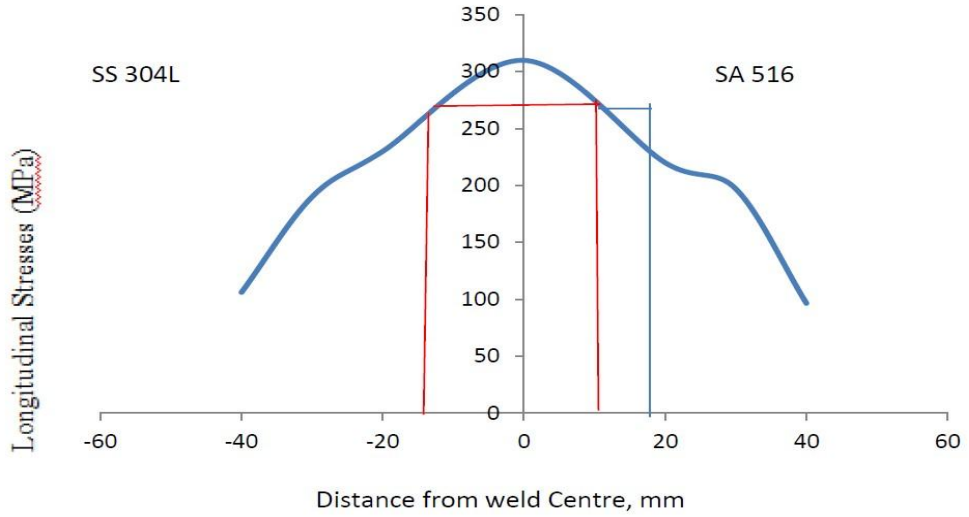

Fig 5.12 Distribution of Longitudinal Residual stresses in specimen of 6mm Buttering Layer

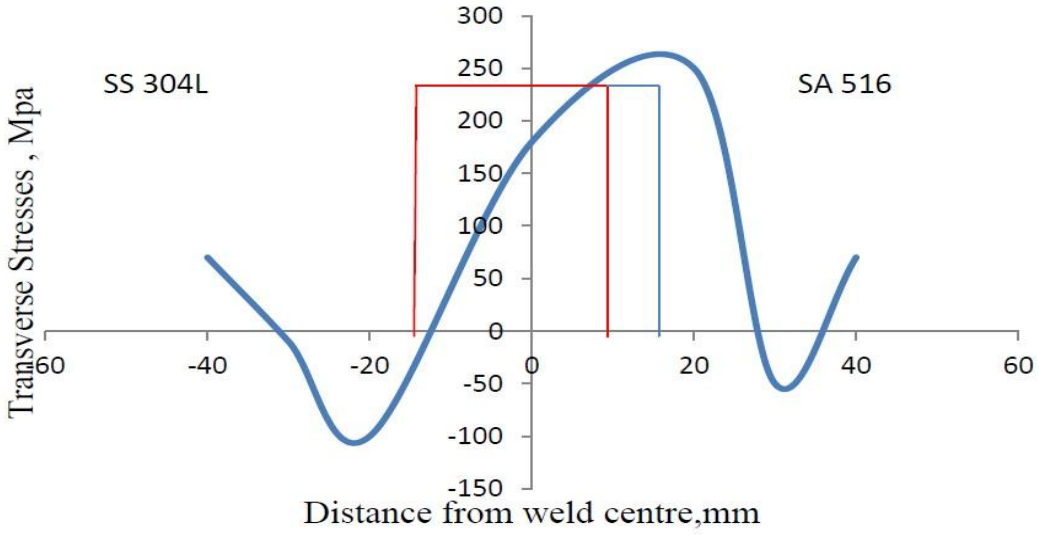

Fig 5.13 Distribution of Transverse Residual stresses in specimen of 6mm Buttering Layer

5.6.5 Welding Procedure to Weld Bimetallic Plates

The plates to be welded were cleaned properly by using emery paper to remove any presence of oil, grease etc. Subsequently, the plain carbon steel plate was tack welded to both the job piece to act as a backing plate. The welding was carried out manually as shown in Fig. 5.14. After the buttering on ferritic side, the groove is filled. It took several number of passes to fill the groove completely. After every deposition of layer, grinding and cleaning with wire brush was applied to remove any pin holes or any discontinuity. Dye penetration test was carried out in the last to

judge any discontinuity in the weld joint. On observing pin hole, grinding was carried out and again welding was carried out.

Fig.5.14 Welding in progress

Fig.5.15 Welded Specimen with 6 mm buttering layer

5.7 Testing of Welded Joint

5.7.1 Non-Destructive Testing of Welds

Ultrasonic Testing was carried out to ensure the soundness of bimetallic weldments.

Equipment:

1. Electronic signal generator

- TR Probe (transmit receive transducer)
- 10 mm diameter
- 4 MHz frequency

2. Straight beam pulse echo system
3. Couplant to transfer the ultrasonic waves into alternating voltage

The setup for present investigation used is shown in Fig. 5.16.

Fig 5.16 Ultrasonic testing

Dye Penetrant Test: The penetrants were applied on the welded surface as shown in Fig. 5.17. There was no defect detected on the surface of bimetallic welded joint.

Fig.5.17 Weld bead profile after application of developer

5.8 Preparation of Specimens:

The samples were prepared from the welded plate and notch was made in the following two zones and the schematic of these zones are clearly visible in Fig. 5.18.

1. Zone A – Weld Metal
2. Zone B – Ferritic HAZ

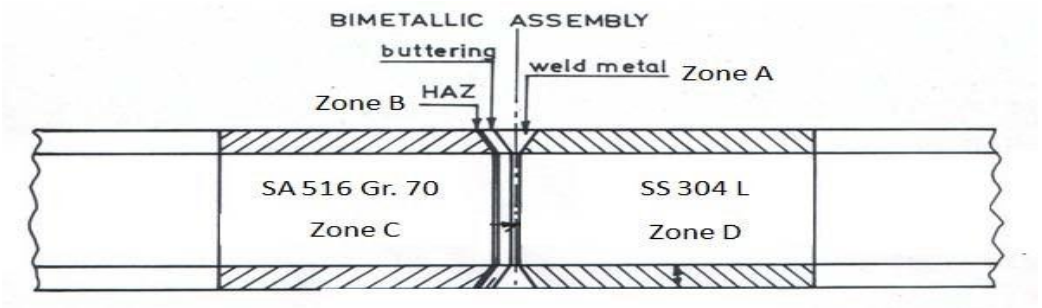

Fig. 5.18 Schematic of weld sample showing different zones

5.8.1 Specimens Geometries Used (Notch in Zone A)

From welded rectangular plates, the cross section of 20 x 20 mm and 140 mm long were cut. Total 32 numbers of the cylindrical specimens were prepared as per ASTM standard by machining on CNC lathe machine. The notch made in the centre of weld pool with radius of 4mm and 2mm and depths of all specimens were made 2.5 mm. The dimensions of prepared specimens are presented in Fig. 19 (a) and (b).

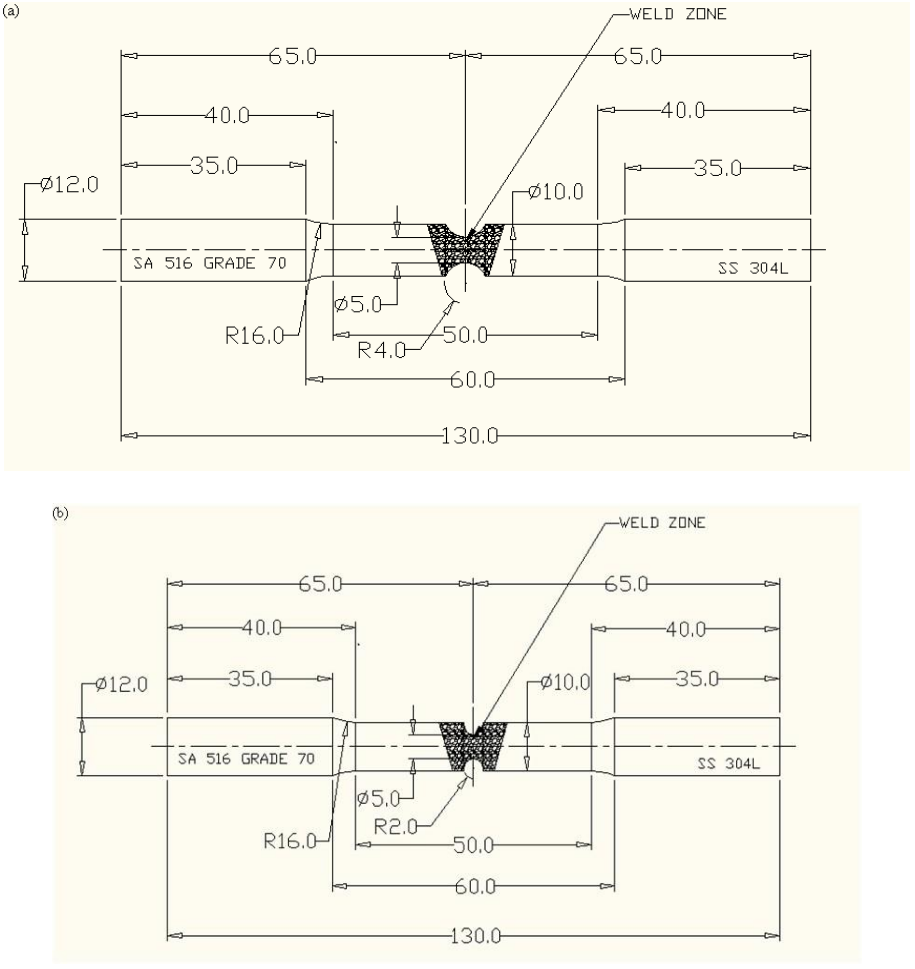

Fig.5.19 Dimensions of specimen having notch in centre of zone A

5.8.2 Notch in Ferritic Side Heat Affected Zone

From welded rectangular plates, the cross section of 20 x 20 mm and 140 mm long were cut. Total 32 numbers of the cylindrical specimens were prepared as per ASTM standard by machining on CNC lathe machine. The notch made in the heat affected zone towards ferritic side with radius of 4mm and 2mm and depths of all specimens were made 2.5 mm. The dimensions of prepared specimens are presented in Fig. 5.20 (a) and (b).

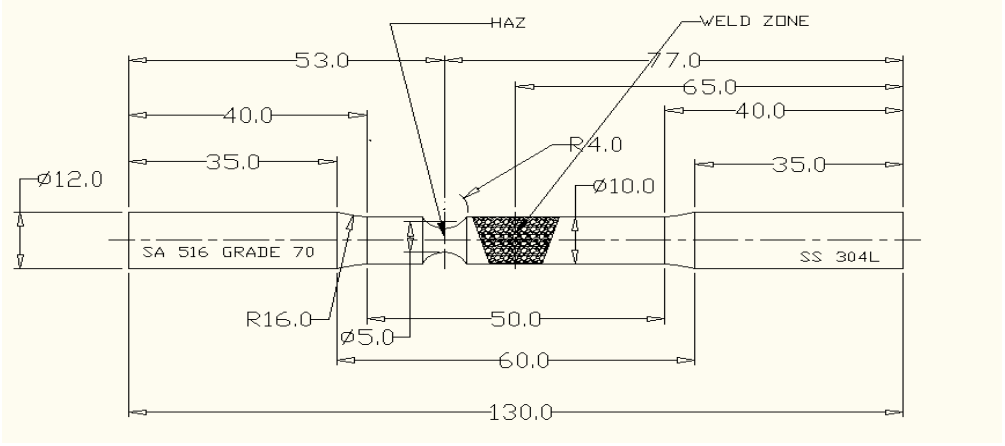

(a)

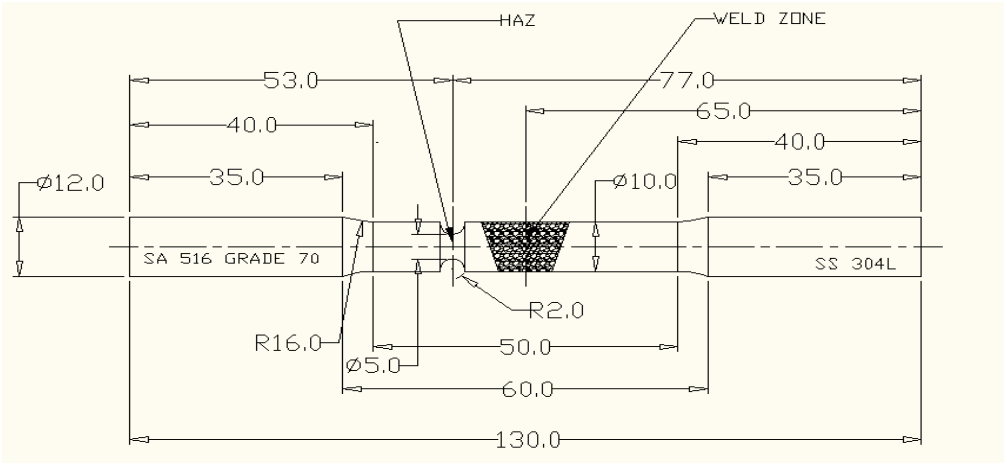

(b)

Fig.5.20 (a) & (b) Dimensions of specimen having notch in centre of zone B

5.9 Thermal Fatigue Parameters

The selection of thermal fatigue parameters i.e. temperature range, heating time, notch radius and number of cycles is shown in Table 5.4. For carrying out the experiment, the following combinations of parameters were selected.

Table 5.4. Thermal fatigue factors and their selected values

Material Code	Temperature Range (^{0} C)	Quenching Time (Sec.)	Parameters		
			Heating Time (HT) Sec.	Notch Radius (NR) MM	Number of cycles (NOC)
1	25 – 283	10	15	2	500
2	25 – 283	10	30	2	500
3	25 – 283	10	15	4	500
4	25 – 283	10	30	4	500
5	25 – 283	10	15	2	1000
6	25 – 283	10	30	2	1000
7	25 – 283	10	15	4	1000
8	25 – 283	10	30	4	1000
9	25 – 283	10	15	2	1500
10	25 – 283	10	30	2	1500
11	25 – 283	10	15	4	1500
12	25 – 283	10	30	4	1500
13	25 – 283	10	15	2	3000
14	25 – 283	10	30	2	3000
15	25 – 283	10	15	4	3000
16	25 – 283	10	30	4	3000

5.10 Thermal Fatigue Tests

Specimens were placed horizontally in the vice and heated rapidly by high frequency induction and cooled by water spray arrangement. The test rig consists of induction coil system with control unit in which heating rate can be vary by varying current, a cooling spray block, PLC and infrared temperature sensor. The various views and components of test rig are as shown in Fig. 5.21 & Fig. 5.22.

5.10.1 Different Views of Test Rig during operation:

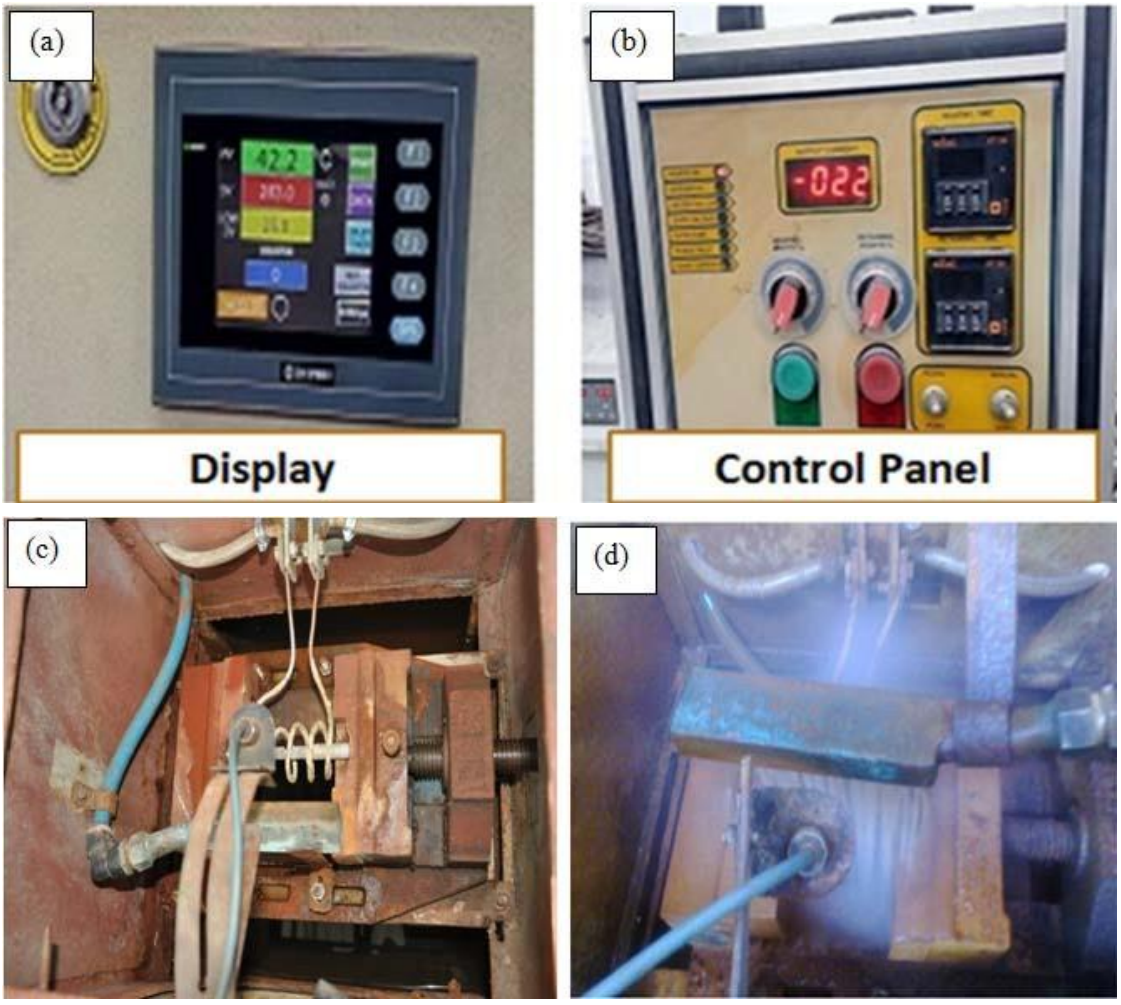

Fig.5.21 (a) and (b) are showing the display unit, (c) and (d) showing the heating and cooling operation.

Fig.5.22 (e), (f), (g) and (h) are the different views of test rig at different locations and (i) cooling tower.

5.10.2 Temperature measurement at different locations of the sample during heating

The temperature was measured with the non contact type infrared temperature sensor. The increasing temperature at different locations is clearly mentioned in the Fig. 5.23.

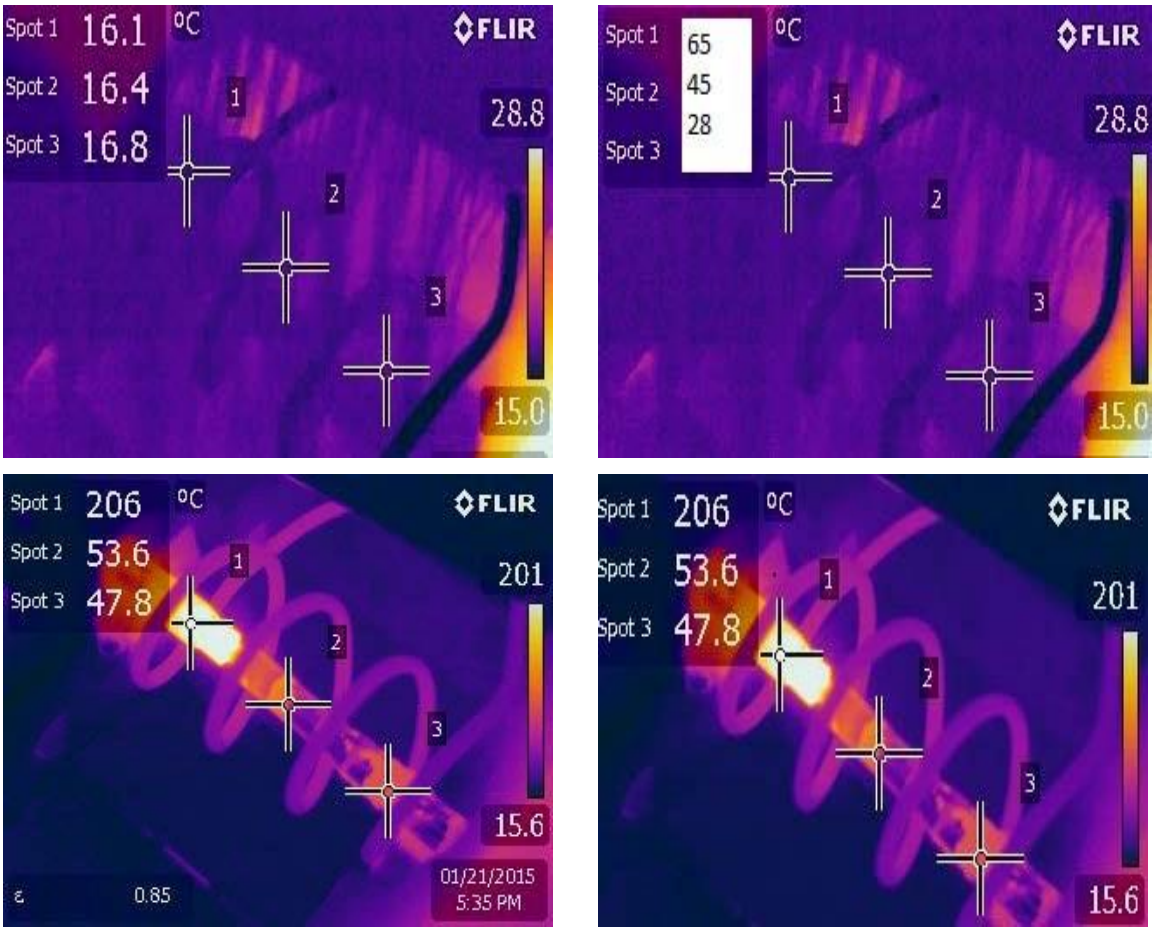

Fig.5.23 Temperature at different locations during heating

5.11 Tensile test

The tensile testing was carried out using round tensile specimen confirming to ASTM ASTM E 8/E 8M – 08 specification and the properties are reported as an average of test results of three specimens. The tests were carried out at a speed of 1mm/min at universal testing machine. The tensile specimens of the base metal and weld joint were machined in transverse direction only. The transverse tensile specimens weld joint were having 45mm gauge length and 9 mm diameters. Fig 5.24 shows the prepared specimen for the test. Fig. 5.26 showing the final sample prepared for tensile testing before thermal fatigue while Fig. 5.27 & Fig. 5.28 are showing the samples after thermal fatigue and fractured.

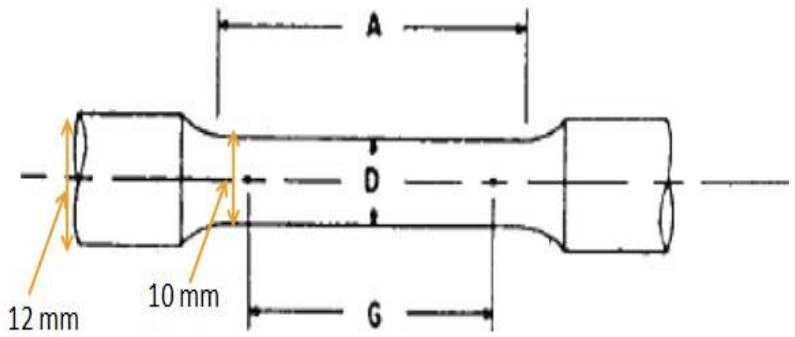

Fig. 5.24 Tensile Specimen

Actual length (A) = 50 mm

Diameter (D) = 10 mm

Gauge length (G) = 45 mm

Tensile tests were carried out on INSTRON 100 ton universal testing machine as shown in Fig. 5.25

Fig.5.25 Tensile Testing Machine loaded with sample

Fig.5.26 Tensile Specimens before Thermal Fatigue

Fig.5.27 Tensile Specimens after Thermal Fatigue

Fig.5.28 Fractured Specimens after Thermal Fatigue

An extensive experimental work was carried out following the above techniques, procedure and data collected was analyzed. The results thus obtained are discussed in Chapter 6.

CHAPTER 6
RESULTS AND DISCUSSION

6.0 Overview

This chapter describes the results obtained from the investigation performed on the designed test rig for thermal fatigue testing. The experimental procedure followed has been discussed in detail in Chapter 5. Here the mechanical behavior of various zones viz. weld metal (Zone A), Ferritic HAZ (Zone B), Base metal SA 516 Gr 70 (Zone C) and Base metal SS 304L (Zone D) has been detailed out along with various thermal fatigue parameters. The discussion has been supported with the help of suitable SEM, EDX, Hardness and residual stresses results.

6.1 Effect of Thermal Fatigue Parameters on Mechanical Behavior in Zone A

6.1.1 Effect on ultimate tensile strength

Fig. 6.1 shows the plots between ultimate tensile strength (UTS) and number of thermal shock cycles for Zone A i.e. notch being provided in weld zone. Fig. 6.2(a) explains the combined effect of notch radius and number of thermal shock cycles on UTS. Fig. 6.2(b) depicts the combined effect of heating time and thermal shock cycles on UTS. These plots show that as the number of thermal shock cycles increase from 500 to 3000 cycles, there is a continous increase in UTS values. It can also be observed that the UTS values are higher for notch radius 2 mm (NR-2) in There are various methods of monitoring temperatures during induction heating. The most common techniques make use of thermocouples and radiation detectors. Despite the widespread use of each method, several major problems should be considered before a final selection is made. These include problems of poor workpiece surface condition, contact resistance and response time for thermocouples comparison to notch radius 4 mm (NR-4), irrespective of the number of thermal shock cycles. The reason for this increase may be the higher degree of constraint in the case of NR-2 than NR-4. It can be further seen that the UTS values are higher for heating time 15 sec (HT-15) than that of heating time 30 sec (HT-30), irrespective of the number of thermal shock cycles. The reason for this increase may be higher temperature gradient for HT-15 than HT-30. The combined effect of the degree of constrained and the temperature gradient is more dominant for all levels of cycles i.e. 500, 1000, 1500 and 3000 cycles.

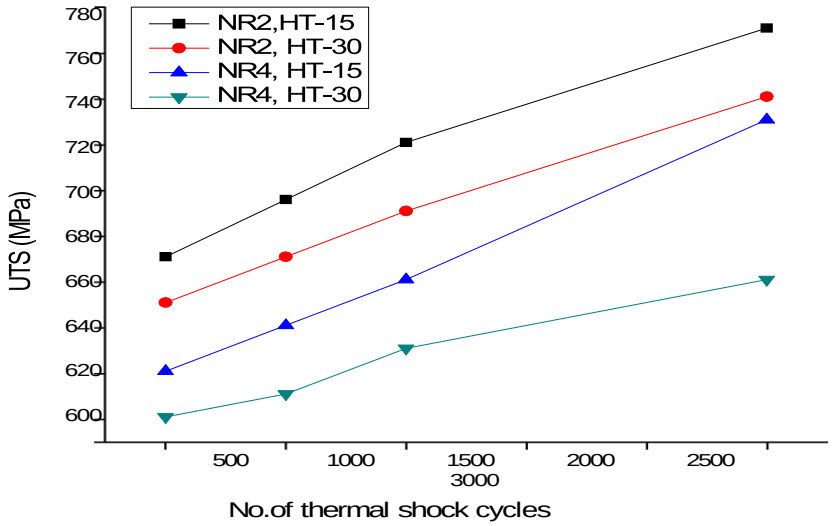

Fig.6.1. UTS vs No. of thermal shock cycles (Notch in the weld zone)

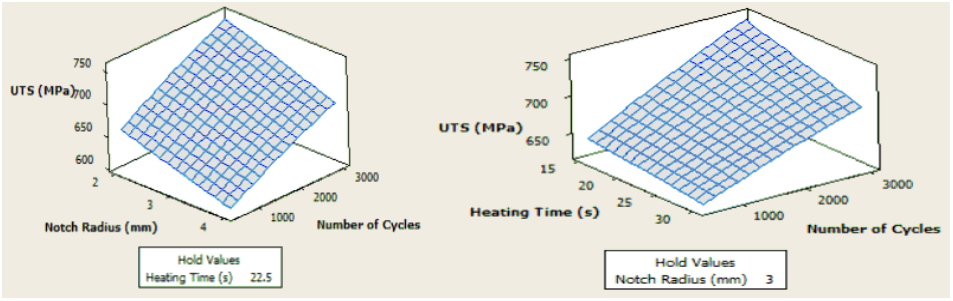

(a) **(b)**

Fig. 6.2(a) 3D surface plot of notch radius and number of thermal shock cycles vs UTS (b) 3D surface plot of heating time and thermal shock cycles vs UTS.

6.1.2 Effect of Percentage Elongation

Fig. 6.3 shows the plot between percentage elongation and number of thermal shock cycles for Zone A i.e. notch being provided in weld zone. Fig.6.4 (a) gives the combined effect of notch radius and number of thermal shock cycles on percentage elongation. Fig. 6.4(b) provides the combined effect of heating time and number of thermal shock cycles on percentage elongation. These plots reflect that as the number of thermal shock cycles increase from 500 to 3000 cycles, there is a continuous decrease in percentage elongation, which means that the ductility is showing a decreasing trend. The percentage elongation values are lower for notch radius 2 mm than notch radius 4 mm and same fact is true for heating time 15 sec than heating time 30 sec. The combined effect of degree of constraint and the temperature gradient is most dominant for all levels of cycles i.e. 500, 1000, 1500 and 3000 cycles.

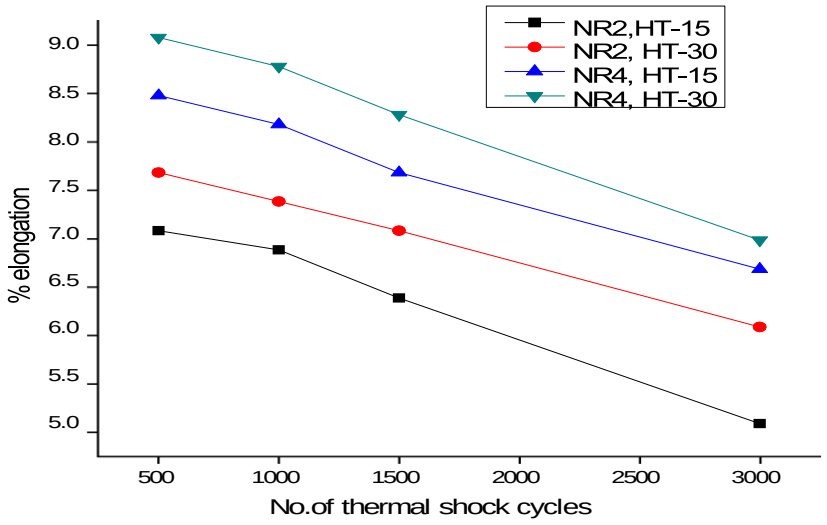

Fig 6.3 Percentage Elongation vs No. of thermal shock cycles (Notch being in the weld zone)

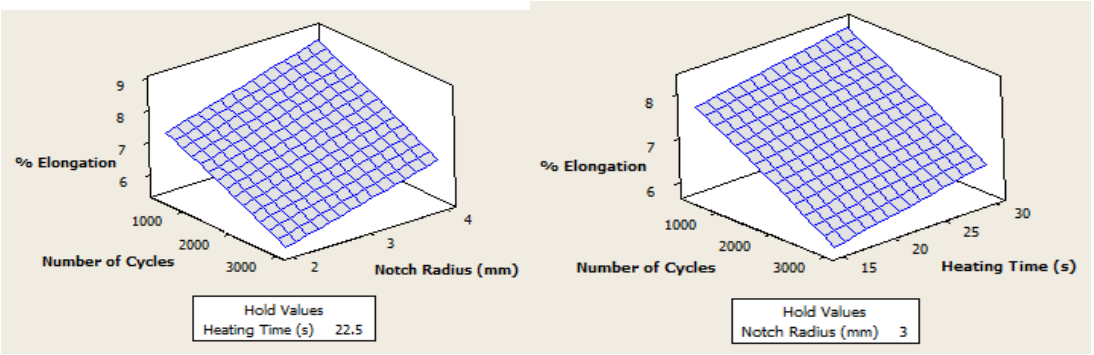

(a) **(b)**

Fig.6.4 (a) 3D surface plot for notch radius and number of cycles vs % Elongation
(b) 3D surface plot for heating time and number of cycles vs % Elongation

Fig. 6.5 and Fig. 6.6 shows microstructure of weld metal before and after thermal shock cycles (3000 cycles) respectively. Further Fig. 6.7 and Fig.6.8 show the EDX of weld metal surface before and after thermal shock cycles (3000 cycles) respectively. There has been seen an increase in carbon percentage in later case i.e. after 3000 thermal shock cycles, which might be responsible for increase in hardness. Further, this may be the very reason for decrease in ductility and reduction in percentage elongation along with increase in number of thermal shock cycles. Fig.

6.9 shows the effect of number of thermal shock cycles on hardness in weld (Zone A), Ferritic HAZ (Zone B) and Base metal SA 516 Gr 70 (Zone C).

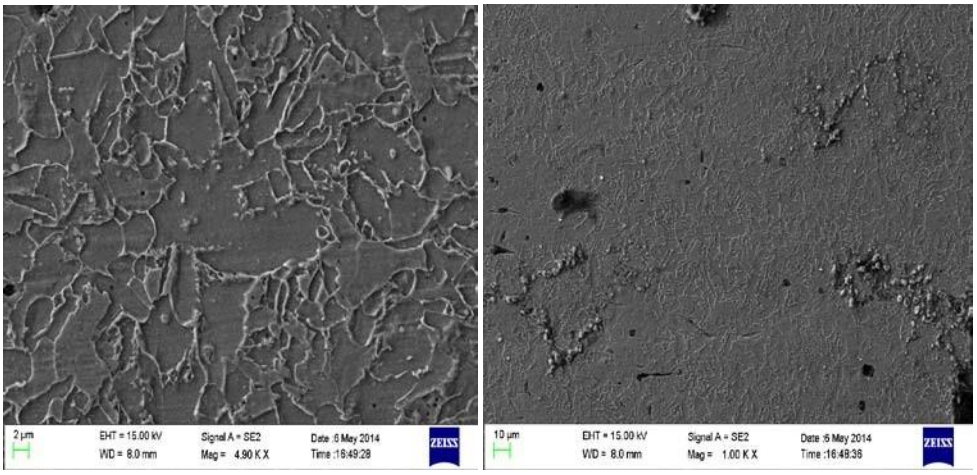

(a) (b)

Fig. 6.5 SEM of weld metal surface before thermal shock at (a) 4900× (b) 1000×

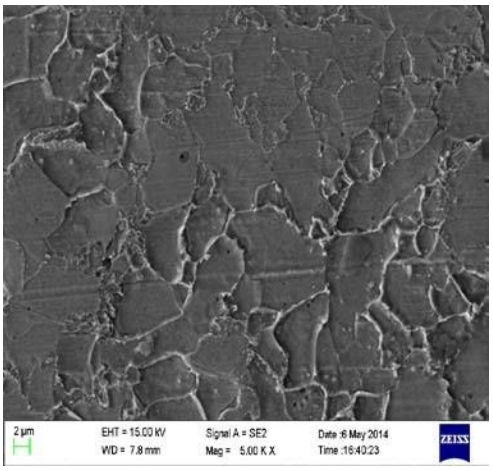

Fig. 6.6 SEM of weld metal surface after thermal fatigue at 5000×

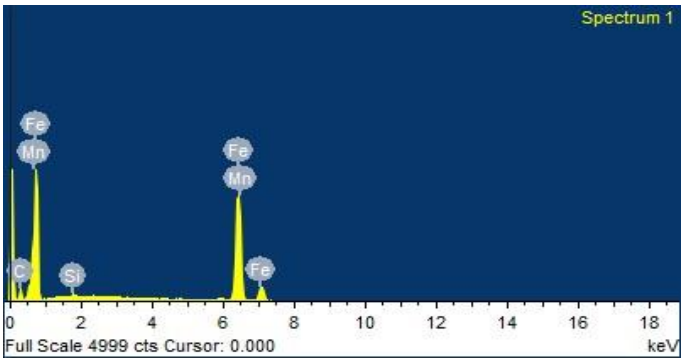

C	Si	Mn
.10	.30	1.40

Fig. 6.7 EDX of weld metal surface before thermal shock

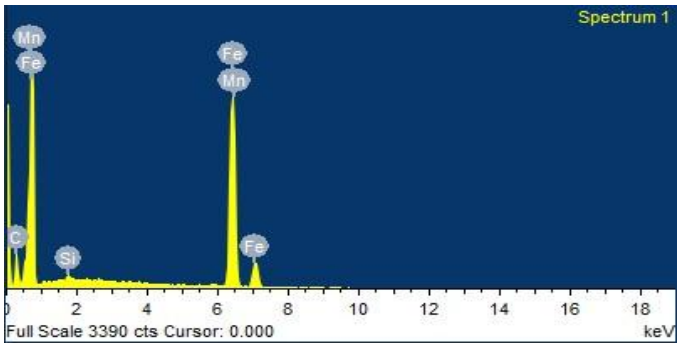

C	Si	Mn
.16	.38	.75

Fig. 6.8 EDX of weld metal after thermal shock

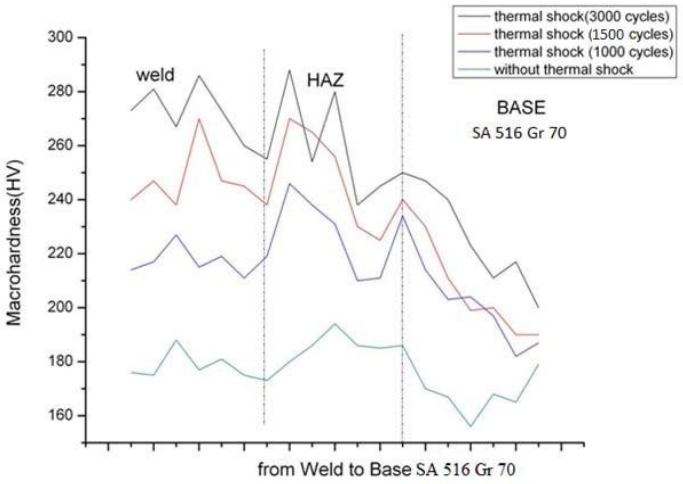

Fig. 6.9 Schematic distribution of macro-hardness across the welded joint

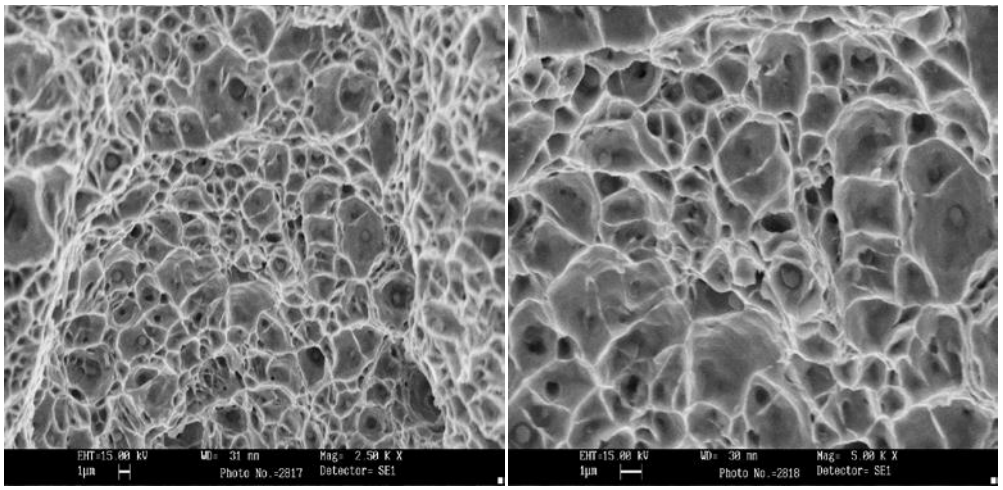

(a) (b)

Fig. 6.10 SEM photograph of weld metal fractured surface of tensile specimen before thermal shock at (a) 2500× (b) 5000×

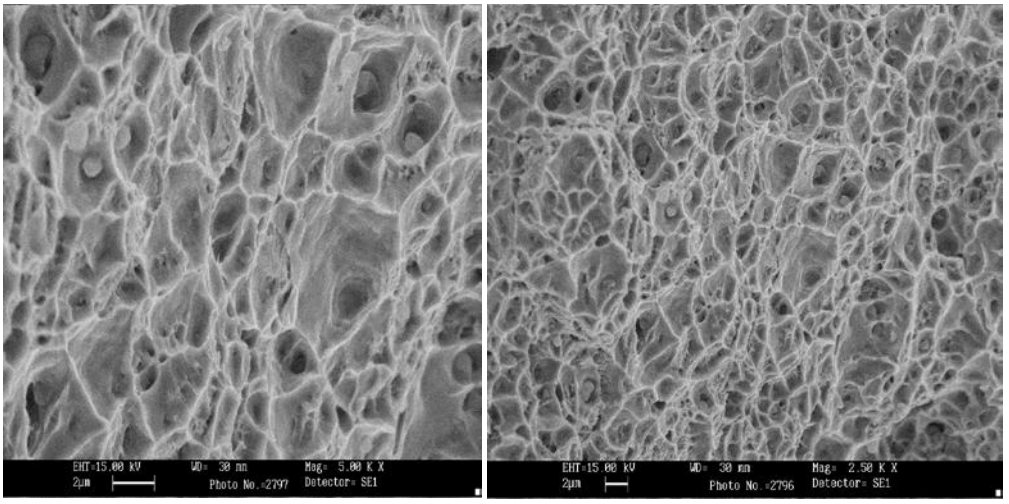

(a) 1500 cycles (b) 1500 cycles

Fig. 6.11 SEM photograph of weld metal fractured surface of tensile specimen after thermal shock cycle at (a) 5000× (b) 2500×

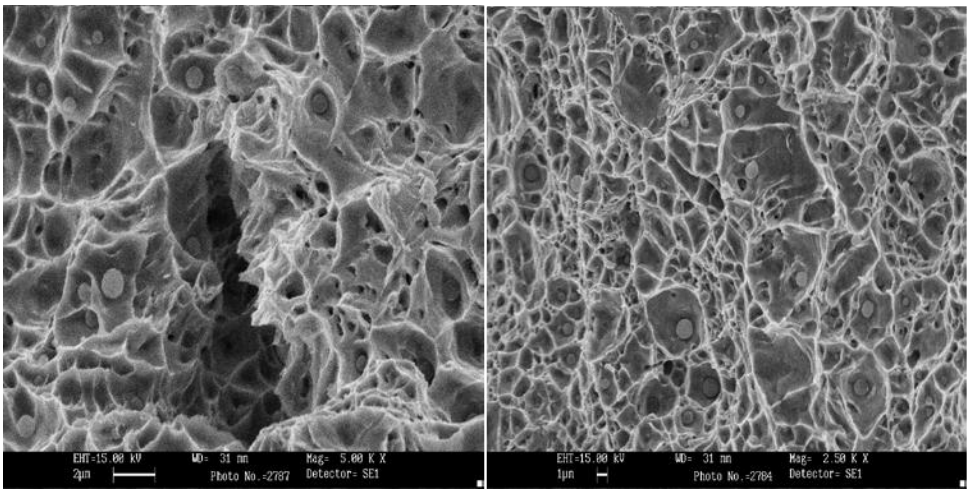

(a) 3000 Cycles (b) 3000 Cycles

Fig. 6.12 SEM photograph of fractured surface of tensile specimen after thermal shock cycle at (a) 5000× (b) 2500×

Fig. 6.10 shows SEM micrograph of weld metal fractured surface of tensile specimen without thermal fatigue. Fig. 6.11 and Fig. 6.12 shows SEM micrographs of weld metal fractured surface of tensile specimen at 1500 and 3000 cycles respectively. Fractography of these surfaces show that as the number of thermal cyclic shock increases, the size of dimple increases. Moreover, the number of dimple decreases due to the coalescence of dimple that shows the reduction in ductility. Fig. 6.12 also shows that at 3000 cycles, the tearing of dimples is taking place.

6.1.3 Effect on Yield Strength

Fig. 6.13 shows the plots between yield strength (YS) and thermal shock cycles, for Zone A i.e. notch being provided in weld zone. It can be observed from these plots that the YS values increase along with the increase in the number of thermal shock cycles from 500 to 3000 cycles. This increase may be due to increased residual stresses in the weldment. Further, it can be observed that the increase in YS is higher for Notch Radius 2 mm (NR-2) as compared to Notch Radius 4 mm (NR-4), which might be due to higher degree of constraint with NR-2. Moreover, the increase in YS is higher for heating time 15 sec (HT-15) as compared to heating time 30 sec (HT-30) irrespective of the number of thermal shock cycles, which might be due to higher temperature gradient for HT-15 than HT-30.

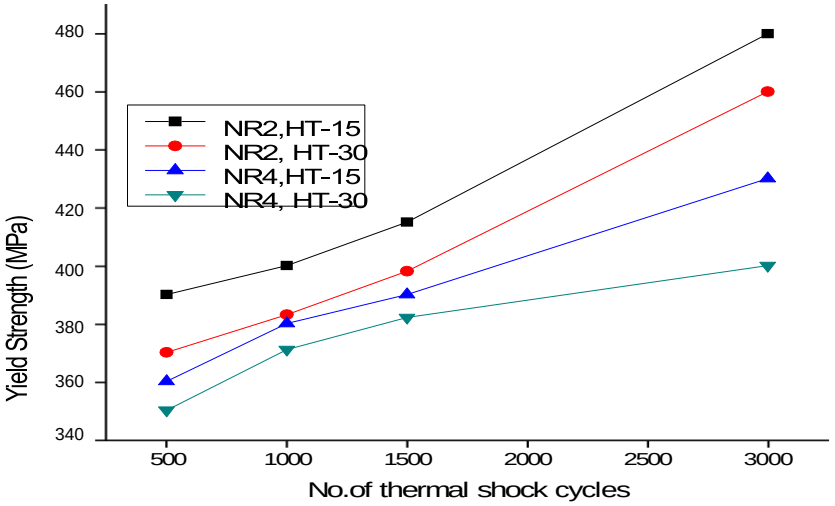

Fig. 6.13 Yield Strength vs No. of thermal shock cycles (Notch being in the weld zone)

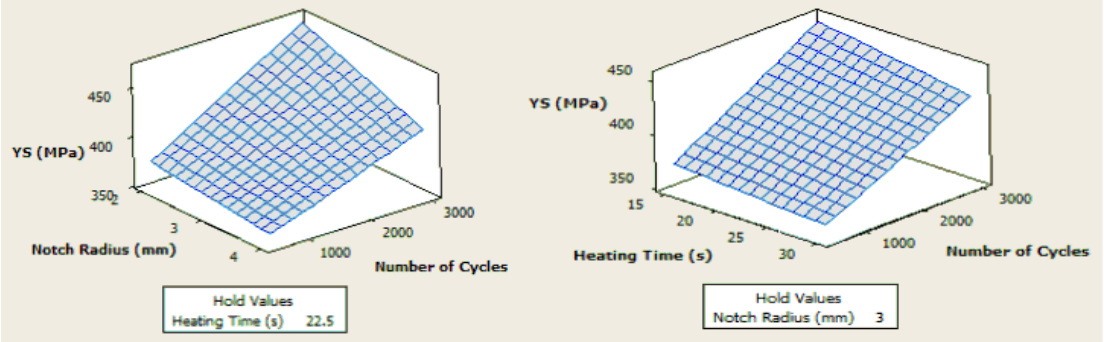

(a) (b)

Fig.6.14 (a) 3D surface plot for notch radius and number of cyclesvs Yield Strength (YS) (b) 3D surface plot for heating time and number of cycles vs Yield Strength(YS).

6.2 Effect of Thermal Fatigue Parameters on Mechanical Behavior in Zone B

6.2.1 Effect on Ultimate Tensile Strength

The plot between Ultimate Tensile Strength (UTS) and number of thermal shock cycles for Zone B i.e. notch being provided in ferrite HAZ is shown in Fig.6.15. Whereas Fig. 6.16(a) reflects the combined effect of notch radius and number of thermal shock cycles on UTS. Fig.6.16(b) depicts the combined effect of heating time and thermal shock cycles on UTS. These plots explain that as the number of thermal shock cycles increase from 500 to 3000 cycles, there is an increase in UTS. It can be observed that the UTS values are higher for notch radius 2 mm (NR-2) as compared to notch radius 4 mm (NR-4) irrespective of the number of thermal shock cycles. The reason for this increase may be the higher degree of

constraint in the case of NR-2 than NR-4. It can be further seen that the UTS values are higher for heating time 15 sec (HT-15) as compared to heating time 30 sec (HT-30) for the most of the number of thermal shock cycles. The reason for this increase may be higher temperature gradient for HT-15 than HT-30.

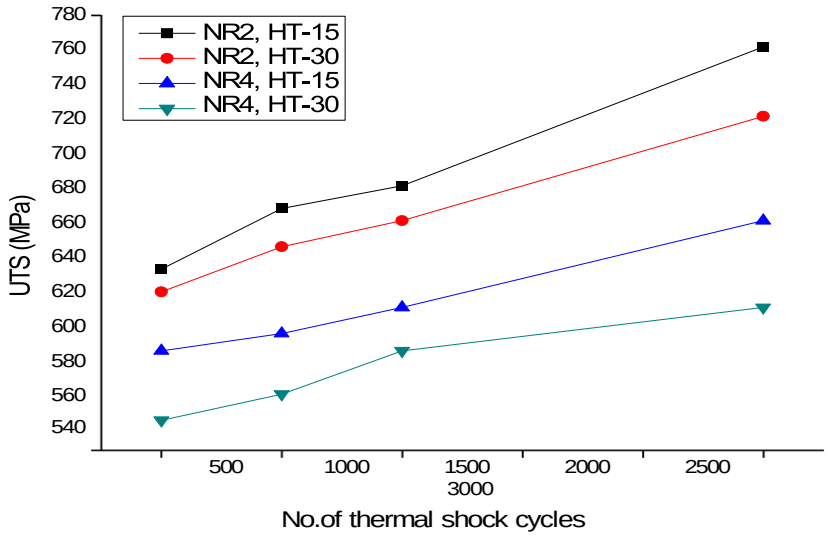

Fig 6.15 UTS vs No. of thermal shock cycles (Notch being in the Ferrite HAZ)

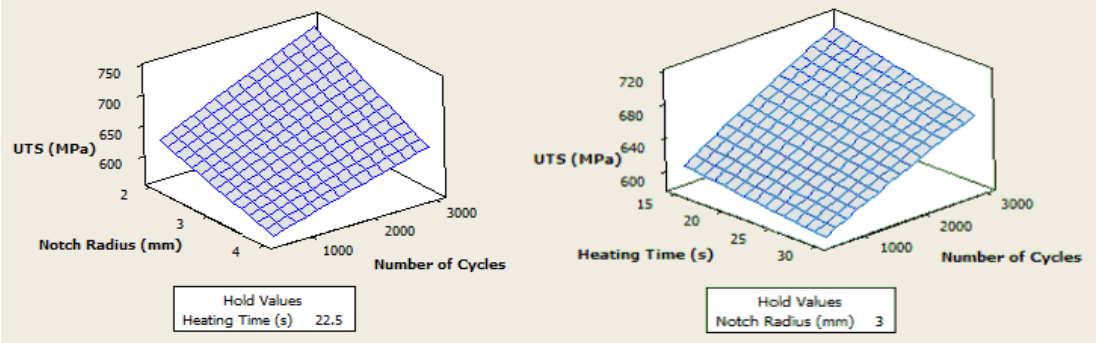

(a) (b)

Fig 6.16(a) 3D surface plot of notch radius and number of thermal shock cycles vs UTS(b) 3D surface plot of heating time and thermal shock cycles vs UTS.

6.2.2 Effect on Percentage Elongation

Fig 6.17 shows the plot between percentage elongation and number of thermal shock cycles for Zone A i.e. notch being provided in weld zone. Fig.6.18 (a) gives the combined effect of notch radius and number of thermal shock cycles on percentage elongation. Fig. 6.18(b) gives the combined effect of heating time and number of thermal shock cycles on percentage elongation. These plots reflect that as the

number of thermal shock cycles increase from 500 to 3000 cycles, there is a continuous decrease in the percentage elongation, which means that the ductility is showing a decreasing trend. The percentage elongation values are lower for notch radius 2 mm than notch radius 4 mm and same fact is true for heating time 15 sec than heating time 30 sec. The combined effect of degree of constraint and the temperature gradient is most dominant for all levels of cycles i.e. 500, 1000, 1500 and 3000 cycles.

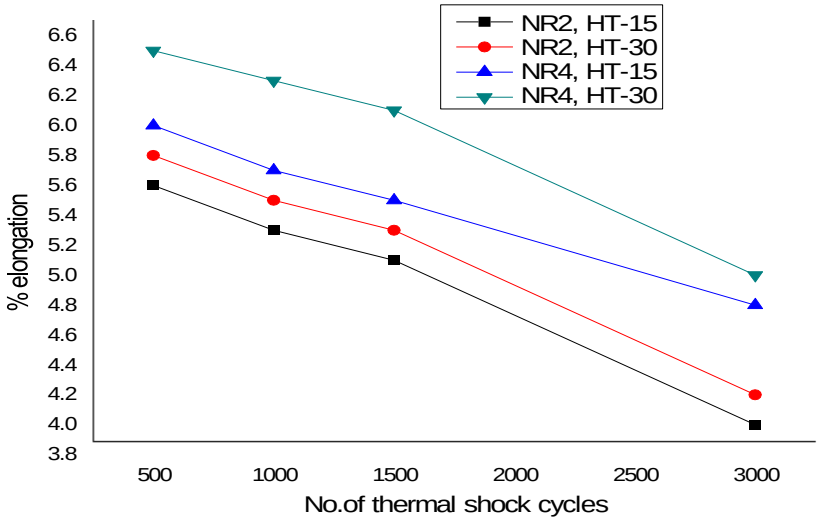

Fig 6.17 percentage Elongation vs No. of thermal shock cycles (Notch being in the Ferrite HAZ)

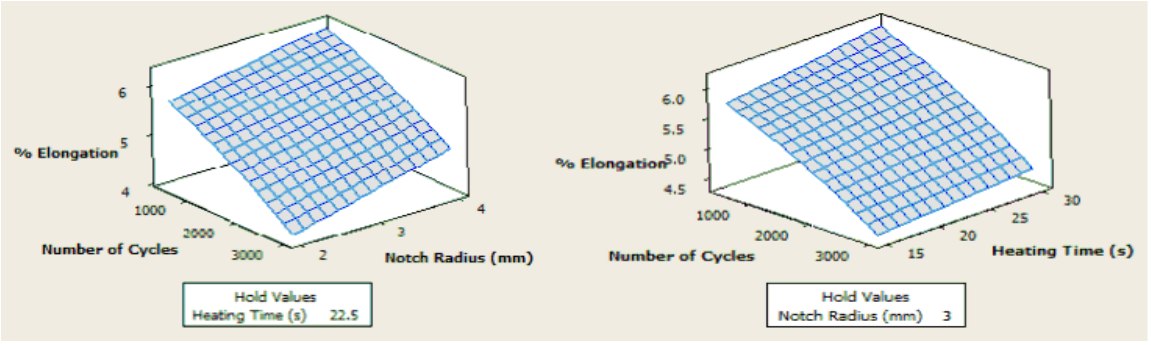

(a) (b)

Fig.6.18 (a) 3D surface plot for notch radius and number of cyclesvs % Elongation(b) 3D surface plot for heating time and number of cyclesvs % Elongation

6.2.3 Effect on Yield Strength

Fig. 6.19 shows the plots between yield strength (YS) and thermal shock cycles, for Zone A i.e. notch being provided in weld zone. It can be observed from these plots that the YS values increase along with the increase in the number of thermal shock cycles from 500 to 3000 cycles. This increase may be due to increased residual stresses in the weldment. Further, it can be observed that the increase in YS is higher for Notch Radius 2 mm (NR-2) as compared to Notch Radius 4 mm (NR-4), which might be due to higher degree of constraint with NR-2. Moreover, the increase in YS is higher for heating time 15 sec (HT-15) as compared to heating time 30 sec (HT-30) irrespective of the number of thermal shock cycles, which might be due to higher temperature gradient for HT-15 than HT-30.

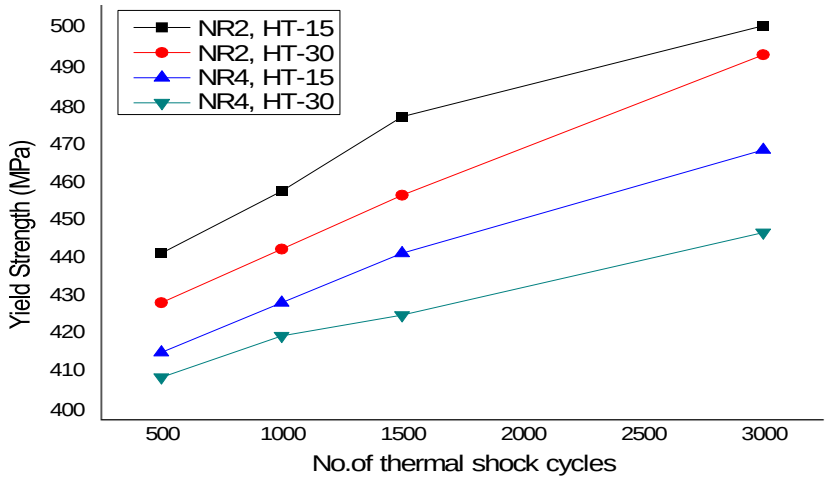

Fig 6.19 Yield Strength vs No. of thermal shock cycles (Notch being in the Ferrite HAZ)

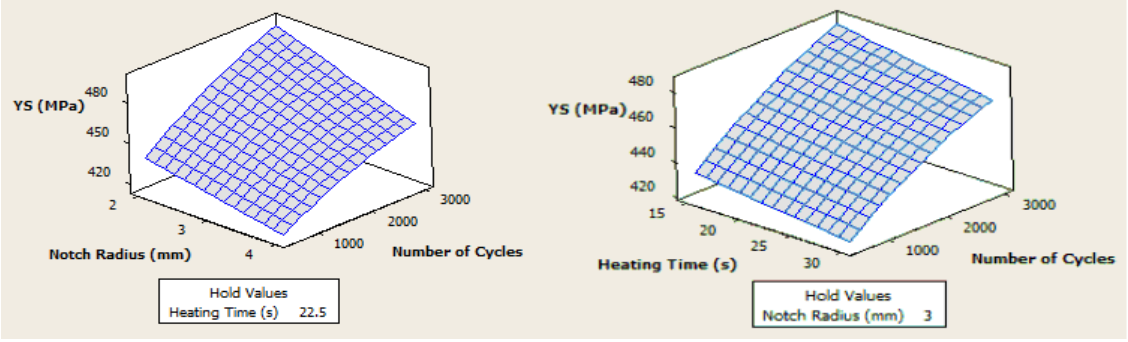

(a) (b)

Fig.6.20 (a) 3D surface plot for notch radius and number of cycles vs Yield Strength(YS) (b) 3D surface plot for heating time and number of cycles vs Yield Strength(YS).

6.3 Effect of Thermal Fatigue Parameters on Mechanical Behavior in Zone C

6.3.1 Effect on Ultimate Tensile Strength

Fig. 6.21 gives the plots between Ultimate Tensile Strength (UTS) and number of thermal shock cycles for Zone C i.e. notch being provided in base metal SA 516. Further, Fig. 6.22(a) explains the combined effect of notch radius and number of thermal shock cycles on UTS. Fig 6.22(b) depicts the combined effect of heating time and thermal shock cycles on UTS. These plots depict that as the number of thermal shock cycles increase from 500 to 3000 cycles, there is an increase in UTS. It can be observed that the UTS values are higher for notch radius 2 mm (NR-2) as compared to notch radius 4 mm (NR-4) for the most of the number of thermal shock cycles. The reason for this increase may be the higher degree of constraint in the case of NR-2 than NR-4. It can be further seen that the UTS values are higher for heating time 15 sec (HT-15) as compared to heating time 30 sec (HT-30) irrespective of the number of thermal shock cycles. The reason for this increase may be higher temperature gradient for HT-15 than HT-30.

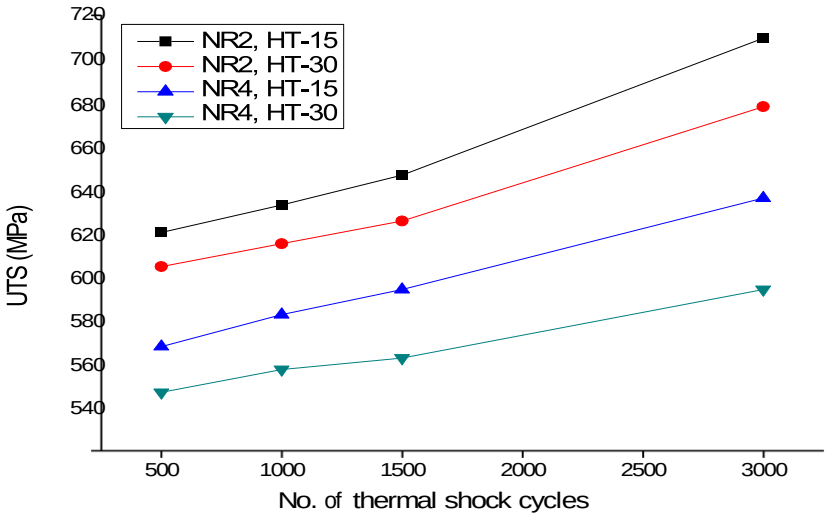

Fig 6.21 UTS vs No. of thermal shock cycles (Notch being in the Base metal SA 516 Gr70)

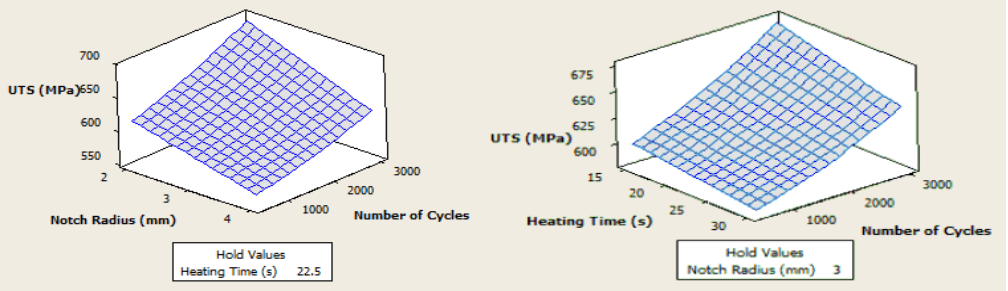

(a) (b)

Fig 6.22(a) 3D surface plot of notch radius and number of thermal shock cycles vs UTS(b) 3D surface plot of heating time and thermal shock cycles vs UTS.

6.3.2 Effect on Percentage Elongation

The relation between percentage elongation and number of thermal shock cycles for Zone A i.e. notch being provided in weld zone is explained with the help of plot shown in Fig.6.23. The combined effect of notch radius and number of thermal shock cycles on percentage elongation is given in Fig.6.24 (a), whereas Fig. 6.24(b) gives the combined effect of heating time and number of thermal shock cycles on percentage elongation. These plots reflect that as the number of thermal shock cycles increase from 500 to 3000 cycles, there is a continuous decrease in percentage elongation, which means that the ductility is showing the decreasing trend. The percentage elongation values are lower for notch radius 2 mm than notch radius 4 mm and same fact is true for heating time 15 sec than heating time 30 sec. The combined effect of degree of constraint and the temperature gradient is most dominant for all levels of cycles i.e. 500, 1000, 1500 and 3000 cycles.

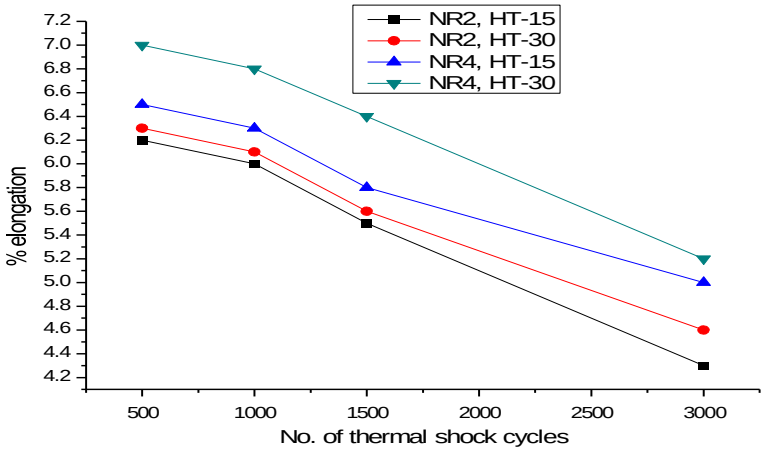

Fig.6.23 Percentage Elongation vs No. thermal shock of cycles (Notch being in the base metal SA 516 Gr70)

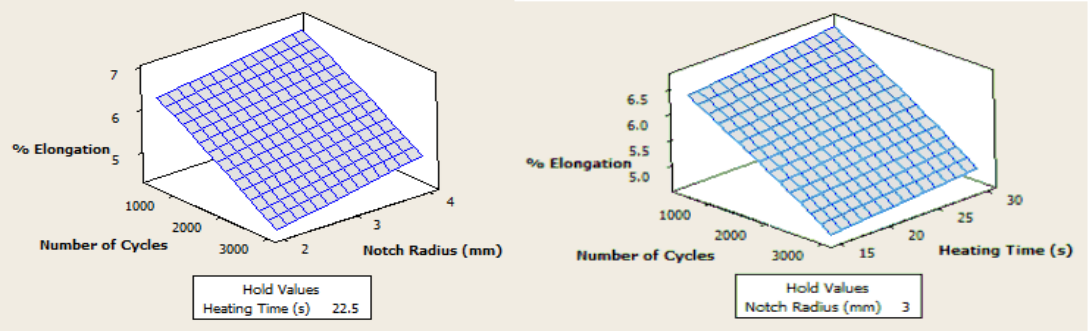

(a) (b)

Fig.6.24 (a) 3D surface plot for notch radius and number of cyclesvs % Elongation (b) 3D surface plot for heating time and number of cyclesvs % Elongation

Fig. 6.25 and Fig. 6.26 show SEM of base metal plain carbon steel SA 516 Gr70 before and after thermal shock cycles (3000 cycles) respectively. Further, the EDX analysis of base metal plain carbon steel SA 516 Gr70surface before and after thermal shock cycles (3000 cycles) is shown in Fig. 6.27 and Fig.6.28 respectively. There has been seen an increase in carbon percentage in later case i.e. after 3000 thermal shock cycles, which might be responsible for increase in hardness. Further, this may be the very reason for decrease in ductility and reduction in percentage elongation along with increase in number of thermal shock cycles.

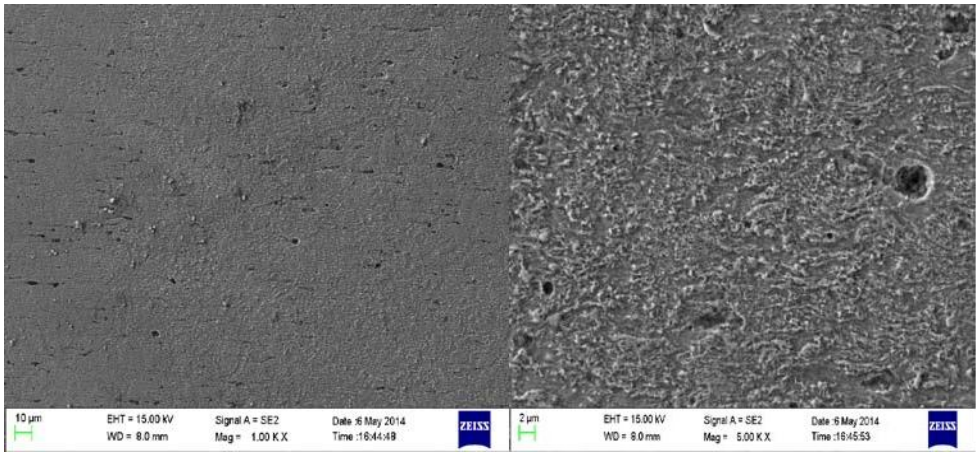

(a) (b)

Fig. 6.25 SEM of base metal surface before thermal shock at (a) 1000× (b) 5000×

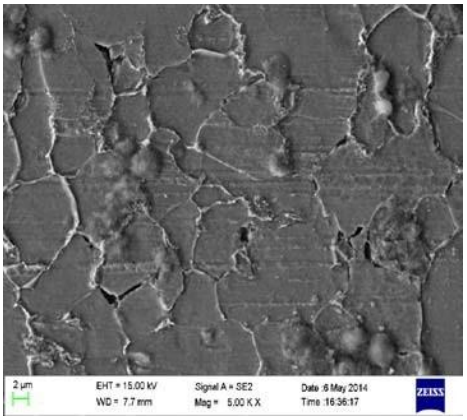

Fig.6.26 SEM of base metal surface after thermal shock

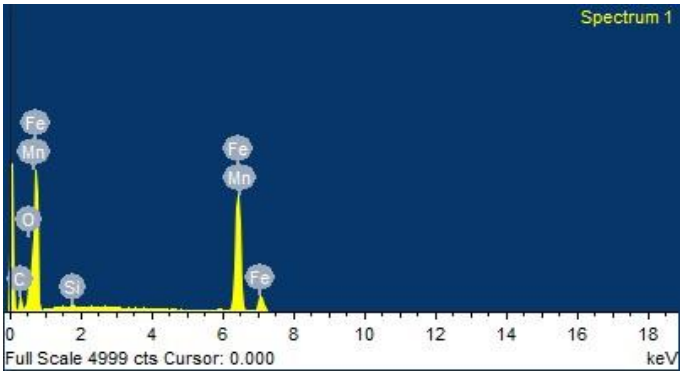

C	O	Si	Mn
.12	3.94	.23	.96

Fig. 6.27 EDX of base metal SA 516 Gr70 surface after thermal shock

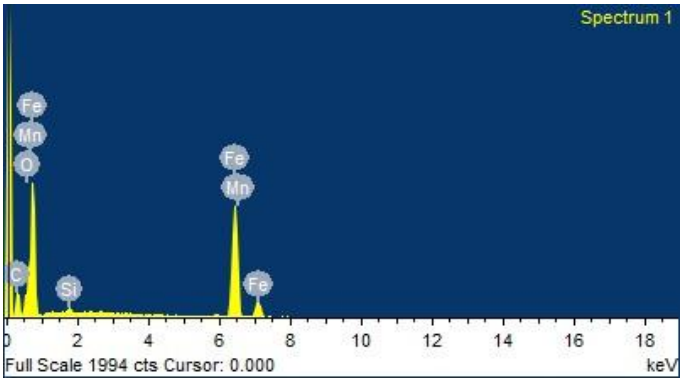

C	O	Si	Mn
.20	3.91	.52	1.02

Fig. 6.28 EDX of base metal SA 516 Gr70 (without thermal shock) surface and percentage chemical composition

6.3.3 Effect on Yield Strength

Fig. 6.29 shows the plots between yield strength (YS) and thermal shock cycles, for Zone A i.e. notch being provided in weld zone. It can be observed from these plots that the YS values increase along with the increase in the number of thermal shock cycles from 500 to 3000 cycles. This increase may be due to increased residual stresses in the weldment. Further, it can be observed that the increase in YS is higher

for Notch Radius 2 mm (NR-2) as compared to Notch Radius 4 mm (NR-4), which might be due to higher degree of constraint with NR-2. Moreover, the increase in YS is higher for heating time 15 sec (HT-15) as compared to heating time 30 sec (HT-30) irrespective of the number of thermal shock cycles, which might be due to higher temperature gradient for HT-15 than HT-30.

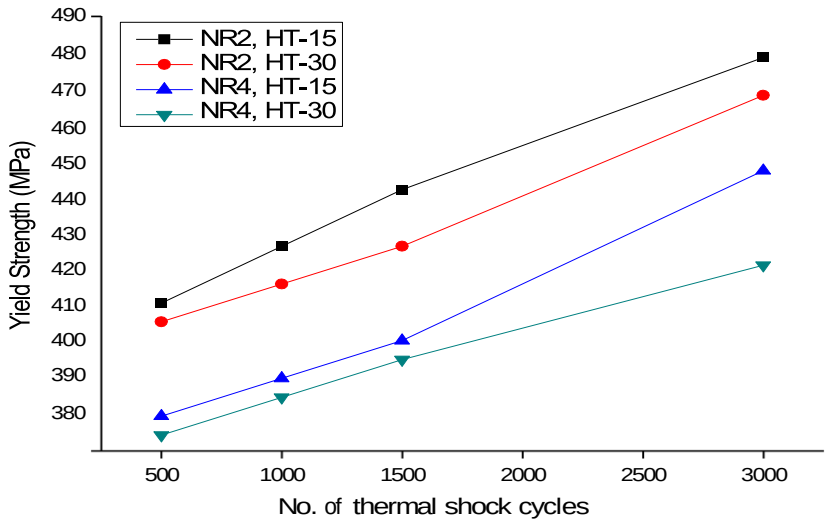

Fig.6.29 Yield Strength vs No. thermal shock of cycles (Notch in the SA 516 Gr70)

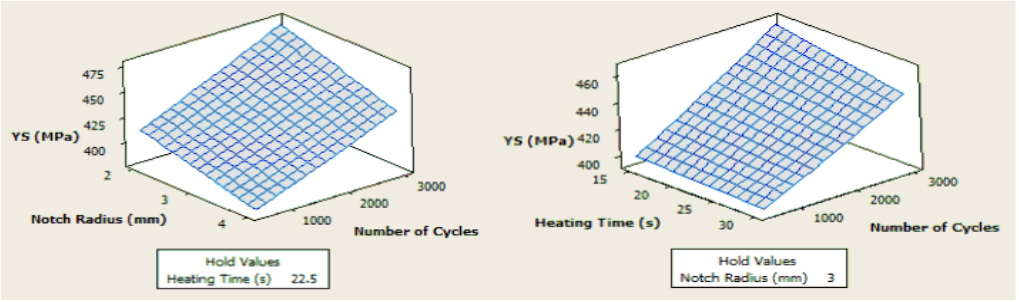

(a) (b)

Fig.6.30 (a) 3D surface plot for notch radius and number of cycles vs Yield Strength(YS) (b) 3D surface plot for heating time and number of cycles vs Yield Strength(YS).

6.4 Effect of Thermal Fatigue Parameters on Mechanical Behavior in Zone D

6.4.1 Effect on Ultimate Tensile Strength

Fig. 6.31 explains the plots between Ultimate Tensile Strength (UTS) and number of thermal shock cycles for Zone D i.e. notch being provided in base metal SS 304L. The combined effect of notch radius and number of thermal shock cycles on UTS is shown in Fig. 6.32(a). The combined effect of heating time and thermal shock cycles

on UTS is explained in Fig 6.32(b). These plots depict that as the number of thermal shock cycles increase from 500 to 3000 cycles, there is an increase in UTS. It can be observed that the UTS values are higher for notch radius 2 mm (NR-2) as compared to notch radius 4 mm (NR-4) for most of the number of thermal shock cycles. The reason for this increase may be the higher degree of constraint in the case of NR-2 than NR-4. It can be further seen that the UTS values are higher for heating time 15 sec (HT-15) as compared to heating time 30 sec (HT-30) irrespective of the number of thermal shock cycles. The reason for this increase may be higher temperature gradient for HT-15 than HT-30.

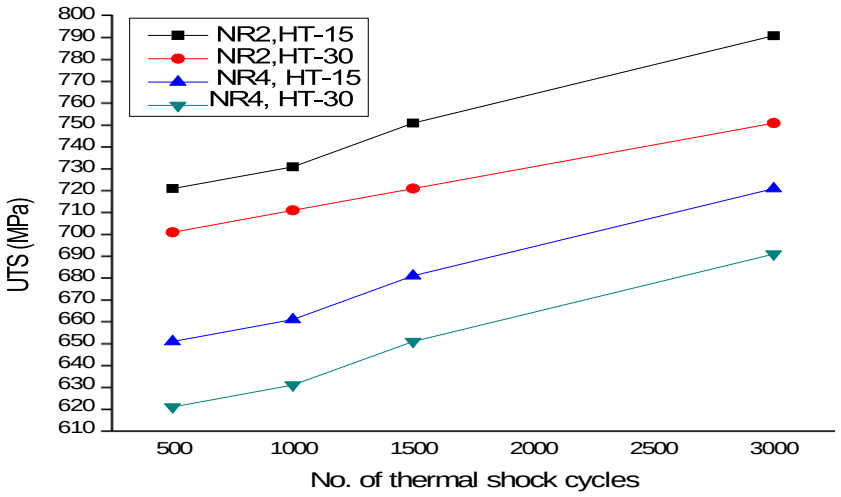

Fig. 6.31 UTS vs No. of thermal shock cycles (Notch in the Base metal SS 304L)

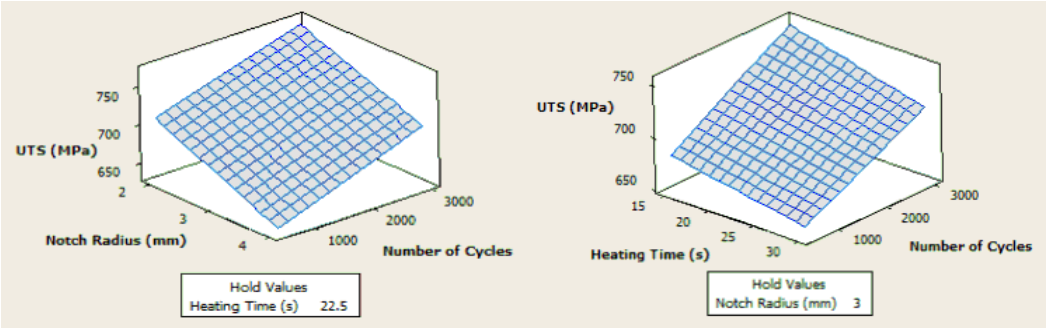

(a) (b)

Fig. 6.32 (a) 3D surface plot of notch radius and number of thermal shock cycles vs UTS(b) 3D surface plot of heating time and thermal shock cycles vs UTS.

6.4.2 Effect on Percentage Elongation

Fig. 6.33 shows the plot between percentage elongation and number of thermal shock cycles for Zone A i.e. notch being provided in weld zone. Fig.6.34 (a) gives the combined effect of notch radius and number of thermal shock cycles on percentage elongation. Fig.6.34(b) gives the combined effect of heating time and number of thermal shock cycles on percentage elongation. These plots reflect that as the number of thermal shock cycles increase from 500 to 3000 cycles, there is a continuous decrease in percentage elongation, which means that the ductility is showing the decreasing trend.The percentage elongation values are lower for notch radius 2 mm than notch radius 4 mm and same fact is true for heating time 15 sec than heating time 30 sec. The combined effect of degree of constraint and the temperature gradient is most dominant for all levels of cycles i.e. 500, 1000, 1500 and 3000 cycles.

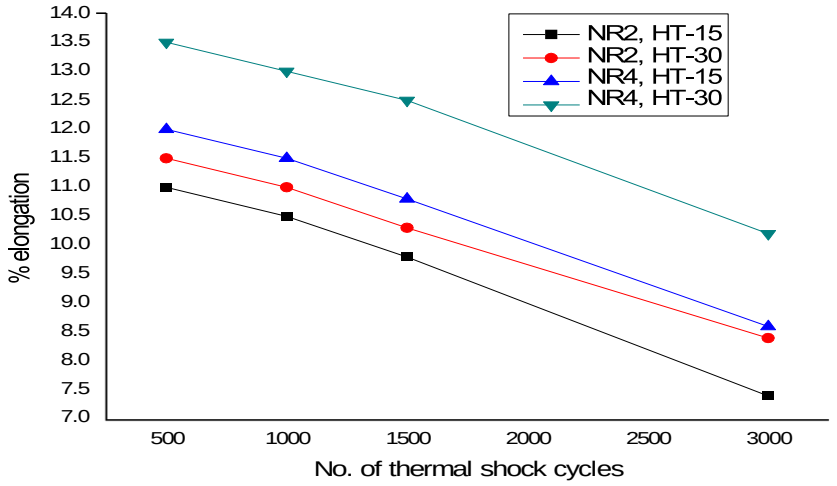

Fig 6.33 UTS vs No. of thermal shock cycles (Notch in the Base metal SS 304L)

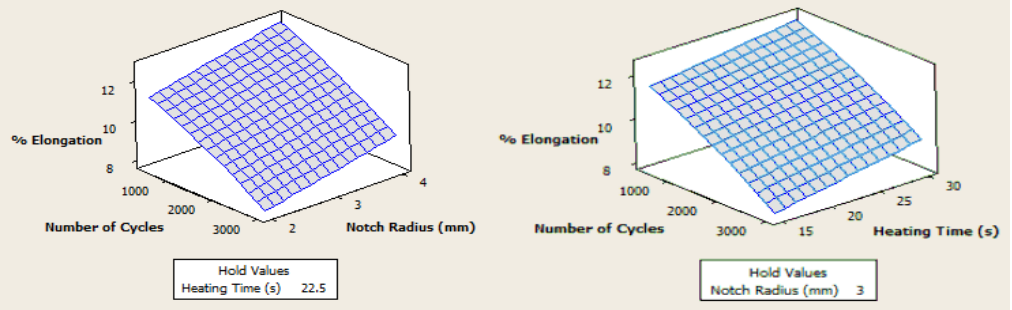

(a) (b)

Fig.6.34 (a) 3D surface plot for notch radius and number of cycles vs % Elongation
(b) 3D surface plot for heating time and number of cyclesvs % Elongation

6.4.3 Effect on Yield Strength

The plots between yield strength (YS) and thermal shock cycles, for Zone A i.e. notch being provided in weld zone are given in Fig. 6.35. It can be observed from these plots that the YS values increase along with the increase in the number of thermal shock cycles from 500 to 3000 cycles. This increase may be due to increased residual stresses in the weldment. Further, it can be observed that the increase in YS is higher for Notch Radius 2 mm (NR-2) as compared to Notch Radius 4 mm (NR-4), which might be due to higher degree of constraint with NR-2. Moreover, the increase in YS is higher for heating time 15 sec (HT-15) as compared to heating time 30 sec (HT-30) irrespective of the number of thermal shock cycles, which might be due to higher temperature gradient for HT-15 than HT-30.

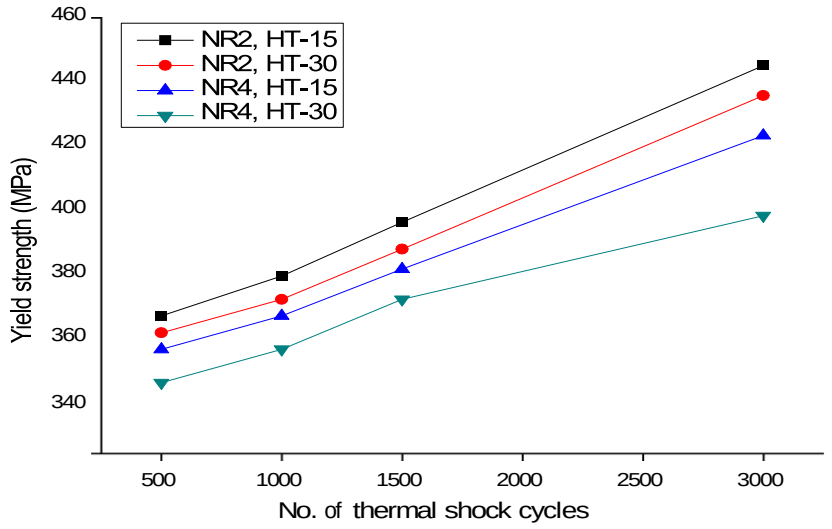

Fig 6.35 UTS vs No. of thermal shock cycles (Notch in the Base metal SS 304L)

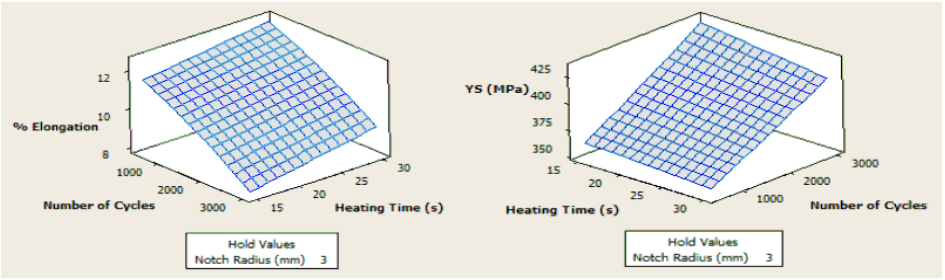

(a) (b)

Fig.6.36 (a) 3D surface plot for notch radius and number of cycles vs Yield Strength (YS) (b) 3D surface plot for heating time and number of cycles vs Yield Strength(YS).

From Ultimate Tensile Strength (UTS) values for all the four regions Weld Zone (Zone A), Ferritic HAZ (Zone B), Base Metal SA 516 Gr70 (Zone C) and Base Metal SS 304L (Zone D), we can observe that for similar notch radius and heating time conditions the UTS values are maximumfor SS 304L and UTS values for weld metal are lower than SS 304L but higher than ferritic HAZ and SA 516 Gr70. Further UTS values for SA 516 Gr70 are lowest among all four zones. Similarly for similar notch radius and heating time conditions the percentage elongation values can be compared for these zones. Percentage elongation values for SS 304L zone is maximum and for ferritic HAZ is minimum. Further percentage elongation values for SA 516 Gr70 zone are higher than ferritic HAZ zone but lower than weld metal zone as far as yield strength is concerned, for similar notch radius and heating time conditions it is observed that the values for ferritic HAZ are maximum and for SS 304L are minimum among all four zones. Further, yield strength for SA 516 Gr70 zones is higher than for weld metal zone but less than for ferritic HAZ.

CHAPTER 7
CONCLUSIONS AND FUTURE SCOPE

7.0 Overview

The current chapter is aimed at drawing conclusions from the present work along with identifying the future scope. The following section describes the contribution to the knowledge from the thesis followed by conclusions aimed at. The last section of this chapter identifies possibility of future wok in the area related to the present thesis.

7.1 Contribution to knowledge

No systematic method was available to study the mechanical behaviour of bimetallic welds in reactor components subjected to thermal shocks. A successful attempt has been made to design and fabricate a test rig for simulating thermal fatigue condition at laboratory scale. Further this test rig has been successfully used to study the mechanical behaviour of bimetallic welds prepared by joining base metal plain carbon steel SA 516 Gr70 and stainless steel 304L with the help this test rig effect of testing parameters such as number of thermal shock cycles, notch radius in specimen, heating time has been successfully studied for weld metal zone, ferrite HAZ, base metal SA 516 Gr70 and base metal SS 304L.

In reference to above stated contributions, the investigation carried out during the present work result in some generic and specific conclusions. The following section lists these conclusions.

7.2 Generic conclusions

The detailed experimental work carried and the date thus generated resulted in some generic thus generated resulted in some generic conclusions listed as follows:

1. An increasing trend has been found for Ultimate Tensile Strength (UTS) in weld metal zone along with increase in number of thermal shock cycles.
2. In weld metal zone the maximum rise in Ultimate Tensile Strength has been found for combined effect of degree of constraint and the temperature gradient i.e. notch radius 2 mm and heating time 15 sec respectively.
3. A decreasing trend has been seen for percentage elongation in weld metal zone along with increase in number of thermal shock cycles.

4. The most dominate effect on percentage elongation in weld metal zone has been seen for notch radius 2 mm and heating time 15 sec and this gives minimum ductility level.
5. An increasing trend also have been found for yield strength in weld metal zone along with increase in number of thermal shock cycles and the maximum rise is seen for notch radius 2 mm and heating time 15 sec.
6. An increasing trend has been found for Ultimate Tensile Strength (UTS) in Ferritic HAZ zone along with increase in number of thermal shock cycles.
7. In Ferritic HAZ zone the maximum rise in Ultimate Tensile Strength has been found for combined effect of degree of constraint and the temperature gradient i.e. notch radius 2 mm and heating time 15 sec respectively.
8. A decreasing trend has been seen for percentage elongation in Ferritic HAZ zone along with increase in number of thermal shock cycles.
9. The most dominate effect on percentage elongation in Ferritic HAZ zone has been seen for notch radius 2 mm and heating time 15 sec and this gives minimum ductility level.
10. An increasing trend also have been found for yield strength in Ferritic HAZ zone along with increase in number of thermal shock cycles and the maximum rise is seen for notch radius 2 mm and heating time 15 sec.
11. An increasing trend has been found for Ultimate Tensile Strength (UTS) in base metal SA 516 Gr70 zone along with increase in number of thermal shock cycles.
12. In base metal SA 516 Gr70 zone the maximum rise in Ultimate Tensile Strength has been found for combined effect of degree of constraint and the temperature gradient i.e. notch radius 2 mm and heating time 15 sec respectively.
13. A decreasing trend has been seen for percentage elongation in base metal SA 516 Gr70 zone along with increase in number of thermal shock cycles.
14. The most dominate effect on percentage elongation in base metal SA 516 Gr70 zone has been seen for notch radius 2 mm and heating time 15 sec and this gives minimum ductility level.
15. An increasing trend also have been found for yield strength in base metal SA 516 Gr70 zone along with increase in number of thermal shock

cycles and the maximum rise is seen for notch radius 2 mm and heating time 15 sec.

16. An increasing trend has been found for Ultimate Tensile Strength (UTS) in base metal SS 304L zone along with increase in number of thermal shock cycles.
17. In base metal SS 304L zone the maximum rise in Ultimate Tensile Strength has been found for combined effect of degree of constraint and the temperature gradient i.e. notch radius 2 mm and heating time 15 sec respectively.
18. A decreasing trend has been seen for percentage elongation in base metal SS 304L zone along with increase in number of thermal shock cycles.
19. The most dominate effect on percentage elongation in base metal SS 304L zone has been seen for notch radius 2 mm and heating time 15 sec and this gives minimum ductility level.
20. An increasing trend also have been found for yield strength in base metal SS 304L zone along with increase in number of thermal shock cycles and the maximum rise is seen for notch radius 2 mm and heating time 15 sec.

In addition to above stated generic conclusion some specific conclusion have also been arrived as given below:

1. By comparing the Ultimate Tensile Strength results for weld metal zone, Ferritic HAZ zone, base metal SA 516 Gr70 zone and base metal SS 304L it can be observed that the Ultimate Tensile Strength values are maximum for base metal SS 304L and minimum for base metal SA 516 Gr70. The Ultimate Tensile Strength values for weld metal zone are higher than for Ferritic HAZ zone.
2. By comparing the percentage elongation for weld metal zone, Ferritic HAZ zone, base metal SA 516 Gr70 zone and base metal SS 304L it can be observed that the percentage elongation values are maximum for base metal SS 304L and minimum for Ferritic HAZ zone. The percentage elongation for weld metal zone is higher than for base metal SA 516 Gr70 zone.
3. By comparing the yield strength for weld metal zone, Ferritic HAZ zone, base metal SA 516 Gr70 zone and base metal SS 304L it can be observed that the yield strength values are maximum for Ferritic HAZ zone and minimum

for base metal SS 304L. The yield strength for base metal SA 516 Gr70 zone is higher than for weld metal zone.

The attempt made in the present work can further be extended in future investigations. The following section discusses the scope of future work in the area under consideration.

7.3 Scope of Future Work

The present work can be further extended into following aspects

1. Effect of variation in temperature range can be studied instead of fixing it to 25 degree Celsius to 283 degree Celsius.
2. Combined effect of thermal shock and mechanical loading can be studied instead of thermal shock only.
3. Studies on crack initiation and propagation leading to failure in various regions of bimetallic weldments can be carried out in detail.

REFERENCES

1. Abdulaliyev Z., Ataoglu S., Guney D., "Thermal stresses in butt joint thick plates from different materials", Welding Journal, 86, 2007, pp 201-204.
2. Agbadual S.A., Mgbemenal C.O., Mgbemna C.E.,Chima L.O., "Thermal cycling effects on the fatigue behaviour of low carbon steel", Journal of Minerals & Materials Characterization & Engineering, 10, 2011, pp 1345-1357.
3. AWS Welding Handbook, seventh edition, "Metals and their Weldabi1ity", vol. 4, 1982, ISBN number: 0-87171-218-0.
4. Ancelet O., Chapuliot S., Henaff G., "Experimental and numerical study of crack initiation and propagation under a 3D thermal fatigue loading in a welded structure", International Journal of Fatigue, 30, 2008, pp 953-966.
5. Anderson W. R.and C. R. Waldron, "High temperature-strain fatigue testing with a modified direct-stress fatigue machine", NA A –SRR,4051 (1959).
6. Assessment and management of ageing of major nuclear power plant components importance to safety, (2003), Report by International Atomic Energy Agency under project TECDOC-1361.
7. ASM Handbook on Welding, Brazing and Soldering, Technology and Engineering, Vol. 6, 1993, Ohio, ASM International.
8. Backer F. De., Schoss V., Maussner G., "Investigation on the evaluation on the residual fatigue life time austenitic stainless steel", Journal of Nuclear Engineering and Design, 206, 2000, pp 201-219.
9. Balbi M., Avalos M., El. Bartali, I. Alvarez-Armas, "Micro-crack growth and fatigue behavior of a duplex stainless steel", International Journal of Fatigue, 31, 2009, pp 2006-2013.
10. Baldwin E.E., Sokol G.J., Coffin L.F., Am. Soc. Testing Mater.,Proe. 57,567-81 (1957).
11. Becker P.C. and Nutting J., "Structural changes during thermal fatigue of two nickel-based alloys" International conference on thermal and high strain fatigue, London, 1967, pp 100.
12. Bentele M. and Lowthian, C.S., "Thermal Shock tests on Gas Turbine Materials," Aircraft Engineering, 1952, 32-38.
13. Beres L., Balogh A., Irmer W., Kirk C. S., "Behavior of welded joints of creep resistant steels at service temperature", Welding Journal, 2003, pp 330-336.

14. Bhaduri A.K., Venkadesan S., Rodriguez P., “Transition metal joints for steam generators”, International Journal of Pressure Vessel and Piping, 42, 1999, pp 51-265.
15. Birger I.A. “Residual stresses in structural members. Residual technological stresses”, Moscow, 1985, pp 5-27.
16. Blumer U., Fricker H., Amacher S., “The bimetallic welds in the THTR steam generators”, IAEA report on specialist meeting on heat exchanging components of gas cooled reactors, 1984, reference no 31051510, published by INIS, Vol. 31, Issue 42.
17. Bradshaw F.J. andLighthill M.J., “Thermal stresses in turbine blades”, Philos. Mag., 40, 1949, pp 770-780.
18. B. Brickstad and B.L. Josefsonb,“A parametric study of residual stresses in multi-pass butt-welded stainless steel pipes”, International Journal of Pressure Vessels and Piping, 75, 1998, pp 11-25.
19. Buckthorpe D., Escaravage, C, Neri P, Pierantozzi P., Schmidt D., Final report CSC-WGCS/AG2, Study contract on Bimetallic weldments (ETNU-CT94-0133UK) and document No. C9731/TR/002, 1997, Vol.2.
20. Buessem W.R.,“Thermal Shock Testing”, Journal of the American Ceramic Society, 38, 1955, pp 15-17.
21. Buni S.Y., Raman N., Seshan S., “The role of graphite morphology and matrix structure on low frequency thermal cycling of cast irons”, Sadhana, 29, 2004, pp 117-127.
22. Burstown M.C., Howard I.C.,Ainsworth R.A., “The influence of constraint on crack tip stress fields in strength mismatched welded joints”, Journal of the Mechanics and Physics of Solids, 46, 1998, pp. 845-872.
23. Busboom H., and Ring P. J., “Dissimilar weld failure analysis and development – comparative behaviour of similar and dissimilar welds”, EPRI Report CS64666, July 1986.
24. Castro R. and Cadenet J.J. de, “Welding metallurgy of stainless and heat resisting steels” ISBN: 052120431, vol. 3, Cambridge University Press, 1974.
25. Changheui J., Lee J., Kim J.S., Jin T.E., “Mechanical property variation within Inconel 82/182 dissimilar metal weld between low alloy steel and 316 stainless steel”, International Journal of Pressure Vessel and Piping, 85, 2008, pp 635-646.

26. Changheui J., Suk-Chull K., Ho-Rim M, Seok J., Tae-Ryong K., "The effects of the stainless steel cladding in pressurized thermal shock evaluation", Journal of Nuclear Engineering and Design, 226, 2003, pp 127-140.
27. Chhibber R., Arora N., Gupta S.R., Dutta B.K., "Use of bimetallic welds in nuclear reactors: associated problems and structure integrity assessment issues", Proc. ImechE, Part C: J. mechanical engineering science, 220, 2006, pp 1121-1133.
28. Chhibber R., Arora N., Gupta S.R., Dutta, B.K., "The problems plaguing the us of bimetallic welds in nuclear reactors", Proc. Of 14th ISME Int. conference on Mechanical Engineering in Knowledge Age, Delhi College of Engineering, New Delhi, pp 8-10, December 12-14, 2005.
29. Christoffel R.J. and Curran R.M., "Carbon migration in welded joints at elevated temperatures", Welding Journal, 35, 1956, pp 457-469.
30. Cipiere M.F. and Le Duff J.A., "Thermal fatigue experience in French piping: influence of local geometry and weld conditions", International Journal of Welding in the World, 46, 2002, pp 23-27.
31. Claud E., Bass P.R., Dickson, T.L., "Role of a probabilistic analysis integrity assessment of reactor pressure vessels exposed to pressurized thermal shock conditions", International Journal of Engineering Failure Analysis, 14, 2005, pp 501-517.
32. Clayton A.M., "Thermal shock in nuclear reactors", Progress in Nuclear Energy, 12, 1983, pp 57-83.
33. Coffin L.F., Jr., Transactions of ASME. Vol 54;pp 931.
34. Cooper A.L. Elevated Temperature Properties of Titanium Carbide Base Ceramals Containing Nickel or Iron.N.A.C.A., RM E 51 110 (1951).
35. Dahlberg M., Nilsson K.F., Taylor N., Faidy C., Wilke U.,Chapuliot S., Kalkhof D., Bretherton I., Church M., Solin J., Catalano J., "Development of a European procedure for assessment of high cycle thermal fatigue in light water reactors": final report of the NESC-thermal fatigue project, European commission joint research centre, December 22, 2011.
36. Davis S.R. "Hardfacing, weld cladding and dissimilar metal joining", Welding Brazing and Soldering, ASM Handbook, Vol. 6., Ohio, ASM International, 1993, pp 789-829.

37. Dean D. and Murakawa H., “Numerical simulation of temperature field and residual stress in multi-pass welds in stainless steel pipe and comparison with experimental measurements”, Computational Materials Science, 37, 2006, pp 269-277.
38. Decamp K., Bauvineau L., Besson J., Pinaeu A., “Size and geometry effects on ductile rupture of notched bars in C-Mn steel: experiments and modelling”, International Journal of Fracture,88, 1998, pp 1-18.
39. Dennis R. Moss, “Pressure vessel design manual”, Golf professional publishing, Elsevier 3rd EDITION, ISBN: 0-7506-7740-62004.
40. Denys R.M., In: Blauel J. G, Schwalbe K-H, editors, “The Fracture Mechanics of Welds, Mechanical Engineering Publications, 1987.
41. Devaux J., Mottet G., Bergheaul J., Bhandari S.K., Faidy C., “Evaluation of the Integrity of PWR Bimetallic Welds”, Transactions of the ASME, 122, 2000, pp 368-373.
42. Dong P., and Gordon J.R., “An investigation to determine the effects of under/overmatching on the accuracy of fracture prediction models, Design and fitness for service of welded structures”, Proceedings of sixth annual north American welding research conference, Columbus, Ohio, 8-10 October, 1990, pp 41-65.
43. Dupont J.N. and Kusko C.S., “Martensite formation in austenitic/ferritic dissimilar alloy welds”, Welding Journal, 2007, pp 51-54.
44. Dutta B. K. andKushwaha H.S., “Application of a modified damage potential to predict crack initiation in welded pipes”, International Journal of Pressure Vessel and Piping, 82, 2005, pp 833-839.
45. Dutta B.K. and Kushwaha H.S., “A modified damage potential to predict crack initiation”, Theory and Experimental Verification Engineering Fracture Mechanics, 71, 2003, pp 263-275.
46. Eckel, J.F., “Diffusion across dissimilar metal joints”. Welding Journal, 43, 1964, pp 170-180.
47. Elmer J.W., Olson D.L., Matlock D.K., “The thermal expansion characteristics of stainless steel weld metal”, Welding Research Supplement, 1982, pp 293-301.
48. EO Correa et al., “Effect of weld metal chemistry on stress corrosion cracking behavior of AISI 444 ferritic stainless steel weldments in boiling chloride solution”, Materials and Corrosion, 64, 2013, 415-421.

49. EO Correa et al.,“Mechanical and microstructural characterization of weldments of ferritic stainless steel AISI 444 using austenitic stainless steels filler metals” 18th International Federation for Heat Treatment and Surface Engineering, ASTM International, 2012.
50. EO Correa et al.,“influence of clad metal chemistry on stress corrosion cracking behaviour of stainless steels claddings in chloride solution”, Scientific Research Publishing, 2, 2010, pp 391.
51. Easterling K. “Introduction to the physical metallurgy of welding”, ISBN: 0 408 01352 4, Butterworth’s & Co Ltd, 1983.
52. Findley W. N., ASTM Bull. No. 147, 50/-6 (August 1947).
53. Firouzdor V. et. al., “Effect of microstructural constituents on thermal fatigue life of A319 Aluminum alloy”, Material Science and Engineering A, 454-455, 2007, pp 428-435.
54. Fissolo A., Amiable S. et. al., “Crack initiation under thermal fatigue: An overview of CEA Experience”, International Journal of Fatigue, 31, 2008, pp. 587-600.
55. Foret R., Zlamal B., SopousekJ., “Structural stability of dissimilar weld between 2 Cr-Mo-V steels”, Welding Journal, 2006, pp 211-217.
56. Füssel Uwe et al.,“Visualization and optimization of shielding gas flows in arc welding”, Welding in the World,56, 2012, pp 54-61.
57. Füssel Uwe et al., “Numerical investigations of the influence of metal vapor in GMA Welding”, Welding in the World, 55, 2011, pp 114-120.
58. Gauther J.P. and Petrequin P., “High cyclic fatigue of austenitic stainless steels under random loading”, International Journal of Nuclear Engineering and Design, 116, 1989, pp 343-353.
59. Genki Y. and Shinobu Y., “A study on probalistic fracture mechanics of nuclear vessel and piping”, International Journal of Pressure Vessels and Piping,73, 1997, pp 97-107.
60. Ginsztler J., “The path to crack initiation during low cycle thermal shock fatigue”, International Journal of Pressure Vessels and Piping, 26, 1986, pp 181-196.
61. Gordon J. Parr and Albert Hanson, “An introduction to stainless steel”, Library of congress catalogue card no: 65 27458, American Society for meals, February 1966.

62. Hass P.E., “Results of industry wide survey on dissimilar metal welds in power plants”, In Proc. AWS/EPRI Conf. Joining Dissimilar Metals, Pittsburg, PA (1982), pp 37-47.
63. Haddar N., Koster A., Kchaou Y., Remy L., “Thermal-mechanical and isothermal fatigue of 304L stainless steel under middle range temperatures”, International Journal of C.R. Mecanique, 340, 2012, pp 444-452.
64. Harvery John F., “Pressure vessel design: nuclear and chemical applications”, D. Vannostr and company, Inc. Princeton, New Jersey, 1969.
65. Hayashi M., “Thermal fatigue strength of type 304 stainless steel in simulated BWR environment”, Nuclear Engineering and Design, 184, 1998, pp 135-144.
66. Hirose T., Sakasegawa A., Kohyama Y., Katoh H., Tanigawa, “Effect of specimen size on fatigue properties of reduced activation ferritic /martenistic steels”, Journal of Nuclear Materials, 283-287, 2000, pp 1018-1022.
67. Howes M.A.H. Fatigue at elevated temperatures, STP 520, ASTM, 242;1973.
68. Ikka V., Ph.D.Dissertion,“Thermal fatigue of austenitic and duplex stainless steel”, Helsinki University of Technology, 2001, Espoo, Finland.
69. Janssens K.G.F, Niffenegger M., ReichlinK., “A computational fatigue analysis of cyclic thermal shock in notched specimens”, Nuclear Engineering and Design, 239, 2009, pp 36-44.
70. Johansson C.A., “Fatigue of steels at constant strain amplitude and elevated temperature”, International Union of Theoretical and Applied Mechanics. Colloquium on Fatigue, Stockholm, ed. by Waloddi Weibull, Springer Verlag, Berlin, 1956, pp 112.
71. Joseph A., Sanjai K.R., Jayakumar T., Murugan N., “Evaluation of residual stresses in dissimilar weld joints”, International Journal of Pressure Vessel and Piping, 82, 2005, pp 700-705.
72. Kacar R. and Baylan O., “An investigation of microstructure/property relationship in dissimilar welds between martensitic and austenitic stainless steel”, International Journal of Materials & Design, 25, 2003, pp 317-329.
73. Kadlec M., Hau P., Sild J., Siegl, A.,Materna, J. Bystriansky, “Thermal fatigue crack growth in stainless steel”, International Journal of Pressure Vessels and Piping, 98, 2012, pp 89-94.

74. Kasatkin B.S.,Kudrin A.B.,Lobanov L.M., et al., “Experimental Methods for the Investigation of Strains and Stresses. A Handbook [in Russian], Naukova Dumka, Kiev, 1981.
75. Keim E. and Lidbury D., Review of assessment method used in nuclear plant life management, based on contributions by members of NULIFE Expert group 2 and 3, Report no. Nulife (12) 2012, 5.
76. Keinanen H., Heli T., Rauno R., Kari T., Ralf A., et.al., “Crack initiation and arrest in a pressurized thermal shock test for a model pressure vessel made of over-440 reactor pressure vessel steel”, Nuclear Engineering and Design, 158, 1995, pp 217-226.
77. Kenneth A.S., David O., William E.K., “Pressure vessel integrity and weld inspection procedure”, Nuclear Engineering and Design, 35, 1975, pp 87-153.
78. Kerezsi B., “Factors affecting crack growth in carbon steel due to repeated thermal shock from temperatures below the creep range”, Ph.D. Thesis Monash University, 2001, Australia.
79. Kerezsi B.B., Kotuusov A.G., Price J.W.H., “Experimental apparatus for thermal shock fatigue investigations”, International Journal of Pressure Vessel and Piping, 77, 2000, pp 425-434.
80. Kerezsi B.B., Price J.W.H., Ibrahim R.N., “Using S-N curves to analyze cracking due to repeated thermal shock”, Journal of Material Processing Technology,145, 2003, pp 118-125.
81. Kerezsi B.B. and Price J.W.H., “Using the ASME and BSI codes to predict crack growth due to repeated thermal shock”, International Journal of Pressure Vessel and Piping,79, 2002, 361-371.
82. Khan M.K., Alam T., Pathak M., Ravi K., Singh R., Gupta S.K.,“A review on the clad failure studies”, Nuclear Engineering and Design, 241, 2011, pp 3658-3677.
83. Khan, M.K., Pathak, M., Suman, S., Deo, A., Singh, R., “Burst Investigation on Zircaloy-4 Claddings in Inert Environment”, Annals of Nuclear Energy, 69, 2014, pp 292-300.
84. Kim J.S., Choi J.B., Kim Y.J., Park Y.W., “Investigation on Constraint effect of reactor pressure vessel under pressurized thermal shock”, Journal of Nuclear Engineering and Design, 219, 2002, pp 197-206.

85. Fefe Klueh R. L., King J. F., Grifth J. L., "A simple test for dissimilar metal welds", Welding Research Supplement, paper presented at the 64th Convention in Philadelphia, 1983, pp154-159. AWS, Annual
86. Klueh R. L., King J. F., Grifth J. L., "Austenitic stainless steel-ferritic steel weld joint failures", Welding Research Supplement, paper presented at the 61st AWS, Annual meeting held in Los Angeles, California, 1982, pp 302-311.
87. Korolev N.M., "The thermal fatigue of weld joints of different types of steels", Plenum Publishing Corporation, 11, 1975, pp 28-29.
88. Koteckia D.J., A martensite boundary on the WRC – 1992 diagram, Welding Research supplement,1999, pp 185-192.
89. Kumar R., Kumar S., Kumar A., "Some studies on Heat Affected Zone (HAZ) toughness behavior of API 5L X52 steel", Indian Welding Journal 2015; Vol 48; No. 2.
90. Kumar R., Gupta S.K., Pandey K.N, "Multi-objective optimization of friction stir welding process parameters for joining of dissimilar AA5083/AA6063 aluminium alloys using hybrid approach", 2016, Proceedings of the Institution of Mechanical Engineers Part L Journal of Materials Design and Applicationsdoi:10.1177/1464420715627294.
91. Kuwabara K., Takahashi Y., Kawaguchi S., Fukuda Y., Fukakura J., "Fatigue strength of dissimilar welded joints for the main vessel of an LMFBR" Nuclear Engineering and Design, 133, 1992, pp 335-344.
92. Laukkanen A., Nevasmaa U., Ehrnsten R., Rintamaa R., Mapping of characteristic features of bimetallic welds from the standpoint of engineering critical analysis, Transactions SMiRT 16, 2001, paper no. 1566, pp 1-8.
93. Lawrence C.M., Wu, Han G.W., "Thermal fatigue behaviour of SiCp/Al composite synthesized by metal infiltration", International Journal of Composites: Part A, 37, 2006, pp 1858-1862.
94. Leggatt R.H., "Residual stresses in welded structures", International Journal of Pressure Vessels and Piping, 85, 2008, pp 144-151.
95. Lloyd G.J and D.S. Wood, "Fatigue crack initiation and propagation as a consequence of thermal stripping", International Journal of Pressure Vessels and Piping, 8, 1980, pp 255-272.
96. Lobanov L.M. andPivtorak V.A. "Development of holographic interferometry for the investigation of the stress-strength state and inspecting the quality of welded joints", In Advanced materials for the 21st-century, Kiev: NaukovaDumk, 1998, pp. 620–636.

97. Lobanov L.M., et al. “Efficient inspection of the quality and determination of residual stresses in welded structures by electronic speckle interferometry”, AvtSvarka, 2005, pp. 10–13.
98. Maillot V., Fissolo A., Degallaix G., Degallaix S., “Thermal fatigue crack networks parameters and stability: An experimental study”, International Journal of Solids and Structures,42, 2004, pp 759-769.
99. Marie S., Menager Y.,Chapuliot S., “Stress intensity factors for unclad and through clad defects in a pressure vessel submitted to a pressurized thermal shock”, International Journal of Pressure Vessel and Piping, 82, 2005, 746-760.
100. Masubuchi K., Analysis of welded structures, Pergamon Press, London 1980. ISBN 008022714-7.
101. Meyer A.M. and M. du. Toit, Interstitial diffusion of carbon and nitrogen into heat affected zones of 11-12% chromium steel welds, supplement to the Welding Journal, 2001.
102. Mitchell M. D., Offer H. P., King P. J., “Carbon migration in transition joint weld”, Report GEFR-00398, General Electric Co., USA, 1978.
103. Murugan S., Rai S.K., Kumar P.V., Jayakumar T., Baldev R., Bose M.S.C.,“Temperature distribution and residual stresses due to multipass welding in type 304 stainless steel andlow carbon steel weld pads”, International Journal of Pressure Vessels and Piping, 78, 2001, pp307-317.
104. Murugan S., Kumar P.V.,Baldev R., “Residual stress analysis in weldments, theoretical approach”, Indian Welding journal,29, 1996, pp7-23.
105. Niffenegger M., Janssens K.G.F.,Reichlin K., Experimental and numerical investigation of cyclic thermal shock, 20th International conference on Structural mechanics in reactor technology (SMiRT 20), Espoo, Finland, SMiRT 20-Division 1, 2009, paper 1998.
106. Paffumi E., Nilson K.F, Taylor N.G., “Simulation of thermal fatigue damage in a 316 model pipe component”, International Journal of Pressure Vessel and Piping, 85, 2008, pp 798-813.
107. Pandey N.D., Bharti A., Gupta S.R. “Effect of submerged arc welding parameters and fluxes on element transfer behaviour and weld-metal chemistry”, Journal of Materials Processing Technology, 40, 1994, pp195-211.
108. Pavlyuk S.K., Rotach A.P., Vecher A.V., “Properties of weld metal in copper low carbon steel joints at elevated temperatures and their thermal fatigue resistance”, Strength of Materials, 18, 1986, pp 292-298.

109. Pham M.S. and Holdsworth S.R., "Role of microstructural condition on fatigue damage development of 316Lat 20and 300^0 C", International Journal of Fatigue, 51, 2013, pp 36-48.
110. Pistorius P.G.H., "Thermal Fatigue of Steel Tyres on Urban Railway Systems", International Journal of Fatigue, 17,1995, pp 471-475.
111. Price J.W.H., Kerezsi B.B., Chang M., "Thermal shock cracking guidelines for acceptance in service", International Journal of Engineering Failure Analysis, 11, 2003, pp 267-277.
112. Ranc N., Wagner D., Paris P.C., "Study of thermal effects associated with crack propagation during very high cycle fatigue tests",Acta Materialia, 56, 2008,pp 4012-4021.
113. Rau C.A. et al. Fatigue at Elevated Temperatures, ASTM STP 520, American Society for Testing and Materials, 1973, 166-178.
114. Reddy G.V., Parsad R., Sandhya M., Valson K., Rao B.S., "High temperature low cycle fatigue properties of 316L(N)/316(N) weld joint", International Journal of Fatigue, 30, 2008, pp 538-546.
115. Requirements of Post Weld Heat Treatment, ASME Boiler and Pressure Vessel code, Rules for Construction of Boilers, Part PW- 39, 2010, pp 101-112.
116. Richard E. Book on Practical Induction Heat treating (2001), Chapter 2 – Theory of Heating by Induction, www.asminternational.org.
117. Schwalbe K.H., Cornec A., Lidbury D., "Fracture mechanics analysis of the BIMET welded pipe tests", International Journal of Pressure Vessel and Piping, Vol. 81, 2003, pp. 251-277.
118. Schwam David, Wallace John F., and Birceanu Sebastian, (2004), Effect of design factors on thermal fatigue cracking of die casting dies, Final technical report submitted to the department of material science, Case Western Reserve University, Cleveland, Ohio, work performed under contract DE-FC07-001D, 138486.
119. Self J.A., Matlock D.K., Olson D. L., "An evaluation of austenitic Fe-Mn-Ni weld metal for dissimilar metal welding", Welding Research Supplement, 1984, 64^{th} annual AWS Convention, Philadelphia, pp 282-288.
120. Shuji T., "Relationship between thermal fatigue and low cycle fatigue at elevated temperature" American Society for Testing and Materials, 1973, pp 80-101.
121. Singh G., Singh K., Singh J., "Effect of process parameters on microstructure and mechanical properties in friction stir welding of aluminum alloy", Journal of Transactions of Indian Institute of Metals, 64, 2012, pp 325-330.

122. Singh G., Singh K., Singh J., “Modelling the effect of process parameters on tensile strength of friction stir welded aluminum alloy joints”, Experimental Techniques, 38, 2014, pp 63-71.
123. Singh R.P., Garg R.K., Kumar D.S., “Mathematical modelling of effect of polarity on weld bead geometry in submerged arc welding”, Journal of Manufacturing Process, 21, 2016, pp 14-22.
124. Sirseesha M., Albert S.K., Sundaresan S., “Thermal cycling of transition joints between modified 9Cr-1Mo steel and alloy 800 for steam generator application”, International Journal of pressure vessels and piping, 79, 2002, pp 819-827.
125. Song J.M., Lui T.S., Kao I.H., Chen L.H., Lin H.M., “Effects of micro structural refinement on tensile behaviour of the AC9A aluminum alloy suffering thermal shock fatigue”, ScriptaMaterilia, 5, 2004, pp1159-1163.
126. Stanley Zinn, Lee Semiatin. Elements of Induction Heating. ASM International, DOI: 10.1361/eoih1988p001.
127. Sudha C., Paul V.T., Terrance L.E., Saroja S.,Vijyalakshmi M., “Microstructure and microchemistry of hard zone in dissimilar weldments of Cr-Mo steels”, Welding Journal supplement, 2006, pp 71-80.
128. Swindeman R. W. Strain-Fatigue Properrtiesof Inconel. Part II. Isothermal Tests with Constant Hold Time, ORNL-3250 March 29, 1962.
129. Swindeman R.W. and Douglas D.A., Trans. ASME, Sera D: J. Basic Eng. 81, 203- 08 (1959) Paper No. 58-A-198.
130. Takagaki M., Toi Y., Asayama, T., “Fatigue damage analysis of reactor vessel model under repeated thermal loading”, Journal of Computational Methods in Engineering and Science, 12, 2006, 21-23.
131. Tarafder S., Ranganath, V.R., Sivaprasad, S., Johri, P., “Ductile fracture behaviour of primary heat transport piping material of nuclear reactors”, Sadhana, 28, 2003, 167-186.
132. Timofeev B.T., Karzov G.P., Blumin A.A., Aikovsky V.V., “Fracture toughness of 15x2 MFA steel and its weldments”, International Journal of Pressure Vessels and Piping, 77, 1997, 41-52.
133. Tucker J.T. and Eberle F., “Development of a ferritic-austenitic weld joint for steam plant application”, Welding Journal, 35, 1956, 529-540.
134. Virkkunn, Ikka, “Thermal fatigue of austenitic and duplex stainless steel” PhD dissertation 2001.

135. Visca E., Libera S., Orcini A., Riccardi B., Sacchetti M., “Thermal fatigue equipment test joints of materials for high heat flux components”, Fusion Engineering and Design, 49-50, 2000, pp 377-382.
136. Weeton John W. Mechanisms of failure of high nickel-alloy turbojet combustion liners. Washington, D.C. : National Advisory Committee for Aeronautics, 1949.
137. Westbrook J.H., “The Thermal Shock Resistance of Metallized Ceramics,” D.Sc. Thesis, 1949, M.I.T., Massachusetts, USA.
138. White D.J., “Some contributions to British work on thermal and high strain fatigue”, International conference on Thermal Stresses and Thermal Fatigue, Berkley, England, 1969.
139. Williams P., Liakat M., Khonsari M.M., Kabir O.M., “A thermographic method for remaining fatigue life prediction of welded joints”, International Journal of Material and Design, 51, 2013, pp 916-923.
140. W.J. Evans, J.E. Screech, S.J. Williams, “Thermo-mechanical fatigue and fracture of INCO718”, International Journal of Fatigue, 30, 2008, pp 257-267.
141. Yen T.C., "Thermal Fatigue - A Critical Review “II Welding Res, Council BulL S. No. 72 (October 1961).
142. Yusufzai M.Z.K. and Dewangan R., “Development of submerged arc welding flux using red mud”, International conference on Agile Manufacturing, IIT BHU, Varanasi, India, 2012.
143. Yusufzai M.Z.K., Singh G., Kumar V., “Effect of process parameters of gas metal arc welding on dilution in cladding of stainless steel on mild steel”, MIT International Journal of Mechanical Engineering, 2, 2012, pp 127-131.
144. Zuchowski R., “Analysis of the thermal fatigue process”, International Journal of Materials Processing Technology, 106, 2000, pp 167-172.
145. Zhang Z.L., Hauge M., Thaulow C., Degard J., “A notched cross weld tensile testing method for determining true stress-strain curves for weldment”, Engineering Fracture Mechanics, 69, 2002, pp 353-366.

PUBLICATIONS FROM THE WORK

1. **H.K. Aggarwal**, Rahul Chhibber and Navneet Arora, "Thermal fatigue of bimetallic weld," Proc. of 21st International Conference on Structural Mechanics in Reactor Technology (SMiRT 21), New Delhi, Vol. 1, pp. 200-201, November 6-11, 2011.
2. **Hamender Kumar Aggarwal**, Rahul Chhibber, Navneet Arora and Rajeev Mehta "Analysis of mechanical behaviour of heat affected zone on ferritic side of bimetallic welds under thermal fatigue conditions" , Material Science Forum, 2016, 880, pp 41-44, doi:10.4028/www.scientific.net/MSF.880.41@2017 Trans Tech Publications, Switzerland.
3. **Hamender Kumar Aggarwal**, Rahul Chhibber, Navneet Arora and Rajeev Mehta "Experimental analysis of thermal fatigue in bimetallic welds", Material Science Forum, 2016, 880, pp 124-127, doi:10.428/www.scientific.net/MSF.880 124@2017 Trans Tech Publications, Switzerland.